Modern Techniques of Measurement of Partial Discharge in High Voltage Systems

Thesis Submitted by

Rakesh Das

Doctor of Philosophy
(Engineering)

Electrical Engineering Department
Faculty Council of Engineering & Technology
Jadavpur University
Kolkata, India

2025

Jadavpur University
Kolkata – 700032, India

INDEX NO. 36/18/E

1. **Title of the Thesis:**

   Modern Techniques of Measurement of Partial Discharge in High Voltage Systems

2. **Name, Designation & Institution of the Supervisors:**

Dr. Kesab Bhattacharya
Professor,
Electrical Engineering Department,
Jadavpur University

Dr. Biswendu Chatterjee
Professor
Electrical Engineering Department,
Jadavpur University

Dr. Sovan Dalai
Professor
Electrical Engineering Department,
Jadavpur University

3. List of Journal Publications:

1. **Rakesh Das**; Arup K. Das; Soumya Chatterjee; Arpan K. Pradhan; Subrata Biswas, Sovan Dalai, Biswendu Chatterjee and Kesab Bhattacharya "A Novel Deep-Learning Framework to Identify and Locate Single and Multiple Partial Discharge Events," in ***IEEE Transactions on Dielectrics and Electrical Insulation***, vol. 30, no. 6, pp. 2633-2641, Dec. 2023, doi: 10.1109/TDEI.2023.3289482.

2. **Rakesh Das**; Arup Kumar Das; Biswajit Chakraborty; Soumya Chatterjee; Sovan Dalai, Biswendu Chatterjee and Kesab Bhattacharya "Mathematical Morphology-Aided Bidirectional Long Short-Term Memory Network- Based Partial Discharge Pulse Sequence Classification," in ***IEEE Transactions on Plasma Science***, vol. 51, no. 12, pp. 3454-3461, Dec. 2023, doi: 10.1109/TPS.2023.3330891.

4. **List of Patents:** Nil

5. List of Presentations in National/International Conferences:

1. **Rakesh Das**; Arup Kumar Das; Soumya Chatterjee; Subrata Biswas; Sovan Dalai, Biswendu Chatterjee and Kesab Bhattacharya, "Time-frequency Representation Aided Deep Transfer Learning Approach for Localization and Identification of Single and Multiple Partial Discharge Events," *2022 IEEE 6th International Conference on Condition Assessment Techniques in Electrical Systems (CATCON)*, Durgapur, India, 2022, pp. 161-165, doi: 10.1109/CATCON56237.2022.10077662.

Statement of Originality

I, **Rakesh Das** registered on **15th June, 2018** do hereby declare that this thesis entitled "***Modern Techniques of Measurement of Partial Discharge in High Voltage Systems***" contains literature survey and original research work done by me as part of Doctoral studies.

All information in this thesis have been obtained and presented in accordance with existing academic rules and ethical conduct. I declare that, as required by these rules and conduct, I have fully cited and referred all materials and results that are not original to this work.

I also declare that I have checked this thesis as per the "Policy on Anti Plagiarism, Jadavpur University, 2018", and the level of similarity as checked by iThenticate software is 03%.

Rakesh Das
(Signature of Candidate)

Date: 23.05.2025

Certified by Supervisors:
(Signature with date, seal)

1. KBhattacharya 23-05-2025
Dr. Kesab Bhattacharya
Professor
Electrical Engineering Department
JADAVPUR UNIVERSITY
Kolkata-700 032

2. 23.05.2025
Professor
Electrical Engineering Department
JADAVPUR UNIVERSITY
Kolkata - 700 032

3. 23.05.2025
Professor
Electrical Engineering Department
JADAVPUR UNIVERSITY
Kolkata - 700 032

Certificate from the Supervisors

This is to certify that the thesis entitled "***Modern Techniques of Measurement of Partial Discharge in High Voltage Systems***" submitted by **Shri Rakesh Das**, who got his name registered on **15th June, 2018** for the award of Ph. D.(Engg.) degree of Jadavpur University is absolutely based upon his own work under the supervision of **Prof. Kesab Bhattacharya**, **Prof. Biswendu Chatterjee** and **Prof. Sovan Dalai** and that neither his thesis nor any part of the thesis has been submitted for any degree/diploma or any other academic award anywhere before.

KBhattacharya 23-05-2025

Signature of the Supervisor and date with Office Seal

Dr. Kesab Bhattacharya
Professor
Electrical Engineering Department
JADAVPUR UNIVERSITY
Kolkata-700 032

BChatterjee
23.05.2025

Signature of the Supervisor and date with Office Seal

Professor
Electrical Engineering Department
JADAVPUR UNIVERSITY
Kolkata - 700 032

23.05.2025

Signature of the Supervisor and date with Office Seal

Professor
Electrical Engineering Department
UNIVERSITY
700 032

Acknowledgement

The author expresses deep gratitude to his esteemed guides Prof. Kesab Bhattacharya, Prof. Biswendu Chatterjee and Prof. Sovan Dalai of Electrical Engineering Department, Jadavpur University for their invaluable guidances in carrying out the thesis work. This work has reached at this stage for their expertise, encouragement and valuable criticisms. The author also expresses his sincere gratitude towards his supervisors for granting the essential freedom for his work, while the close oversight from the mentor directed the work towards excellence.

The author expresses his deep sense of appreciation to the Head of the Department of Electrical Engineering, Jadavpur University for his kind accordance in providing necessary departmental facilities for implementation of this work. The author also acknowledges the financial support provided by State Research Fellowship, Government of west Bengal (SRF 2018-22).

It is the author's pleasure to acknowledge his respected teachers Prof. Sivaji Chakravorti, Prof. Debangshu Dey, and Dr. Arpan kumar Pradhan for their advice and encouragement in completing the research work.

The author also wants to acknowledge contributions of Dr. Subrata Biswas Dr. Soumya Chatterjee, Dr. Arup Kumr Das, Mr. Biswajt Chakraborty in the course of the research work.

The author is thankful to his colleagues Dr. Suhas Deb and Mr. Subhajit Maur for providing support in various ways for carrying out the work.

The author would like to express his heart-felt gratitude to all his family members and friends for their never-ending support and encouragement during the course of the thesis work.

The author also extends thanks to all the members of the HighTension Laboratory of Electrical Engineering Department, Jadavpur University for making it possible to work in a homely atmosphere. Last but not least, the author remains indebted to all the resources that he was fortunate to have during the work.

Dedicated to

My Parents and Teachers

Contents

Chapter 1

Theory of Partial Discharge

Chapter 2
Experimental Setup & Measurement Procedure

Chapter 3
Identification and Classification of Partial Discharge Pulse Sequence based on Mathematical Morphology aided Bi-directional Long-Short Term Memory Network

ABSTRACT

This thesis presents a comprehensive study on the modern measurement techniques of Partial Discharge (PD). **Chapter 1** presents a comprehensive literature review that outlines the recent status and trends of research on Partial Discharge diagnostics, highlighting existing methods for detection, locating and measurement along with identifying the key gaps that present work aims to address. In **Chapter 2**, an experimental setup and data acquisition system were developed for the accurate detection, localization and measurement of Partial Discharge in solid insulation. The Partial Discharge signal detection serves as a critical diagnostic tool for assessing the insulation condition. **Chapter 3** introduces a conventional but advanced methodology to detection, locate, identification and classification of the three types of discharge in solid insulation (Corona discharge, surface discharge and internal discharge or partial discharge (PD) in high voltage equipment with the help of Pulse Sequence Analysis of PD signal by Mathematical Morphology based Bi-directional Long Short Term Memory (Bi-LSTM) Network. In **Chapter 4**, a modern and advanced technique is proposed to locate the Single Location PD (SLPD) and Multiple Location PD (MLPD) from the captured Acoustic signal by the sensors are analysed and classified by time frequency aided deep learning network. In **Chapter 5** presents the development of a modern and advanced methodology to locate the Single Location PD (SLPD) and Multiple Location PD (MLPD) from the signal of Optical sensors are analysed and classified with the help of a 1-Dimensional local binary pattern based novel deep learning network.

List of Figures

List of Tables

List of Abbreviations

Abbreviations	Full-Form
PD	Partial Discharge
IEC	International Electrotechnical Commission
DWT	Discrete Wavelet Transform
ML	Machine Learning
DL	Deep Learning
FIS	Fuzzy Inference System
ANN	Artificial Neural Network
SVM	Support Vector Machine
HV	High Voltage
EMI	Electromagnetic Interference
RFI	Radio frequency Interference
UV	Ultraviolet
IR	Infrared
PMTs	Photomultiplier Tubes
FTIR	Fourier Transform Infrared Spectroscopy
IMS	Ion mobility spectrometry
UHF	Ultra High Frequency
RF	Radio Frequency
VHF	Very High Frequency
WK-CNN	wavelet kernel convolutional neural network
TFR	Time Frequency Representation
PRPD	Phase Resolved Partial Discharge
IEEE	Institute of Electrical and Electronics Engineers
PRPS	Phase Resolved Pulse Sequence

1-D	1 (one) Dimension
LBP	Local Binary Pattern
TRPD	Time Resolved Partial Discharge
HFCT	High Frequency Current Transformer
UWB	Ultra Wide Band
CNN	Convolutional Neural Network
DNN	Deep Neural Network
RNN	Recurrent Neural Network
MM	Mathematical Morphology
LSTM	Long Short Term memory
Bi-LSTM	Bidirectional Long Short Term memory
PSA	Pulse Sequence Analysis
EPDS	Electrical Partial Discharge Source
APDS	Acoustic Partial Discharge Source
STFT	short-time Fourier transform
CWT	continuous wavelet transforms
WVD	Wigner Ville distribution
SPWVD	Smoothed Pseudo Wigner Ville distribution
OPDS	Optical Partial Discharge Source
PDLE	Partial Discharge Location Emulator
SPDE	Single Partial Discharge Emission
MPDE	Multiple Partial Discharge Emission
SLPD	Single Partial Discharge Event
MLPD	Multiple Partial Discharge Event
SE	Structure Element
CV	Convolutional
GNB	Gaussian Naive Bayes
KNN	k-nearest neighbourhood

TN	Truly Negative
TP	Truly postive
FN	False Negative
FP	False Positive
SNR	Signal to noise ratio
CP	Classification Problem

List of Mathematical Symbols

Symbol	Meaning
u_i	flattened output corresponding to i^{th} channel
w_i	indicates the fusion weight of the flattened output u_i
v	fused output
$x(t)$	a cross-term reducing window in the time domain
$y(t)$	the window which reduces cross-terms in frequency domain
ϕ	Phase angle
q	magnitude of the charge
n	number of PD occurrences over predefined time duration
$E(i)$	erosion
$D(i)$	dilation
$O(i)$	opening
$C(i)$	closing
$n-\Delta u$ pattern	variation of n versus Δu , with n being the number of occurrence of pulses

Chapter 1

1.1. Introduction

Electricity supply networks demand continuous condition assessment and monitoring due to the essential role of insulation in high-voltage power equipment. Insulation in such equipment must endure electrical, mechanical, and thermal stresses, and any defect—particularly from Partial Discharge (PD)—can severely impact the equipment, potentially leading to failures if undetected [1]. According to the IEC 60270 Standard, PD is defined as "a localized electrical discharge that only partially bridges the insulation between conductors" [2]. This localized discharge degrades insulation and can result in power interruptions if left unaddressed.

Partial Discharge occurs as a localized breakdown of insulation under electric stress, which may or may not be adjacent to a conductor [1-2]. Although PD does not immediately cause full insulation failure, prolonged undetected activity can eventually lead to complete breakdown, endangering the life of high-voltage (HV) equipment [1-6]. PD can appear at single or multiple sites within an HV apparatus, making precise location identification essential for utility providers [3-6]. Detecting PD early allows preventive actions to be taken, which can prevent premature equipment failure.

Effective PD monitoring involves detecting, locating, recognizing, and measuring discharge levels. Techniques for PD detection range from analyzing discharge current impulses to assessing chemical by-products, acoustic emissions, and electromagnetic radiation. These methodologies are categorized into off-line and on-line systems, with on-line monitoring being preferred for critical systems to reduce power interruptions.

PD monitoring systems must be sensitive, accurate, and precise. Various analysis methods, including statistical, time-based, and frequency-based feature extraction, are used [3]. Advanced techniques such as discrete wavelet transform (DWT) enhance feature extraction, while machine learning (ML) approaches—including artificial neural networks (ANNs), support vector machines (SVMs), and fuzzy inference systems (FIS)—are frequently applied for classification and regression [3]. Recently, deep learning (DL) techniques have become more prevalent, offering robust solutions for PD diagnostics by automating feature extraction and classification.

Studies on PD detection and classification have evolved from early explorations of ANNs [4] to more comprehensive reviews on ML techniques [3,5] and, recently, DL methods [6]. However, the literature still lacks an in-depth discussion of certain ML techniques. This thesis focuses on the

application of ML, particularly DL, in PD diagnostics, aiming to improve detection, location, and classification accuracy. Future research will need to address existing challenges and unlock the full potential of these techniques to enhance the reliability and maintenance of electrical equipment.

1.2. Concept of Electrical Discharge

The concept of electrical discharge involves the flow of electricity through a medium—typically gas, liquid, or solid—when there is an electrical potential difference (voltage) between two electrodes [7-18]. This discharge often results in the release of energy in the form of light, heat, or sound. The phenomenon occurs when the potential difference across the electrodes ionizes the medium, enabling the flow of electric current. Electrical discharges are pivotal in various applications, from lighting systems like fluorescent lamps and neon signs to industrial processes such as welding and cutting, as well as in natural events like lightning. However, these discharges can also pose risks; unwanted discharges can lead to equipment damage, electrical interference, or safety hazards.
Understanding electrical discharges is essential across fields such as electrical engineering, physics, and materials science. This knowledge enables the advancement of technologies, while also equipping engineers and scientists to manage and mitigate the potential risks associated with these discharges.

1.2.1. Types of Electrical Discharge

Electrical discharge occurs when the voltage between two electrodes is such that the resulting electric field exceeds the dielectric strength of the intervening medium. Dielectric strength is the maximum electric field a material can withstand before breaking down, allowing electrical current to pass through. When breakdown occurs, it leads to an electrical discharge, which manifests in various forms:

i. **Sparks**: Short, high-energy bursts of electrical discharge, often accompanied by visible light and heat. Sparks are commonly observed in everyday situations, such as rubbing feet on a carpet and then touching a metal object or in the operation of spark plugs in internal combustion engines.

ii. **Arcs**: Continuous electrical discharges that maintain a conductive path between two electrodes. Industrial applications like arc welding

use electrical arcs to generate the intense heat required for welding metals.

iii. **Corona Discharge**: A type of discharge that occurs in high-voltage systems, such as power lines and transformers, where the electric field intensity is high enough to ionize the surrounding air, resulting in a visible glow and a hissing sound.

iv. **Surface Discharge**: Occurs on the surface of insulations, especially when surface imperfections or contaminants create weak points that facilitate breakdown.

v. **Localized Discharges**: Partial discharges (PD) that happen when the electric field in a localized region within the insulation exceeds the material's breakdown strength, resulting in small electrical discharges or sparks. These discharges are typically short-lived and may repeat at irregular intervals.

vi. **Internal Discharge**: Discharge occurring within the bulk of the insulating material due to embedded voids or impurities.

vii. **Glow Discharge**: A low-energy discharge often characterized by a visible glow, commonly used in devices like neon signs and fluorescent lamps.

viii. **Streamers**: Thin, branching channels of discharge that can form during lightning strikes or in laboratory experiments.

In summary, electrical discharge is a fundamental phenomenon in electricity and physics, encompassing diverse events where current flows through a medium due to voltage differences. These discharges can occur naturally, as in lightning, or be used in technological and industrial applications, making them a critical area of study and application in electrical engineering and science.

1.3. Background Theory of Partial Discharge

Partial Discharge (PD) is a localized phenomenon occurring within electrical insulation when subjected to high electric stress, often due to imperfections or contaminants. Although PD does not immediately lead to insulation failure, its repetitive occurrence progressively deteriorates insulation, which

can ultimately compromise the reliability of high-voltage equipment [19-24]. Understanding the causes and mechanisms of PD is essential for effective diagnostics and preventive maintenance, as early detection of PD helps extend equipment lifespan and mitigate the risk of catastrophic failure.

1.3.1. Partial Discharge (PD)

Partial Discharge (PD) is a localized breakdown within electrical insulation that occurs under electrical stress, but it does not fully bridge the insulation between conductors. This discharge may or may not occur near a conductor, and while it does not lead to immediate failure, repeated PD events can progressively weaken the insulation. If undetected, PD can eventually lead to complete insulation breakdown, posing risks to the life of high-voltage (HV) equipment [19-24].

PD can appear in single or multiple locations within HV equipment [21-24], making precise identification crucial for electrical utilities. Accurately locating PD allows utilities to implement preventive measures that extend equipment lifespan and prevent premature failures. PD incidents within HV systems emit a range of signals, including electrical, optical, and acoustic, along with chemical by-products. While the electrical measurement method is well-established, it may not always capture PD at the origin site.

PD pulses exhibit unique characteristics that offer insights into the type and severity of the defect causing the discharge. Analyzing these characteristics enables effective evaluation of insulation condition, helping utilities make informed decisions for maintenance and risk mitigation.

1.3.2. Reasons Behind Partial Discharge

Partial discharge (PD) can arise from various factors, including manufacturing flaws, poor workmanship, design limitations, contamination within insulation, voltage stress, and environmental conditions. Over-voltages from switching operations or lightning strikes can also trigger PD. Typically, PD occurs when localized electric field stress within insulation escalates, often due to imperfections such as voids, cracks, or contamination. Insulation materials in high-voltage equipment like transformers, cables, switchgear, and motors serve to prevent unintended electrical contact between conductive components. However, insulation degrades over time due to aging, environmental factors, and mechanical stresses. This degradation can create weak spots, such as voids or cracks, within the insulation material. When electric field strength in these areas exceeds the

insulation's dielectric strength, localized breakdown occurs, allowing electrical discharge to pass through. If left unaddressed, this localized discharge can ultimately result in insulation failure, posing a risk of catastrophic equipment breakdown [18,25,26].

1.4. Effect of Partial Discharge in Insulating Systems

Partial discharge (PD) in high-voltage (HV) equipment can have severe consequences for insulation integrity and system reliability. As a key early indicator of insulation degradation, PD leads to several adverse effects, including:

i. **Insulation Degradation**: Unchecked PD progressively weakens insulation materials, will reduce or degrade their ability to withstand high electric fields and increasing the risk of failure.

ii. **Reduced Dielectric Strength**: Repeated PD activity gradually lowers the insulation's dielectric strength, making it more susceptible to breakdown under electrical stress.

iii. **Localized Stress and Accelerated Aging**: PD creates high-stress points within the insulation, accelerating the aging process, especially in regions prone to recurring discharges.

iv. **Formation of Conductive Paths**: PD can create conductive paths along or within insulation surfaces, potentially resulting in electrical tracking and further degradation.

v. **Corona and Ozone Formation**: In surface discharges, PD can generate corona effects and ozone, both of which contribute to localized heating and chemical reactions that deteriorate material.

vi. **Heat Generation**: PD events generate heat, creating localized hotspots. Over time, these hotspots increase the risk of insulation failure due to thermal degradation.

vii. **Acoustic Noise and Vibration**: PD events can emit characteristic acoustic signals and cause vibration, enabling detection through acoustic monitoring techniques.

viii. **Electromagnetic Interference (EMI)**: PD generates electromagnetic waves that may interfere with nearby electronic equipment, posing a risk to the operation of sensitive devices.

ix. **Increased Maintenance Costs**: Continuous PD activity necessitates frequent inspections and preventive maintenance to avoid costly repairs and downtime.

x. **Risk of Catastrophic Failure**: If left unaddressed, PD can progress to complete insulation breakdown, leading to catastrophic equipment failure and potentially hazardous situations.

xi. **Reduced Equipment Lifespan**: The cumulative effects of PD significantly shorten the operational life of HV equipment, emphasizing the importance of early detection and intervention.

Table 1.1. Nature of insulations related to different types of PD

SL **NO**	**DISCHARGE TYPE**	**REMARKS**
1.	Low magnitude, short time	Insulation condition not bad
2.	Low magnitude, sustained	Moderate insulation, breakdown occurs after long time
3.	High magnitude, short time	Bad insulation
4.	High magnitude, sustained	Very bad, cannot be used as insulation purpose

In summary, effective monitoring and diagnostics, such as PD measurement and analysis, are critical for identifying the effects of PD in high-voltage systems. Early detection enables proactive maintenance, reduces the risk of equipment failure, and ensures the long-term reliability and safety of electrical power systems.

1.5. Need to Detect Partial Discharge

Detecting Partial Discharge (PD) in high-voltage systems is essential for ensuring the reliability, safety, and lifespan of electrical power infrastructure [18,25,26,28]. PD detection offers multiple benefits:

i. **Early Warning of Equipment Deterioration**: PDs are minor electrical discharges occurring within insulation materials of equipment like transformers, cables, and switchgear, often signaling more serious issues. Detecting PD early allows for timely maintenance, which helps avoid catastrophic failures and costly downtime.

ii. **Enhanced Equipment Reliability**: Identifying and addressing PD activity promptly extends the life of high-voltage equipment. This proactive approach reduces emergency repairs and replacements, cutting maintenance costs while ensuring a more reliable power supply.

iii. **Safety Assurance**: PD can lead to the release of gases and contaminants in equipment, which could pose hazards or indicate potential equipment failure. Early PD detection enhances safety for personnel and mitigates environmental risks from oil leaks or gas emissions.

iv. **Preventing Power Outages**: PD-induced failures can cause power outages that impact entire regions, leading to inconvenience and economic loss. Early detection helps prevent such disruptions and ensures stable energy delivery.

v. **Cost Savings**: Replacing or repairing high-voltage equipment is costly. PD detection allows for planned, efficient maintenance schedules, minimizing unexpected expenses and reducing reliance on emergency repair teams.

vi. **Electrical equipment Management**: PD detection aids in the effective management and reliability assessment of electrical equipment over the long term [18,19,25,26]. Condition monitoring using PD diagnosis helps identify early faults, enabling maintenance before equipment reaches critical failure.

vii. **Compliance with Standards**: Many international standards and regulations mandate regular PD testing in high-voltage systems for legal and operational reasons.

viii. **Environmental Impact**: Detecting PD helps mitigate environmental pollution by reducing the release of greenhouse gases, such as sulfur hexafluoride, and preventing contamination from oil leaks.

ix. **Diagnostic Significance**: PD measurements are vital for condition monitoring in high-voltage equipment, offering early identification of insulation defects, potential risks, and equipment condition. This diagnostic information supports informed maintenance decisions and risk management.

In inference, partial discharge (PD) detection is essential for the effective management of high-voltage equipment. Early identification of PD activity supports proactive maintenance, enhancing equipment reliability, safety, and longevity. Integrating PD diagnostics into condition monitoring allows utilities to mitigate environmental impact, comply with industry standards, and optimize asset performance, ultimately ensuring a more stable and cost-effective power infrastructure.

1.6. Classification of Partial Discharge

Partial discharges (PD) can be classified based on their occurrence location, discharge type, and behaviour relative to applied voltage. Understanding these classifications is vital for accurately diagnosing insulation defects and assessing the overall health of high-voltage equipment [11-15,28]. Key classifications include:

i. **Internal Partial Discharge**: Occurs within the bulk of insulation material, typically due to voids or air pockets embedded within the insulation. These discharges often signal material imperfections or degradation over time.

ii. **External Partial Discharge**: Occurs on the insulation's outer surface rather than within it, often due to contaminants, surface damage, or high humidity, which can cause localized breakdown on the insulation exterior.

iii. **Corona Discharge**: This low-level discharge arises in gaseous media around conductors, usually accompanied by a visible glow or corona effect. Corona discharge is common in high-voltage environments where sharp edges or points generate intense electric fields.

iv. **Surface Discharge**: Develops along the surface of insulation and is frequently linked to environmental contaminants or surface irregularities that weaken dielectric properties over time.

v. **Treeing Discharge**: Characterized by the formation of branching, tree-like degradation paths within or along the surface of the insulation material, treeing discharge is often a precursor to complete insulation failure.

vi. **Capacitive and Inductive PD**: Capacitive PD occurs in areas of high capacitance within the system, such as between transformer windings, while inductive PD occurs within inductive components, like the windings of transformers or inductors.

vii. **Radio Frequency Interference (RFI) PD**: Produces electromagnetic waves that can interfere with nearby communication systems and sensitive electronic devices, creating an additional operational challenge in industrial environments.

viii. **Free-Moving Particle Discharge**: Caused by the movement of conductive particles within the insulation, this type of discharge creates localized electric fields, typically in transformers or switchgear.

Additionally, PD can be categorized by the behaviour of discharge pulses relative to the phase of applied voltage:

i. **Phase-Resolved PD Pulse**: Analyzes PD pulses concerning the phase angle of the applied voltage, helping identify the discharge's location and type.

ii. **Periodic and Non-Periodic PD**: Periodic PD pulses occur at regular intervals, whereas non-periodic PD pulses appear irregularly, often indicating intermittent issues within the insulation.

Table 1.2. Some common classifications of different types of PD

SL NO	Internal Partial Discharge Occurs within the bulk of the insulation material.	External Partial Discharge External partial discharge specifically refers to discharges that happen on the outer surface of the insulation rather than within it.
1.	**Internal Void Discharge –** PD that occurs within voids or air pockets within the insulation material.	**Surface PD -** Takes place on the surface of the insulation.
2.	**Treeing Discharge -** PD associated with the development of "tree-like" degradation patterns within the insulation material.	**Corona Discharge -** Low-level PD that occurs in gaseous media around conductors, often characterized by a visible glow or corona.
3.	**Capacitive PD -** Occurs in capacitive components of the system, like between windings in a transformer.	**Surface Treeing Discharge:** PD associated with the development of "tree-like" degradation patterns in the surface of insulation material.
4.	**Inductive PD -** Occurs in inductive components, such as within the windings of an inductor or transformer	**Surface Tracking Discharge:** PD caused by the formation of conductive paths on the surface of insulating materials due to erosion or tracking.
5.	**Free-Moving Particle Discharge** PD caused by the movement of free particles within the insulation, creating localized electric fields.	**Radio Frequency Interference (RFI) PD:** PD that generates electromagnetic waves, leading to interference in communication systems.
According to PD pulse	**Phase-Resolved PD Pulse** Analysis of PD pulses with respect to the phase of the applied voltage, helping to identify the location and type of discharge. **Periodic PD:** Repeats at regular intervals. **Non-periodic PD:** Occurs irregularly.	**Pulse sequence** The sequences of three consecutive PD pulses are used to generate the PSA pattern related to their external test voltage and their phase angle within one period. **Periodic PD:** Repeats at regular intervals. **Non-periodic PD:** Occurs irregularly.

These classifications provide valuable insights into the nature of PD events and help in identifying the specific defects within the insulation system, thus guiding maintenance and risk assessment strategies.

1.7. PD Detection Methods

Various methodologies are employed to detect and quantify partial discharges (PD) in high-voltage systems. These techniques range from traditional electrical measurements to advanced sensing approaches [16,18,25,26,27,28], each offering unique insights into PD activity:

i. **Electrical Measurement Methods**: Electrical measurements involve using high-frequency current transformers, capacitive couplers, or voltage dividers to detect PD signals. Electrical methods conforming to the IEC 60270 Standard primarily capture discharge current impulses, with online and offline setups enabling versatile PD

ii. **Optical Detection Methods**: Optical sensors capture and analyze light emissions in the ultraviolet (UV), visible, or infrared (IR) spectra generated during PD events. This method utilizes photomultiplier tubes (PMTs), photodiodes, and infrared cameras to detect optical signals associated with PD.

iii. **Acoustic Detection Methods**: Acoustic sensors detect ultrasonic waves produced by PD events, typically in the frequency range of 20 kHz to 1 MHz. Piezoelectric acoustic sensors, mounted externally on equipment, capture sound waves associated with PD without interrupting power. Signal processing techniques help filter out noise and enhance PD signal detection.

iv. **Radio Frequency (RF) Detection Methods**: RF-based detection utilizes high-frequency current transformers (HFCTs) and antennas

to detect electromagnetic waves emitted by PD events. HFCTs are commonly placed on neutral or ground paths of HV equipment for PD detection, offering high-frequency response for real-time monitoring.

v. **Ultra-High Frequency (UHF) Detection Methods**: UHF-based methods capture PD signals within the range of 300 MHz to 3 GHz, reducing noise and enabling precise PD localization. UHF sensors are typically mounted on equipment via oil drain valves or dielectric windows, providing high sensitivity to PD events.

Each of these PD detection techniques provides unique advantages, and often a combination of methods is used for comprehensive monitoring. Online monitoring systems offer real-time insights, facilitating preventive maintenance and reducing equipment failure risks. Selecting the appropriate method depends on specific requirements, equipment characteristics, and desired sensitivity. The different techniques of PD detection methods are depicted in Figure. 1.1.

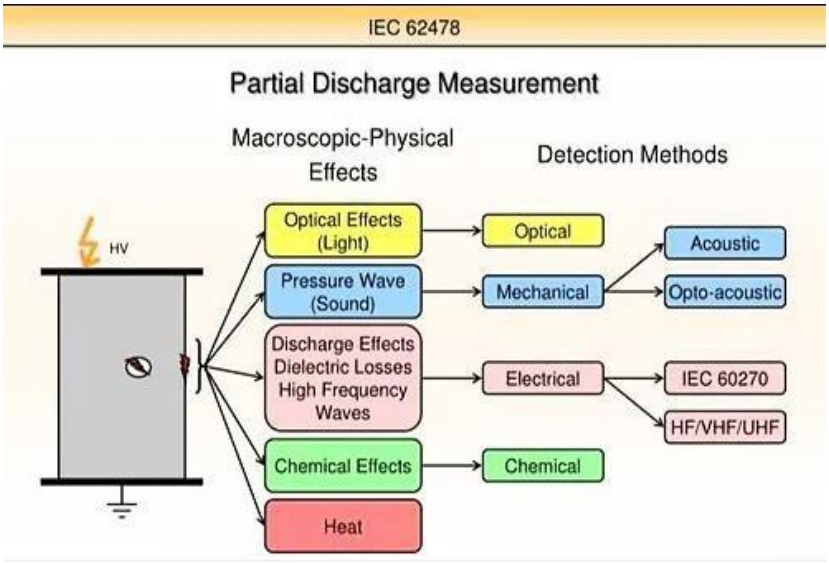

Figure. 1.1. Different types of Partial Discharge detection method.

While PD has numerous manifestations, there are accordingly several detection methods available to capture these varied activities. Among them,

some typical methods are going to be discussed below in the next sub-sections, each chosen based on specific requirements, equipment characteristics, and desired sensitivity.

1.7.1. Electrical Method

The electrical method is one of the most widely used techniques for detecting partial discharge (PD) in high-voltage systems. By measuring the electrical pulses generated during PD events, this method provides direct insight into the insulation condition and helps in identifying defects within high-voltage equipment. The approach relies on capturing high-frequency discharge currents, typically using components such as coupling capacitors, high-frequency current transformers (HFCTs), and impedance measuring devices. The electrical method, particularly under the IEC 60270 Standard, can be implemented in both online and offline setups. Offline detection enables detailed diagnostics in controlled environments, while online monitoring facilitates continuous PD tracking without the need to disrupt operations. Due to its accuracy and adaptability, the electrical method is commonly adopted in the power industry, enabling timely maintenance and reducing the risk of equipment failure across a range of high-voltage applications.

1.7.1.1. IEC 60270 Method

The IEC 60270 method is a standardized approach for detecting partial discharge (PD) activity in high-voltage systems [2-3]. This method employs electrical detection techniques to measure PD pulses generated within insulation or around conducting parts. Using high-frequency current transformers, capacitive couplers, and coupling capacitors, the IEC 60270 method captures discharge current impulses, providing a reliable framework for PD measurement.

The components of an IEC 60270-based PD detection system include:

i. **Coupling Capacitor**: Connects directly to the high-voltage line, allowing only the high-frequency PD signals to pass while blocking the power frequency. This capacitor is essential for isolating PD signals from background noise.

ii. **High-Frequency Current Transformer (HFCT)**: Positioned around conductors to detect PD pulses without direct contact. The HFCT converts the PD current into a measurable voltage signal.

iii. **Measuring Impedance**: Converts the PD pulses into measurable signals that can be processed and analyzed. It is typically designed to match the impedance of the measurement system for optimal accuracy.

iv. **Bandpass Filter**: Filters out low-frequency noise and power-frequency components, isolating the high-frequency PD signals for clearer detection.

v. **Amplifier**: Increases the signal strength of PD pulses, ensuring they are strong enough for accurate analysis and recording.

Adhering to the IEC 60270 Standard, this method allows for accurate PD assessment through these specialized components and circuits [shown in Figure. 1.2 and Figure. 1.3]. It can be applied in both online and offline monitoring setups. Offline systems enable comprehensive diagnostics in controlled environments, while online monitoring provides continuous PD tracking without interrupting normal operations. Due to its high sensitivity and ability to capture high-frequency discharge events, the IEC 60270 method remains a trusted choice for PD monitoring in various high-voltage applications.

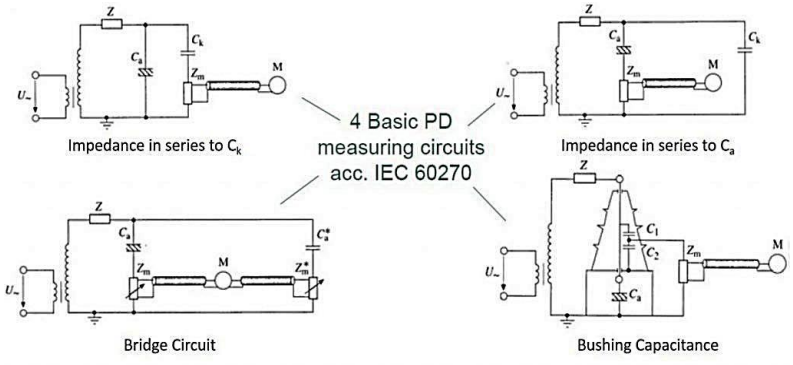

Figure. 1.2. Schematic of Electrical detection method of PD [2].

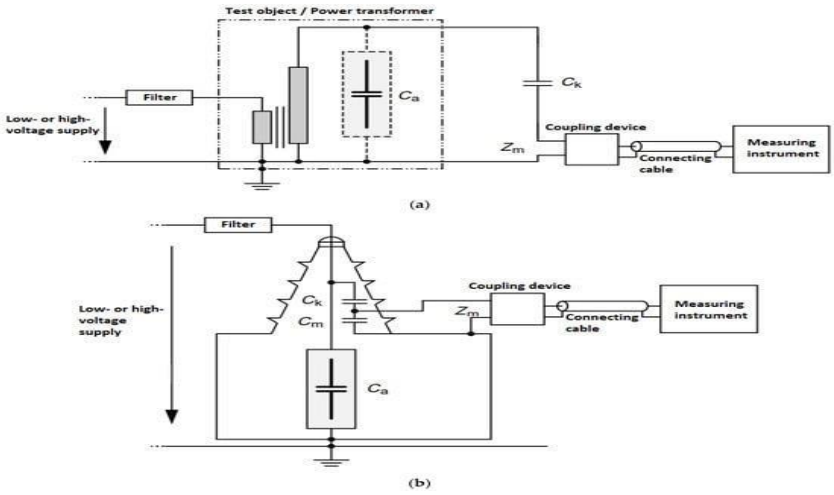

Figure 1.3. Schematic of Electrical detection method of PD (a) Laboratory method (b) on field method.

1.7.2. Acoustic Detection Methods

Acoustic detection methods identify partial discharge (PD) activity by capturing ultrasonic or acoustic signals generated during PD events. These methods are non-intrusive and rely on sensors to detect sound waves in the ultrasonic frequency range, typically between 20 kHz and 1 MHz. When PD occurs, it generates pressure waves that travel through the insulation material and surrounding medium [16,18,25.26,27]. By placing acoustic sensors on the equipment surface, these waves can be detected without interrupting system operations.

There are two primary acoustic detection approaches:

i. **Direct Acoustic Detection**: Involves placing piezoelectric sensors directly on the equipment surface, where they capture ultrasonic signals produced by PD [shown in Figure. 1.4]. These sensors convert the mechanical vibrations from PD into electrical signals, which are then processed for analysis. This method is particularly effective for PD localization, as the sound intensity decreases with distance, allowing for triangulation to pinpoint the PD source.

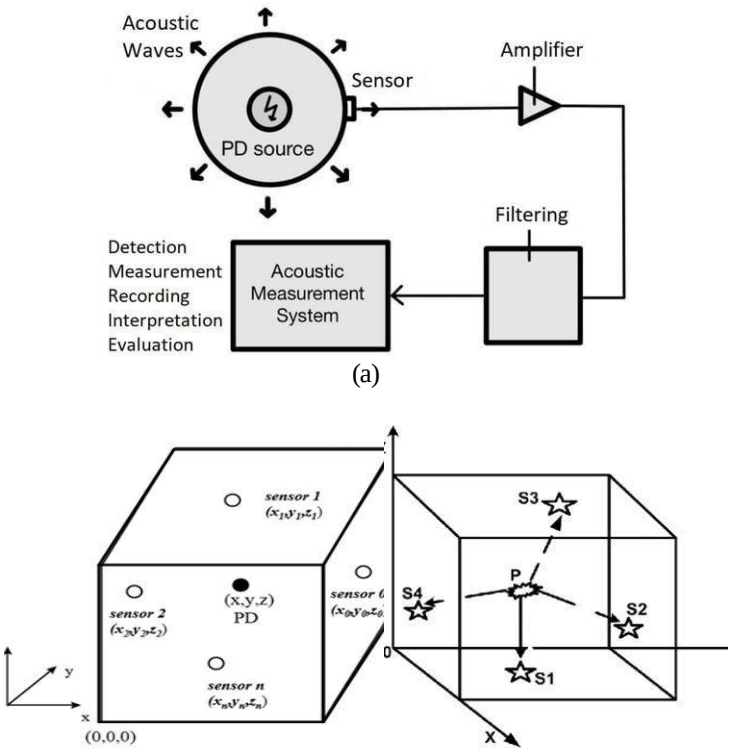

Figure. 1.4. (a) Schematic of acoustic detection method (b) placement of sensors according to 3D system

ii. **Ultrasonic Detection in Air**: This technique utilizes ultrasonic detectors to capture airborne ultrasonic signals emitted by PD activity [shown in Figure. 1.5]. Often used in open environments, ultrasonic detection is sensitive to surface discharges or corona effects and can be implemented using portable hand-held devices. This method is valuable for rapid inspections and preliminary PD assessments in accessible locations [37,38].

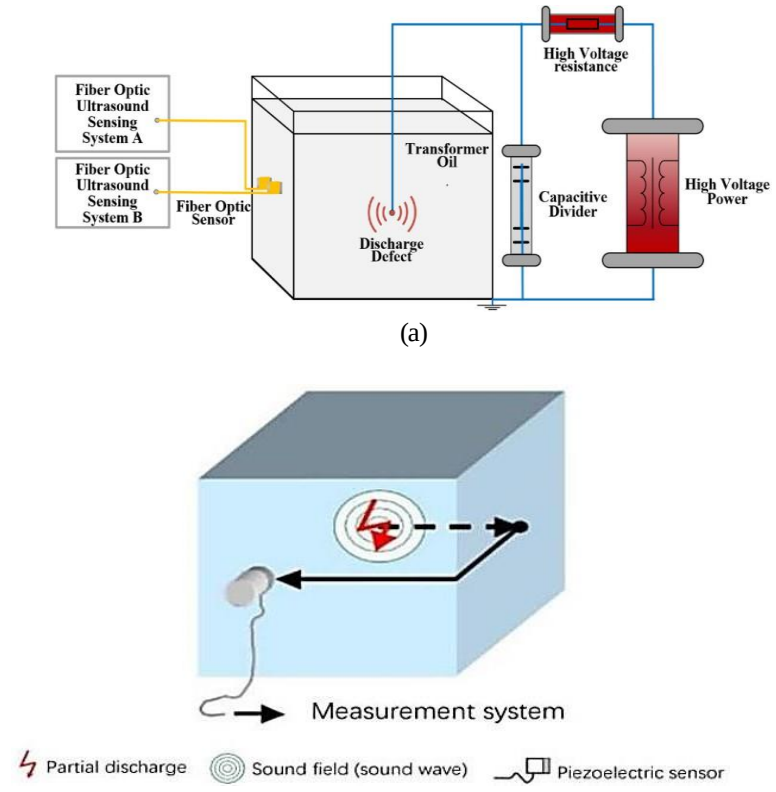

Figure. 1.5. (a) Schematic of Ultrasonic detection of PD Placement of sensor, (b) placement of Sensor.

Both approaches benefit from signal processing techniques, which help filter background noise and enhance the clarity of PD signals. Acoustic detection is widely applicable across different types of high-voltage equipment, as it enables real-time monitoring and early PD identification, reducing the risk of severe equipment damage [30-38].

1.7.3. Optical Detection Method

The optical detection method for partial discharge (PD) involves capturing and analyzing light emissions that occur during PD events [shown in Figure. 1.6]. When PD activity generates photons, particularly in the ultraviolet (UV), visible, or infrared (IR) spectra, these emissions can be detected using optical sensors. Photomultiplier tubes (PMTs), photodiodes, and infrared cameras are commonly employed to capture these light signals and analyze them for PD activity [16,18,25.26,27].

Optical detection is highly effective for identifying corona and surface discharges, especially in environments where electrical interference might affect other detection methods. By monitoring the intensity and location of light emissions, optical sensors can provide information on the severity and position of PD, facilitating accurate diagnostics. Since optical detection methods are non-intrusive, they are suitable for online monitoring, enabling continuous tracking without disrupting equipment operations.

This method is particularly useful in outdoor and high-voltage substation environments, where it can monitor exposed conductors and insulators. Despite its advantages, the optical method may be limited by environmental factors such as ambient light, which can interfere with accurate detection. Nevertheless, with appropriate filtering and shielding techniques, optical detection remains a valuable tool for identifying PD in critical power infrastructure [28,29].

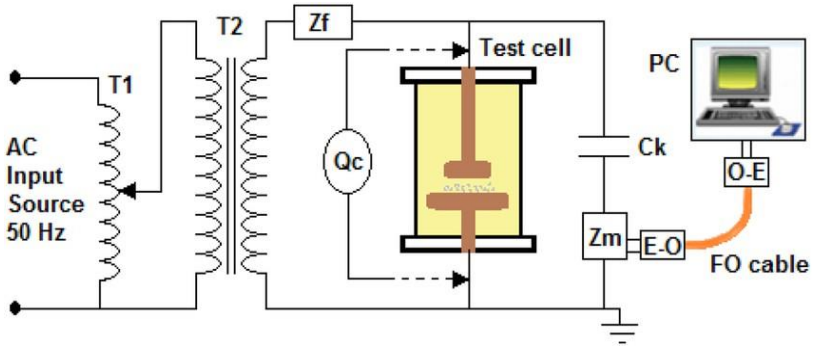

Figure. 1.6. Schematic of Optical detection method.

1.7.4. Radio Frequency Detection Method

The radio frequency (RF) detection method identifies partial discharge (PD) activity by capturing electromagnetic waves emitted during PD events [shown in Figure. 1.7]. When PD occurs, it generates high-frequency electromagnetic emissions within the RF range, typically the measurement frequencies range from MHz to several GHz (300 MHz to 3 GHz)[39-49]. RF detection systems, including UHF sensors, high-frequency current transformers (HFCTs) and antennas, are used to capture these emissions, providing a non-intrusive means of detecting PD activity [shown in Figure. 1.8]. UHF frequency range, typically above 300 MHz[44-49].
RF detection is particularly advantageous in scenarios where traditional electrical methods might be impractical, as it allows for real-time monitoring without requiring direct contact with high-voltage components. HFCTs [shown in Figure. 1.9 and Figure. 1.10] are often placed on grounding paths or conductors to capture PD signals, while antennas can be positioned externally to detect RF emissions in the surrounding environment [39-41].

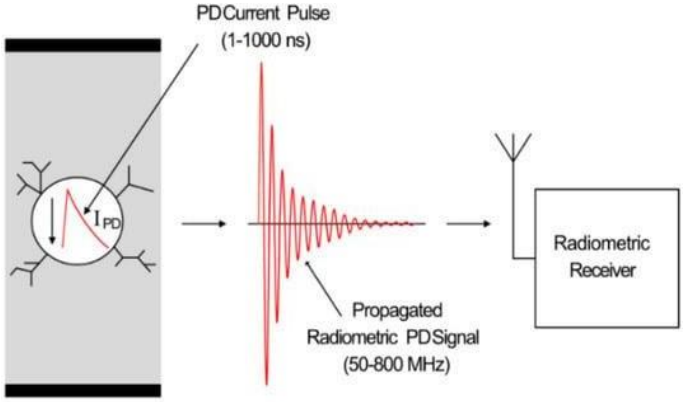

Figure. 1.7. Radio frequency (RF) detection method of PD.

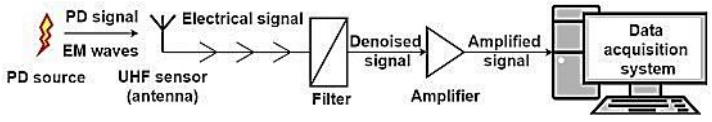

Figure. 1.8. Schematic of RF and UHF Detection.

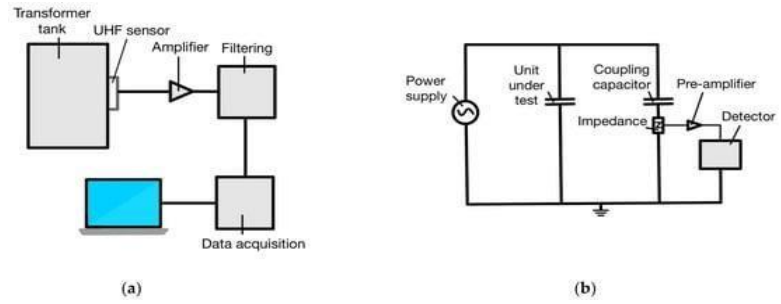

Figure. 1.9. (a) Block diagram of UHF based PD detection (b) schematic circuit.

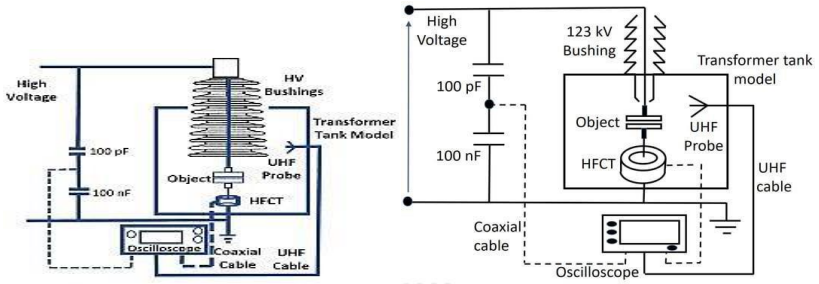

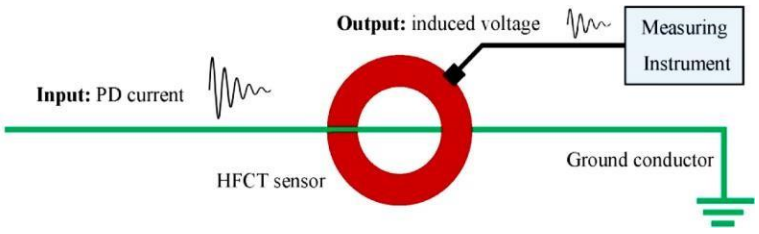

Figure. 1.10. Schematic of (a) UHF and (b) HFCT based on field PD detection with (c) HFCT sensor.

This method is effective for continuous online monitoring and provides valuable information for locating PD sources, as RF signals can be analyzed to triangulate the discharge location. However, RF detection is sensitive to

external electromagnetic interference, which can affect accuracy. Despite this, with appropriate filtering and shielding, RF detection remains a widely used technique for PD diagnosis, especially in environments where real-time, non-intrusive monitoring is crucial.

1.8. Measurement and Data Acquisition Technique of Partial Discharge

Partial discharge (PD) measurement and data acquisition techniques are essential for accurately identifying and analyzing PD events within high-voltage equipment. These techniques are designed to capture PD signals in real-time, enabling engineers to evaluate the insulation condition and predict potential equipment failures. Advanced measurement methods utilize various sensors and specialized circuits to acquire PD data across different domains, such as time, phase, and frequency. The data collected through these techniques provide comprehensive insights into PD characteristics, including the location, magnitude, and pattern of discharge activity. By capturing this information, PD measurement and acquisition systems support effective diagnostics, timely maintenance, and overall system reliability.

1.8.1. Partial Discharge Signal Analysis

Partial discharge signal analysis interprets the data captured during PD events to assess insulation performance and detect early signs of deterioration. Several analytical methods, including Phase Resolved Pulse Sequence Analysis (PRPS), Phase-Resolved Partial Discharge (PRPD), and Time-Resolved Partial Discharge (TRPD), provide insights into PD activity from different perspectives. These approaches analyze PD signals with respect to factors such as phase angle, pulse sequences, and timing, offering a detailed understanding of discharge behaviour. Additionally, software tools equipped with classification algorithms enhance the precision of PD diagnostics by categorizing PD patterns and supporting the identification of specific defect types. Through these signal analysis methods, utilities gain a clearer view of insulation condition, enabling predictive maintenance and minimizing risks of unexpected equipment failure.

1.8.1.1. Phase Resolved Pulse Sequence Analysis (PRPS)

Phase Resolved Pulse Sequence Analysis (PRPS) is a technique used to measure and analyses partial discharge (PD) signals, extracting

valuable information about their characteristics [11,13]. It involves examining the time-domain attributes of the pulses emitted during partial discharge events [shown in Figure. 1.11]. PD signals are captured using suitable measurement techniques such as high-frequency current transformers (HFCT), ultrasonic sensors, or optical sensors [15]. These signals are typically recorded as voltage or current waveforms, which are then pre-processed to eliminate noise that could impact the analysis. Filtering methods, including band-pass or high-pass filters, are often employed to isolate the PD pulses from other forms of interference. The PD pulses are subsequently identified and extracted from the pre-processed waveforms using various algorithms [63]. Techniques such as threshold-based methods, peak detection, or pattern recognition algorithms may be used to distinguish individual pulses. Once identified, the pulses are segmented into distinct events [50-58]. This segmentation process involves separating the pulses based on time and amplitude, ensuring each pulse is analyzed independently. Features related to time-domain and amplitude are then extracted from these segmented pulses. These features include parameters such as pulse duration, rise time, peak amplitude, pulse repetition rate, and pulse charge, which provide valuable insights into the characteristics of the PD events [50-58]. The extracted features are examined to reveal patterns and correlations within the pulse sequence. Statistical analysis, clustering algorithms, or pattern recognition techniques can be applied to identify specific patterns or classes of PD events. The analyzed pulse sequence data is interpreted to assess the severity, location, and type of partial discharge activity [50-58]. Comparisons with established databases or expert knowledge assist in diagnosing the condition of the electrical insulation or identifying potential faults. By analyzing the pulse sequence data over time, trends and changes in PD behaviour can be detected, allowing for the identification of early signs of insulation deterioration or fault progression.

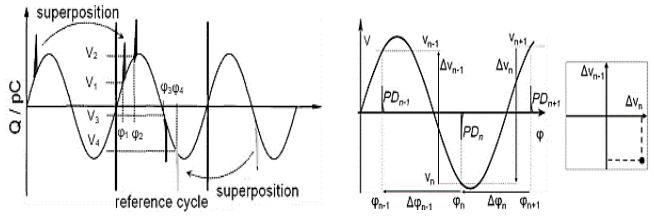

(a) (b)

Figure. 1.11. (a)Phase Resolved pulse sequence of Partial Discharge plot and (b) n-Δu pattern.

Pulse sequence analysis in partial discharge (PD) provides valuable insights into the characteristics and behaviour of partial discharge events. It aids in identifying specific PD patterns, classifying PD types, and evaluating the condition of insulation. This analytical technique is crucial for condition monitoring, making informed maintenance decisions, and ensuring the reliability and safety of electrical systems [55-58].

1.8.1.2. Phase-resolved partial discharge (PRPD)

Phase Resolved Partial Discharge (PRPD) analysis is a method utilized in partial discharge measurement and analysis to understand and scrutinize the characteristics of partial discharge events based on their occurrence within specific phases of the electrical signal [46,59]. It encompasses the segmentation and examination of partial discharge pulses concerning the phase of the voltage or current waveform. PD signals are captured using suitable measurement techniques such as high-frequency current transformers (HFCT), capacitive couplers, or other PD sensors. These PD signals are typically recorded as voltage or current waveforms, which are then pre-processed to eliminate noise and interference that may hinder the analysis [60]. Techniques like band-pass or high-pass filters are often employed to isolate the PD pulses and their corresponding phase components. The PD pulses are segmented based on their occurrence within specific phases of the electrical signal. The waveform is partitioned into distinct phases (e.g., phase A, phase B, phase C in three-phase systems), and each phase is scrutinized independently [61]. Within each phase, the PD pulses are detected and extracted using various algorithms. Techniques such as threshold-based methods, peak detection, or pattern recognition may be utilized to identify individual pulses within the designated phase. Diverse time-domain and amplitude-related features are then extracted from the segmented pulses within each phase, including parameters like pulse duration, rise time, peak amplitude, pulse repetition rate, and pulse charge [46,62]. These features furnish insights into the characteristics of the PD events within each phase. The extracted features are employed to construct a Phase-Resolved Partial Discharge (PRPD) plot. The PRPD plot is a two-dimensional scatter plot wherein the x-axis represents the phase angle of the electrical signal, while the y-axis signifies the pulse amplitude or another pertinent feature [shown in Figure. 1.12]. Each data point on the plot corresponds to a detected PD pulse within a specific phase [46,63]. The PRPD plot is analysed to identify patterns and correlations within the PD events transpiring in each phase. Specific patterns or clusters of PD events can be understood, offering insights into the type of PD activity or the state of the insulation system [64-66]. The

scrutinized PRPD plot is interpreted to evaluate the severity, location, and type of partial discharge activity within each phase. Comparisons with established databases or expert knowledge aid in diagnosing the condition of the electrical insulation or identifying potential faults.

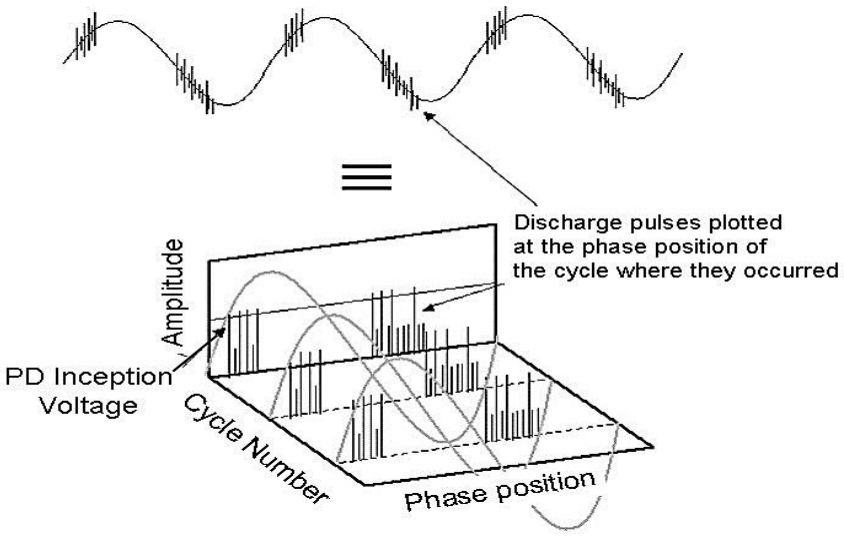

Figure. 1.12. Phase Resolved Partial Discharge plot.

Phase-resolved partial discharge analysis offers valuable insights into the occurrence and characteristics of partial discharge (PD) events within each phase of the electrical signal. It facilitates the identification of phase-related patterns, classification of PD types, and assessment of insulation condition on a per-phase basis [59-67]. This analytical technique plays a pivotal role in the detection and monitoring of partial discharge activity in electrical systems, particularly in three-phase power systems.

Partial discharge events resulting in current pulses below 1 MHz in the test object are captured using a coupling capacitor and measuring impedance. The PD signal is represented in both the time-domain and phase-domain to illustrate the features of the PD activity [2]. Phase-resolved PD (PRPD) and phase-resolved pulse sequence (PRPS) are two methods used to present the pattern of PD activities, demonstrating the relationship among discharge amplitude (q), cycle number (n), and phase position (φ). These methods were initially proposed in 1990 [7] and are primarily based on statistical features to illustrate unique patterns for different types of PD

defects. Three distinct types of PD patterns, namely surface discharge, void discharge, and corona discharge, can be identified based on the information from the φ-q-n representation, as established by previous contributions [3]. However, a significant limitation of PRPD and PRPS is their inability to differentiate between source types if multiple types of defects are involved. Additionally, overlaps in the phase domain information can adversely affect the performance of PD classification [46,55].

1.8.1.3. Time-Resolved Partial Discharge (TRPD)

Time-Resolved Partial Discharge (TRPD)

Time-Resolved Partial Discharge (TRPD) is an advanced technique used to analyze and characterize partial discharge events in high-voltage equipment. Unlike conventional partial discharge measurements, which focus on detecting the presence of partial discharges, TRPD provides detailed information about the temporal behaviour and characteristics of the discharge pulses over time [25-28,46]. This allows for a more in-depth analysis of the partial discharge phenomenon. In TRPD measurements, the partial discharge pulses are captured and recorded with high time resolution.

The measurement setup typically includes the following components:

i. **Sensor:** A sensor is used to detect the partial discharge pulses. Various types of sensors can be employed depending on the specific application, including high-frequency current transformers, capacitive sensors, or electromagnetic wave sensors. The sensor converts the partial discharge signals into electrical signals that can be measured and recorded.

ii. **Amplification and Conditioning:** The detected partial discharge signals are typically weak, so amplification and conditioning circuitry is used to enhance the signal-to-noise ratio and prepare the signals for further analysis. This may involve amplifiers, filters, and impedance matching networks.

iii. **Analog-to-Digital Converter (ADC):** The amplified and conditioned partial discharge signals are digitized using an ADC. The ADC converts the analog signals into digital format, allowing for digital processing and analysis.

iv. **Data Acquisition System:** A data acquisition system is used to capture and store the digitized partial discharge signals with high time resolution. This system typically consists of a fast sampling rate and sufficient memory capacity to capture and store the transient discharge pulses.

v. **Time Synchronization:** To ensure accurate temporal analysis, a time synchronization mechanism is employed to synchronize the data acquisition system with a reference time base. This allows precise alignment of the captured partial discharge pulses in time.

The time-resolved measurements have gained significant importance in the field of studying discharge mechanisms on different kinds of insulations. The availability of highly sensitive and large bandwidth RC type detectors for measuring partial discharge signals has made it possible to observe and analyse the shape characteristics of discharge pulses in both the time and frequency domains. Previously, due to the phase-shaping circuitry and low bandwidths of the detection system, it was not possible to preserve the shape of the electrical discharge pulse.

Furthermore, if the time constant of the detector is longer than the width of the discharge pulse, integration of the discharge pulse occurs, which is not a well-suited method for studying discharge mechanisms. The ultra-wideband or time-resolved system can be used to study the temporal behaviour of the discharge process in the nanoseconds range. With the development of ultra-wideband digital oscilloscopes having bandwidths up to several GHz, the true pulse shape can be preserved and can be further related to the physics of the discharge process.

When the partial discharge signal is recorded with the help of an Ultra-Wideband (UWB) detection circuit, several discharge parameters can be measured to describe the true shape of the PD pulse [shown in Figure. 1.13].

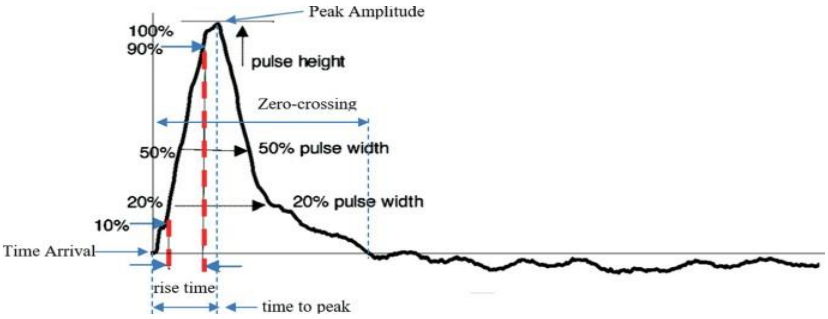

Figure. 1.13. Graphical representation of time resolved partial discharge parameters (Courtesy: Ahmed, Zeeshan. (2016). Analysis and De-Noising of Partial Discharge Signals in Medium Voltage XLPE Cables).

The discharge pulse shape parameters which are described below:

Rise Time: the time interval between 10% and 90% of PD pulse amplitude.
50% pulse width: it is the time interval between 50% PD pulse amplitude duringrise and fall of pulse.
20% pulse width: it is the time interval between 20% PD pulse amplitude duringrise and fall ofpulse.
Pulse height: The maximum PD pulse amplitude.

The recognition of partial discharge characteristics based on time-resolved parameters provides significant information regarding the physics of the discharge process. It has been observed that the shape of PD pulses changes significantly with prolonged insulation ageing. Discharge pulses with extremely short rise time and pulse width are observed during the initial phase of an electrical tree inside the insulation. These discharge pulses have characteristics like streamer-like discharge pulses.

After severe degradation of the insulation over a long period, the discharge pulses exhibit characteristics of very high-intensity discharge activity. The pulses are quite similar to pitting-type discharge pulses, indicating the formation of small pits across the discharge cavity. These discharge pulses have very small rise times and relatively smaller discharge pulse widths. The very fast rising front of the discharge pulse also indicates the presence of high-frequency energy content in the frequency spectrum. These discharge theories have been observed during the lifetime tests of insulation ageing and verified by the experimental results provided later in this study.

Once the TRPD signals are acquired, various analysis techniques can be applied to study the characteristics of the partial discharge events [25-28,55]. This includes analysing the pulse shape, magnitude, duration, repetition rate, and other parameters. Advanced signal processing methods, such as waveform analysis, statistical analysis, and pattern recognition algorithms, may be employed to extract relevant information and identify potential issues in high-voltage equipment. Time-Resolved Partial Discharge measurements provide valuable insights into the behaviour and nature of partial discharge events. They can be used for condition monitoring, diagnostics, and maintenance planning to ensure the reliable operation of high-voltage equipment and prevent potential failures.

1.8.1.4. Software Tool for Partial discharge signal analysis and Interpretation

1.8.1.4.1 Signal processing-based classifications

Signal processing-based classifications are instrumental in analyzing partial discharge (PD) signals, enabling the extraction of meaningful features that reveal underlying patterns in discharge activity. Techniques such as Wavelet Transform and Mathematical Morphology are commonly employed to process PD signals, enhancing their clarity and interpretability. The Wavelet Transform decomposes PD signals into different frequency components, allowing for the detection of transient features across multiple scales. Mathematical Morphology, on the other hand, applies shape-based filtering to analyze the structure of PD pulses, isolating essential details and removing noise. Together, these signal processing methods facilitate more precise PD classification, aiding in the diagnosis of insulation defects and contributing to reliable equipment maintenance.

1.8.1.4.1.1 Wavelet Transform

Wavelet Transform is a powerful signal processing technique that can be used for partial discharge (PD) signal analysis. It offers the ability to analyse signals in both the time and frequency domains simultaneously, making it suitable for detecting and characterising PD events [21]. The PD signal data is prepared by ensuring it is in a suitable format for the Wavelet Transform. This typically involves pre-processing steps such as noise removal, filtering, and normalisation to enhance the quality of the PD signals. The Wavelet Transform decomposes the PD signal into different frequency components at different scales. It achieves this by convolving the signal with wavelet functions, which are small, localised, and oscillatory functions. The result is a time-frequency representation of the PD signal, which provides information about the presence and characteristics of PD events. Different wavelet functions can be used for the Wavelet Transform, each with its own properties and suitability for PD analysis. Commonly used wavelets include the Haar wavelet, Daubechies wavelets, and Morlet wavelet [18]. The choice of wavelet depends on the specific characteristics of the PD signal and the analysis objectives [18]. The Wavelet Transform enables the extraction of various features from the decomposed PD signal. These features can include wavelet coefficients, energy distribution across different scales and frequencies, or statistical measures such as variance or entropy. The extracted features capture important information about the PD events and serve as

input for further analysis. The Wavelet Transform can also be used for de-noising and enhancing the PD signal. By thresholding or filtering certain wavelet coefficients, noise and unwanted components can be suppressed, enhancing the visibility and detection of PD events. The extracted features can be used for pattern recognition and classification of PD events. Machine learning algorithms such as Artificial Neural Networks (ANNs), Support Vector Machines (SVMs), or Random Forests can be trained on the wavelet-based features to classify PD events, determine their severity, or identify different types of PD [73]. The Wavelet Transform allows for visualising the time-frequency distribution of PD events, providing insights into their temporal and spectral characteristics. Time-frequency plots, scalograms, or spectrograms can be generated to facilitate the interpretation and analysis of PD signals [74].

Wavelet Transform-based methods offer the advantage of capturing both the time and frequency information of PD signals, allowing for more detailed analysis and detection of transient PD events. However, it is important to select an appropriate wavelet, choose suitable decomposition levels, and carefully interpret the results to avoid errors or misinterpretations. Additionally, feature selection and the choice of machine learning algorithms are crucial for accurate classification and interpretation of PD signals in the wavelet domain.

1.8.1.4.1.2 Mathematical Morphology

Mathematical morphology is a key technique in image and signal processing, focusing on the shape and structure of objects [18,127]. Applied to partial discharge (PD) signal analysis, it enhances the detection and characterization of PD events. Operations like erosion, dilation, opening, and closing modify signal shapes, improving feature detection and reducing noise [96,125,127,128]. For instance, morphological filtering can enhance the signal-to-noise ratio by minimizing interference. Gradient and edge detection operations highlight distinct PD event boundaries, facilitating their identification.

Mathematical morphology also aids in feature extraction, such as measuring the area, length, or shape of PD pulses, and in analysing the morphological characteristics like symmetry and elongation to classify PD types. Additionally, it helps in identifying clusters of PD events, indicating insulation defects or localized breakdowns, and in segmenting signals to isolate PD events from background noise [97,126,98,99]. Proper selection of

morphological operations and parameters is crucial for accurate PD signal analysis and interpretation of insulation defects.

1.8.1.4.2 Machine Learning

Machine learning develops algorithms that enable computers to learn from data and make predictions without explicit programming. In PD signal analysis, machine learning algorithms are trained on labelled data to identify patterns and characteristics of PD signals [18,97]. These algorithms classify, detect, or interpret PD signals based on features derived from time-domain, frequency-domain, or statistical analyses [98]. During training, the algorithm learns relationships between features and labels (e.g., healthy, or faulty) [99]. The trained model then classifies new, unlabelled PD signals. Model performance is evaluated using metrics like accuracy, precision, recall, and F1-score, with techniques such as cross-validation assessing generalization ability.

1.8.1.4.2.1 Artificial Neural Networks (ANNs)

Artificial Neural Networks (ANNs) are widely used for partial discharge (PD) analysis due to their capability to learn complex patterns in data [4,18,75]. The process begins with preparing PD signal data, including noise removal, normalization, and feature extraction from time-domain or frequency-domain analyses [5,76]. During training, ANNs use a structured dataset where signals are associated with outcomes like healthy or faulty. The network adjusts its parameters through backpropagation to minimize prediction errors [77]. After training, the ANN model classifies new, unlabeled PD signals. Model performance is evaluated with metrics such as accuracy, precision, recall, and F1-score, using techniques like cross-validation to avoid overfitting [78]. ANNs excel in detecting PD signal patterns and handling diverse features, making them effective for real-time PD monitoring and equipment assessment. However, sufficient, and representative training data are crucial, and overfitting can be mitigated with techniques like regularization [79]. ANN-based PD analysis has demonstrated effectiveness in equipment like transformers and cables, improving condition monitoring and maintenance strategies [80].

1.8.1.4.2.2 Support Vector Machines (SVMs)

Support Vector Machines (SVMs) are effective for partial discharge (PD) signal analysis due to their classification and regression capabilities [17,18]. To prepare PD signal data, relevant features are extracted using techniques such as statistical measures, frequency-domain analysis, or time-frequency analysis [88]. Feature selection can enhance SVM efficiency by reducing dimensionality [89]. SVMs train on labeled datasets where extracted features indicate PD presence, type, or severity. They use kernel functions to map the input space to a higher dimension for better data separation [90]. The choice of kernel (linear, polynomial, radial basis) depends on data characteristics, and model parameters like the regularization parameter (C) are fine-tuned through cross-validation [91]. Model performance is evaluated with metrics such as accuracy and precision, using cross-validation or test datasets [92]. Once trained, SVMs can predict PD events in real-time or analyze historical data. They excel in high-dimensional spaces but may struggle with large datasets or imbalanced classes. Careful feature selection and parameter optimization are crucial for accurate PD analysis.

1.8.1.4.2.3 Random Forest

Random Forest, a robust ensemble learning method, is effective for partial discharge (PD) signal analysis [18]. It combines multiple decision trees to improve prediction accuracy. To prepare PD signal data, features are extracted using techniques such as statistical, frequency-domain, or time-frequency analysis [24]. The Random Forest model is trained on a labeled dataset, where features represent PD characteristics and labels indicate the presence, type, or severity of PD. The algorithm builds multiple decision trees, each trained on a random subset of data, and makes predictions through voting [94]. For classification, the majority vote determines the final class; for regression, the average of predictions is used [18,24,95]. Feature selection and dimensionality reduction enhance model efficiency. Performance is evaluated using metrics like accuracy and precision, with cross-validation ensuring robustness [93-95]. Once trained, the model can classify new PD signals or assess historical data. Random Forest handles high-dimensional data well, is robust against overfitting, and provides insights into feature importance. However, careful feature selection, hyper-parameter tuning, and addressing class imbalance are essential for accurate results.

1.8.1.4.3 Deep Learning

Deep learning, a subset of machine learning, leverages neural networks with multiple layers to automatically learn data representations, showing promise in PD signal analysis [6,11,18,100]. Models like Convolutional Neural Networks (CNNs) and Recurrent Neural Networks (RNNs) effectively capture complex patterns in PD signals. These models consist of layers that process and pass data, learning hierarchical features from raw signals [101]. Trained using backpropagation, deep learning models adjust weights to improve prediction accuracy [102]. They often require large datasets but can benefit from end-to-end learning, which automates feature extraction, and transfer learning, which adapts pre-trained models to specific tasks with limited data. These techniques improve classification accuracy and interpret complex patterns, enhancing condition monitoring and maintenance strategies for electrical equipment [103].

1.8.1.4.3.1 Recurrent Neural Networks (RNNs)

Recurrent Neural Networks (RNNs) excel in analysing sequential data, making them suitable for partial discharge (PD) signal analysis [18,104]. They capture temporal dependencies by processing data segmented into time intervals or frames, creating input sequences of PD signal samples. RNNs often use Long Short-Term Memory (LSTM) or Gated Recurrent Unit (GRU) layers, which retain information over long sequences and effectively capture temporal patterns [105,106]. The model is trained with supervised learning, where input sequences are matched with labels (e.g., PD presence or severity) [107]. During training, RNNs learn to predict target values from these sequences, with hidden states encoding temporal patterns [108]. The trained model can perform classification (e.g., identifying PD types or severity) or regression (e.g., estimating PD intensity). Model performance is evaluated using metrics like accuracy, precision, recall, or mean squared error, with cross-validation or separate test datasets assessing generalization [109]. Post-validation, RNNs can predict PD events in real-time or analyze historical data, aiding maintenance, asset management, and risk assessment decisions. While RNNs capture temporal dynamics well, their performance depends on data quality, model architecture, and hyper-parameter tuning [120]. Proper pre-processing and optimization are crucial for accurate results.

1.8.1.4.3.2 Convolutional Neural Networks (CNNs)

Convolutional Neural Networks (CNNs) are highly effective for partial discharge (PD) signal analysis due to their capability to analyse grid-like data, such as images or spectrograms [13,18,110]. For PD analysis, PD signals are transformed into spectrograms—2D representations showing frequency content over time—which serve as input for the CNN model. The CNN architecture typically includes convolutional layers for feature extraction, pooling layers for dimensionality reduction, and fully connected layers for classification or regression tasks [111]. During training, CNNs use supervised learning with spectrograms as input and labels indicating PD presence or severity [112]. Convolutional layers detect various patterns, like pulse shapes or frequency components, while pooling layers simplify feature maps to retain essential information. Fully connected layers use these features for predicting PD characteristics [113]. The CNN model can perform classification tasks, such as detecting PD presence, identifying event types, or estimating severity. For regression, it estimates the magnitude or intensity of PD events.

Model performance is evaluated with metrics like accuracy, precision, recall, or mean squared error, using cross-validation or test datasets for generalization [121]. Once validated, CNNs can predict PD events in real-time or analyse historical data, aiding maintenance, and risk assessment. Despite their advantages in capturing local patterns, CNN performance can be affected by spectrogram quality, model architecture, and hyper-parameter tuning. Effective spectrogram generation, model design, and optimization are crucial for accurate PD signal analysis with CNNs [121].

1.8.1.4.3.3 Long short-term memory (LSTM) networks

Long Short-Term Memory (LSTM) networks, introduced by Hochreiter and Schmidhuber in 1997, are advanced Recurrent Neural Networks (RNNs) designed to handle sequential data and address limitations of traditional RNNs [114,115]. LSTMs excel in capturing long-term dependencies through a memory cell structure, which allows them to selectively retain or forget information over time. This is achieved via three main components: the input gate (regulates incoming information), the forget gate (controls discarded information), and the output gate (determines exposed information) [115]. LSTMs are trained using backpropagation through time, an extension of standard backpropagation, adjusting gates and memory cells to learn relevant

patterns [116]. This architecture effectively addresses the vanishing gradient problem—a common issue in RNNs where gradients diminish exponentially, hindering learning of long-range dependencies. LSTMs mitigate this with gating mechanisms that maintain gradient flow, enabling effective long-term learning.

LSTMs have demonstrated impressive performance across various domains, including natural language processing, time series analysis, and speech recognition [117]. In electrical systems, LSTMs and Bi-LSTM (Bidirectional LSTM) networks are promising for partial discharge detection due to their proficiency in handling sequential data and capturing temporal patterns [119,122]. The structure of Bi-LSTM is shown in Figure. 1.14.

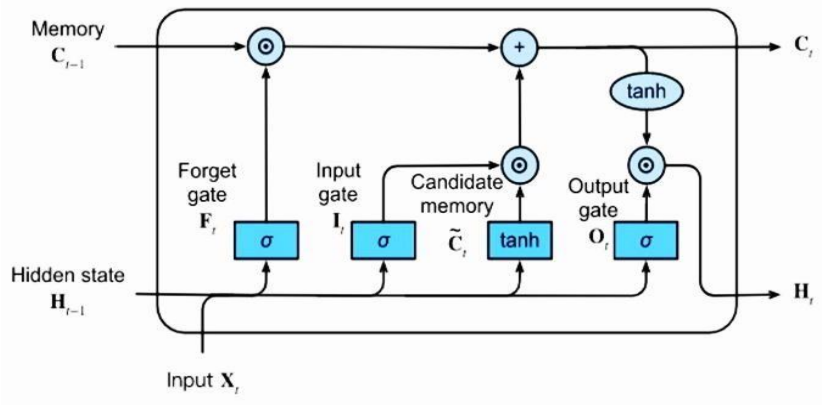

Figure. 1.14. Structure of Bi-LSTM Network.

1.9. Challenges

Despite advancements in partial discharge (PD) detection and analysis, several challenges continue to affect the accuracy, safety, and cost-effectiveness of PD monitoring in high-voltage systems. Addressing these challenges is critical for developing robust and reliable PD measurement and diagnostic systems that can operate effectively across various applications and environmental conditions.

1.9.1. Noise and Interference

One of the primary challenges in PD detection is the presence of noise and interference from external sources, such as switching transients, electromagnetic interference, and ambient noise. These unwanted signals can mask PD activity, making it difficult to distinguish true PD signals from background noise. Effective filtering and noise reduction techniques are essential to improve detection accuracy.

1.9.2. High Voltage and Safety Concerns

PD measurement often involves working with high-voltage equipment, which poses inherent safety risks to personnel and equipment. Ensuring safe measurement setups and employing proper isolation techniques are crucial to mitigate these risks. Additionally, robust equipment and protocols are required to handle high voltages safely during both online and offline monitoring.

1.9.3. Frequency Range of PD Signals

PD signals span a wide frequency range, from a few kHz to several GHz, depending on the type of insulation material and defect. Designing detection systems that can accurately capture this broad frequency range without losing signal fidelity is challenging. Selecting the appropriate sensors and measurement devices to cover the relevant frequency range is essential for effective PD analysis.

1.9.4. Detection Sensitivity

High detection sensitivity is required to identify weak PD signals, especially in the early stages of insulation degradation. However, increased sensitivity may also make the system more susceptible to noise and interference. Balancing sensitivity with noise immunity is a challenge that demands sophisticated signal processing and equipment calibration.

1.9.5. Transient Nature of PD

PD events are inherently transient and may occur sporadically, making continuous monitoring necessary to capture these brief occurrences.

Developing equipment capable of capturing transient PD signals in real-time without missing critical events is a technical challenge, particularly for online monitoring applications.

1.9.6. Environmental Conditions

Environmental factors, such as humidity, temperature, and pressure, can influence PD activity and affect measurement accuracy. These conditions can lead to variations in PD signals, requiring detection systems to be resilient to environmental fluctuations and to compensate for such effects in their analysis.

1.9.7. Compatibility with Different Insulation Materials

PD characteristics vary with insulation materials, such as oil, gas, solid, or polymeric insulations, each presenting unique PD signal profiles. Designing universal detection and diagnostic systems that are compatible across different materials and accurately interpret their PD signals remains a significant challenge in PD research and application.

1.9.8. Validation of Laboratory Findings in Practical Settings

Techniques that are effective in controlled laboratory conditions may face challenges when applied in real-world high-voltage environments. Validating the accuracy, reliability, and repeatability of PD measurement and analysis methods in practical settings is essential to ensure that laboratory findings can be translated to field applications.

1.9.9. Cost and Complexity of Equipment

High-quality PD detection equipment is often costly and complex, limiting its accessibility for widespread implementation, especially in older infrastructure. Balancing the need for sophisticated measurement systems with budget constraints remains a challenge for utilities and industries aiming to implement comprehensive PD monitoring.

1.9.10. Aging and Degradation Effects

Over time, aging and degradation of insulation materials can alter PD characteristics, complicating the interpretation of PD signals and potentially masking or mimicking other defects. Accurate PD assessment in aged equipment requires continuous calibration and updates to detection models to account for these changes.

1.10. Organisation of the thesis

Chapter 1 reviews the potential for advancing partial discharge (PD) detection using pulse sequence analysis, acoustic sensors, and optical sensors. The focus should be on combining these modalities to enhance detection accuracy. Develop signal processing algorithms with techniques like wavelet transform and machine learning. Explore fusion methods such as Kalman filters to integrate data for better PD localization. Design real-time monitoring systems for electrical insulation in applications like power transformers and high-voltage cables. Investigate optical fiber-based sensors, including Fiber Bragg gratings, for non-intrusive detection and explore remote sensing challenges. Contribute to standardized testing procedures and industry best practices for PD monitoring.

In Chapter 2, two experimental setups will be designed for accurate PD localization using optical and acoustic sensors. The optical setup will simulate single and multiple PD events in an air-insulated steel tank with five sensors placed on the tank's wall. The acoustic setup will emulate PD events in an oil-filled cubical tank using five sensors to capture sound waves emitted by the PD sources.

In Chapter 3, a novel method for automated defect identification in insulation systems based on PD measurements will be proposed. PD pulse sequences from three artificial faults will be recorded and represented in PRPS format. These patterns will be analysed using MM and novel morphological features, which will be fed to a Bi-LSTM network for accurate PD defect classification. This method outperforms other deep learning frameworks and is suitable for real-time defect detection.

In Chapter 4, an innovative framework using acoustic sensors installed on the outside wall of power equipment will be introduced. The acoustic data, reflecting PD source locations and numbers, will be analysed in the time-frequency space. This information will be processed using transfer learning and classification modules for accurate PD localization in real-life applications.

In Chapter 5, an automated framework using a multi-channel fusion hybrid MFCNN-BiLSTM deep network will be proposed for identifying and localizing PD events with data from five optical sensors. The framework will leverage PD signatures for accurate type and location detection, with 1-D LBP enhancing classification accuracy.

In Chapter 6, the conclusions and future scope of the thesis have been discussed. This chapter has provided valuable insights into PD detection and measurement techniques, highlighting the importance of continued research and development and a comprehensive investigation into pulse sequence analysis, optical, and acoustic sensor-based PD detection techniques, providing valuable insights and paving the way for future advancements in this field. By advancing our understanding of PD phenomena and exploring innovative sensing technologies, we can mitigate the risks associated with insulation degradation, minimize downtime, and enhance the reliability of electrical systems. Future research directions may include further optimization of sensor performance, validation of techniques in real-world operating conditions, and the development of advanced data analytics methodologies for predictive maintenance applications.

1.11. Originality of the thesis

- The originality of the thesis based on "Pulse Sequence Analysis, Optical, and Acoustic Sensor-Based Partial Discharge Detection" is highlighted by its innovative integration of pulse sequence analysis with optical and acoustic sensors. This method offers significant advantages over single-sensor approaches by providing complementary data and enhancing detection accuracy.

- This thesis makes substantial contributions by developing advanced algorithms that incorporate machine learning, pattern recognition, and statistical signal processing to effectively analyze sensor data.

- The application of these proposed techniques adds unique value to the condition monitoring of high-voltage systems, health assessment of electrical insulation, and predictive maintenance. The credibility of this advanced technique is reinforced through validation via laboratory experiments, field trials, and comparisons with existing methods.

- Additionally, the thesis introduces novel sensors with improved sensitivity and cost-effectiveness, fostering innovation by bridging disciplines such as electrical engineering, signal processing, photonics, and acoustics. Addressing practical challenges like sensor placement, environmental noise, and real-time processing further underscores the thesis's significance in advancing partial discharge detection.

Chapter 2

2.1 Introduction

This chapter presents the comprehensive experimental setup and methodology for detecting Partial Discharges (PD) using both optical and acoustic techniques. Partial Discharge (PD) detection is crucial in assessing the health and reliability of high-voltage equipment. Three experimental approaches are elaborated upon: Electrical, Acoustic and Optical Partial Discharge Detection.

For Electrical detection of Partial Discharges (PD) is based on capturing signals generated during discharge events, which provides a non-intrusive means of monitoring PD activity within high-voltage equipment. This section describes the experimental framework for Electrical PD detection, including the preparation of the Electrical Partial Discharge Source (EPDS), Electrode arrangement, and data acquisition methodology

For Acoustic PD Detection, an Acoustic Partial Discharge Source (APDS) is employed. This source is tested within the PDLE using acoustic sensors to capture and analyze sound waves emitted by the discharge events. The acoustic detection framework simulates realistic conditions by employing an oil-filled tank to mimic transformer-like environments.

Similarly, Optical PD Detection, a specially designed Optical Partial Discharge Source (OPDS) is prepared and tested within a custom-built Partial Discharge Location Emulator (PDLE). The PDLE, a controlled environment resembling high-voltage equipment enclosures, ensures accurate detection and localization of PD sources using strategically placed optical sensors.

Each section of this chapter provides detailed descriptions of the experimental setup, including the electrode configurations, sensor arrangements, and procedures for data acquisition. The results contribute to developing robust methodologies for localizing PD events and understanding their characteristics.

2.2 Partial Discharge Laboratory

Partial Discharge (PD) measurements are highly susceptible to electromagnetic interference (EMI), as the frequency ranges of

communication signals and other radio-frequency devices overlap with those of PD signals. To ensure accurate data collection, the Partial Discharge Laboratory is designed to minimize EMI and provide a controlled environment for experimentation.

At Jadavpur University, a dedicated double-shielded laboratory has been established specifically for PD detection. This laboratory consists of two enclosures:

Outer Enclosure: The primary structure is fully shielded with copper plates welded together to block external electromagnetic waves effectively.

Inner Enclosure: Inside the copper shielding, a secondary enclosure is constructed using galvanized iron (GI) sheets. This double-layer design significantly reduces EMI, ensuring the integrity of PD measurements.

The laboratory dimensions are approximately 7.5 m x 4 m x 6 m for the outer enclosure and 3.9 m x 3.75 m x 3 m for the inner enclosure. This setup allows the PD laboratory to maintain a noise-free environment necessary for precise data acquisition.

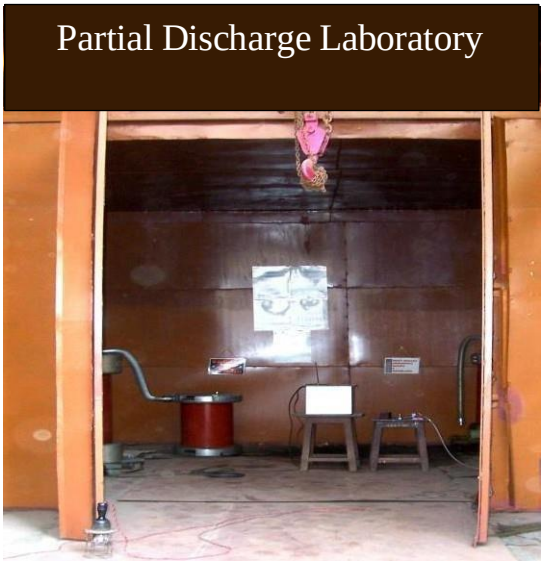

Figure. 2.1. Photograph of the Partial Discharge Testing laboratory at Jadavpur University.

The Partial Discharge Laboratory (Figure.2.1) is equipped with high-voltage transformers, coupling capacitors, damping resistors, and measurement

terminals to simulate real-world high-voltage equipment. Additional care is taken to ensure that all test equipment is free from inherent PD activity before the experiments begin.

This controlled environment forms the foundation for reliable testing of both optical and acoustic PD detection methodologies, supporting the subsequent experiments described in this chapter.

2.3 Conventional Electrical Detection

Electrical detection, also known as conventional detection, is a widely used method for identifying and analyzing partial discharges (PD) in high-voltage insulation systems. This method relies on capturing electrical signals generated by PD activity and is crucial for diagnosing insulation health. The technique involves using high-voltage electrodes, coupling capacitors, and detection impedances to measure PD pulses. These pulses are then analyzed to determine the nature, intensity, and location of the discharge. Conventional detection is highly effective in laboratory settings and controlled environments, allowing researchers to accurately assess insulation degradation and predict failures.

2.3.1 Preparation of Electrical Partial Discharge Source (EPDS) for Experiment

The preparation of the Electrical Partial Discharge Source (EPDS) involves creating a standard dielectric sample sandwiched between two electrodes. The shape and position of the electrodes are adjusted based on the type of partial discharge being investigated. A high-voltage transformer applies the necessary voltage to one electrode, while the other electrode is grounded. The coupling capacitor, connected through an appropriate impedance, is used to collect the discharge signals. This setup ensures reliable data acquisition by maintaining a consistent and repeatable discharge environment. The dielectric material used in the EPDS plays a significant role in determining the type and characteristics of partial discharge that will be observed during the experiment.

2.3.2. Electrode Configuration

The EPDS incorporates a pair of brass electrodes to generate partial discharges. The high-voltage (HV) electrode is suspended and is connected to an external high-voltage source. The ground electrode is placed at the base of the chamber, ensuring a well-defined electric field distribution.
The electrode surfaces are polished to maintain consistent discharge characteristics and minimize unwanted noise in the recorded electrical signals.
The electrode configuration and arrangement are crucial for generating and detecting different types of partial discharges. The following configurations are commonly employed:

2.3.2.1 Corona Discharge:

A pointed electrode is placed in air with an air gap between the dielectric material. When high voltage is applied, ionization occurs at the sharp tip, leading to corona discharge.

2.3.2.2 Surface Discharge:

A cylindrical electrode is positioned to make contact with the surface of the dielectric. This arrangement simulates surface discharges, which occur due to imperfections or contaminants on the dielectric surface.

2.3.2.3 Internal Discharge:

Both electrodes are in direct contact with the dielectric, with an intentional internal void present. When voltage stress is applied, discharges occur within the void, mimicking real-world insulation defects.
Each of these configurations allows researchers to study specific types of PD, helping in the assessment of insulation performance and degradation over time.

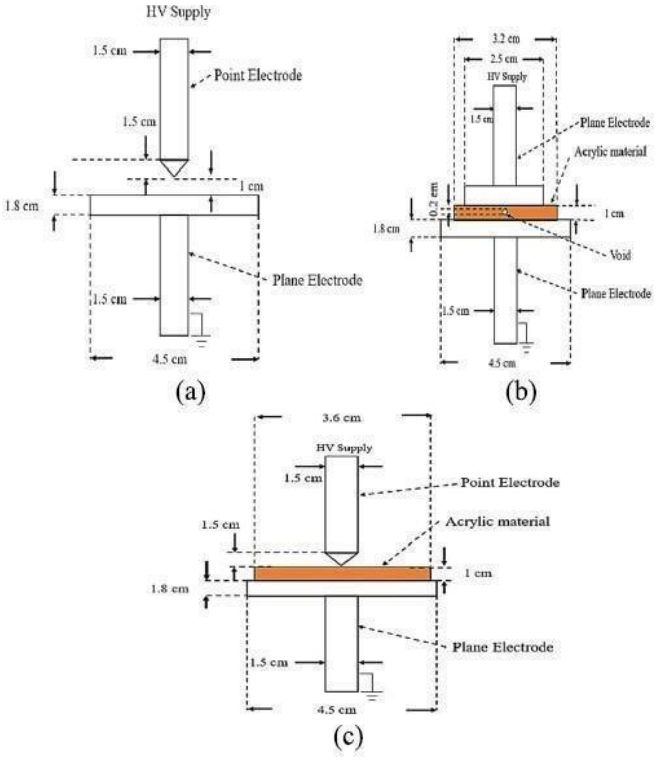

Figure.2.2. Electrode arrangement for PD measurement for (a) corona discharge, (b) internal discharge, and (c) surface discharge.

In Figure2.2, the electrode arrangement for PD measurement of three PD defects, i.e., corona discharge, surface discharge, and internal discharges are shown. The electrodes were made of brass. The dimensions of the electrode and the insulation specimen are shown in the Figure.2.2.

2.3.3 Experimental Setup for Electrical Detection

The experimental setup for electrical detection of Partial Discharges (PD) integrates the Electrical Partial Discharge Source (EPDS), the Partial Discharge Location Emulator (PDLE) and measuring instruments to create a controlled environment for studying PD-induced electrical signal emissions.

This setup ensures reliable data acquisition and facilitates precise localization of PD events.

2.3.3.1 Key Components of the Setup

The high-voltage system includes a 0.23/50 kV, 10 kVA testing transformer, providing the required excitation voltage. A variable autotransformer regulates the input voltage, allowing controlled voltage ramping for PD initiation. The setup has also coupling capacitor, capacitive potential divider and parallel combination of inductor with damping resistor for appropriate detection and measurement of discharge signals.

2.3.3.2 Assembly of the Setup

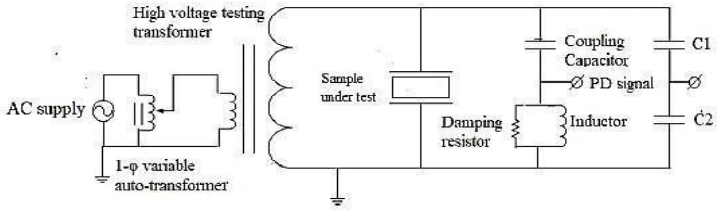

Figure.2.3 Schematic diagram of PD measurement

The experimental setup for electrical detection involves assembling the high-voltage system, coupling capacitor, detection impedance, and data acquisition system. The setup is depicted in Figure.2.3, which illustrates the connections and measurement points. The experimental arrangement is designed to isolate and capture partial discharge signals effectively, minimizing external noise and interference. This setup enables precise measurement of PD characteristics, including magnitude, frequency, and occurrence patterns, which are crucial for insulation diagnostics.

2.3.3.3 Experimental Procedure

For PD measurement, high voltage was applied across the test sample via a 0.23/50 kV, 10 KV. A high voltage test transformer, the primary of which is connected to an autotransformer. The primary of the test transformer is grounded to allow the flow of third-harmonic currents, so that there is no distortion in the applied voltage. Before the start of the experiment, investigation was done to ensure that the test equipment was PD free.

Thereafter, the voltage is increased in steps of 1 kV till PD inception voltage is obtained. Once the PD inception is attained, the high-frequency PD pulses appear across the test object via a coupling capacitor. The damping resistor was used to avoid the sustained oscillation of the PD pulses across the inductor as the PD pulses appear across the inductor. Since the inductor offers high impedance to the high frequency PD pulses, the PD pulses appear across the measuring terminal (as shown PD signal terminal in Figure2.3) via coupling capacitor as the latter provides low impedance to the PD signals. Capacitors C1 and C2 serve as the potential divider for the applied high voltage at power frequency. Capacitor C2 in the low voltage side acts as phase reference of the PD pulses. In this work, the PD measurement has been performed for three different PD defects like corona, surface, and internal discharges.

2.3.4 Recorded Electrical Partial Discharge Data

The recorded electrical partial discharge data will be presented in graphical format, illustrating the discharge patterns observed during the experiment. Figure2.5 is given to showcase the captured PD signals and variations under different conditions. A more detailed discussion will be provided in Chapter 3. This data forms the foundation for further analysis, helping to understand the behaviour of different discharge types and their implications on insulation performance.

2.3.4.1 Data Recording Methodology

PD data acquisition by Pulse Sequence Analysis (PSA) is basically the differences in voltage magnitude between two successive PD pulses are considered as Δu features (Figure.2.4)

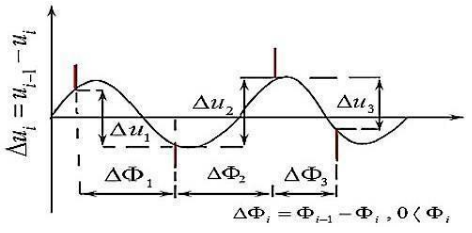

Figure. 2.4. PSA data acquisition

2.3.4.2 Key Observations

The Δu features are important parameters to analyze the PSA for data acquisition, PD pulses are kept in phase-resolved pulse sequence (PRPS) format. These data are synchronized with power frequency cycle during the entire data acquisition period and are never overlapped on a single cycle. In this way, Δu features can be obtained from consecutive PD pulses, which provide key information regarding the type of discharge, i.e., the nature of defect within the insulation system. From the Δu feature, a specific pattern known as the $n-\Delta u$ pattern (variation of n versus Δu , with n being the number of occurrence of pulses) can be obtained which bears close correlation with the change in space and surface charges, which remain at the discharge site. The presence of residual charges can directly influence the generation of PD pulse sequences which lead to memory effect during PD activities.

2.3.4.3 Visualization and Data Interpretation

In this work, PSA has been examined to identify defects inside a solid insulation based on the nature of deviation of $n-\Delta u$ pattern. The PD data have been recorded in PRPS format as reported in section 1.8.1.1. The, Δu parameter from consecutive pulses have been extracted to analyze each category of PD data. Then, the variation of $n-\Delta u$ sequence is plotted for each type of defect (Figure.2.5).

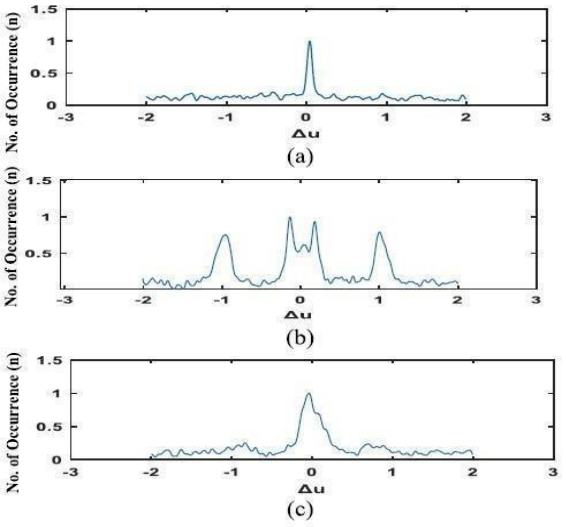

Figure.2.5. Normalized Δu pattern for (a) "corona discharge", (b) "internal discharge" and (c) "surface discharge".

Table.2.1. Classification of PD defects

PD defect event	Class	PD defect type
Corona	PD1	Single
Surface discharge	PD2	Single
Internal discharge	PD3	Single

2.3.4.4 Significance of Recorded Electrical PD Data

The graphical representation of recorded electrical PD data by PSA technique as $n - \Delta u$ pattern for corona discharge, internal discharge, and surface discharge has been shown in Figure2.5(a-c), where the magnitude of Δu feature have been varied from −2 up to +2 in the X-axis, whereas on the Y - axis, corresponding frequency of occurrences "n" is displayed. Here, "n" has been normalized between the values 0 and 1. The detailed description of the defects has been reported in Table.2.1

2.4 Acoustic Detection

Acoustic detection of Partial Discharges (PD) is based on capturing ultrasonic signals generated during discharge events. Unlike optical detection, which relies on light emissions, acoustic detection provides a non-intrusive means of monitoring PD activity within high-voltage equipment. This section describes the experimental framework for acoustic PD detection, including the preparation of the Acoustic Partial Discharge Source (APDS), sensor placement, and data acquisition methodology.

The acoustic detection setup follows a structured approach to ensure precise PD localization. The Acoustic Partial Discharge Source (APDS) is positioned within a controlled environment inside the Partial Discharge Location Emulator (PDLE). The enclosure is designed to isolate external noise and maintain a consistent medium for sound propagation. Acoustic sensors are strategically placed to capture pressure variations caused by PD events, enabling signal analysis and localization.

The experimental framework consists of multiple sub-sections. Section 2.4.1 describes the preparation of the APDS, including the materials and electrode configuration used to generate stable acoustic PD signals. Section 2.4.2 details the electrode configuration and arrangement, ensuring optimal discharge conditions for generating acoustic waves. Section 2.4.3 focuses on the PDLE setup for acoustic detection, ensuring an isolated and controlled test environment. Section 2.4.4 explains the placement of the APDS within the PDLE, maintaining consistency in experimental conditions. Section 2.4.5 describes the acoustic sensor arrangement inside the PDLE, ensuring uniform coverage and avoiding blind spots. Section 2.4.6 outlines the experimental setup, detailing the signal processing techniques used to capture and analyse acoustic PD data. Section 2.4.7 presents the recorded acoustic PD data, highlighting key observations and signal characteristics. Section 2.4.8 provides a database description, compiling structured data for future analysis and validation of acoustic PD detection techniques.

2.4.1 Preparation of Acoustic Partial Discharge Source (APDS) for Experiment

The Acoustic Partial Discharge Source (APDS) is designed to simulate real-world PD events and generate stable acoustic signals for detection and analysis. The APDS setup ensures a controlled and repeatable discharge environment, facilitating accurate data acquisition for acoustic PD

localization. This section details the preparation of the APDS, including material selection, electrode configuration, and discharge characteristics.

2.4.1.1 Material Selection and Design

The APDS consists of a specially fabricated oil-filled chamber, designed to enhance acoustic wave propagation and minimize signal attenuation. The chamber is constructed from an acrylic cylinder, which provides electrical insulation while allowing uniform acoustic transmission. Transformer oil is used as the dielectric medium, mimicking the insulation environment of high-voltage power transformers.

A void or defect is intentionally introduced within the dielectric medium to simulate real-world insulation failures that lead to partial discharges. The void is created using a thin gas-filled cavity, which ensures consistent PD generation when subjected to high voltage. The size and placement of the void are carefully controlled to maintain reproducibility in discharge events.

2.4.1.2 Electrode Configuration

The APDS incorporates a pair of brass electrodes to generate partial discharges. The high-voltage (HV) electrode is suspended inside the oil-filled chamber and is connected to an external high-voltage source. The ground electrode is placed at the base of the chamber, ensuring a well-defined electric field distribution. The chamber or tank with electrode arrangement has been depicted in Figure.2.6.

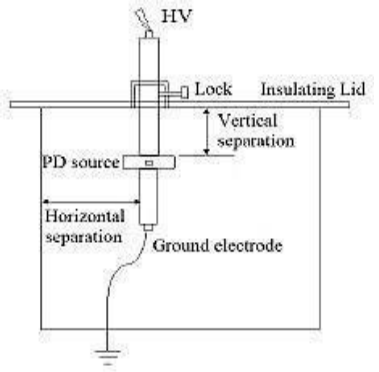

Figure. 2.6. Stainless steel tank with electrode arrangement.

To achieve a concentrated PD event, the electrode gap is optimized based on the dielectric strength of the oil and the expected inception voltage. The spacing between the electrodes is calibrated to initiate discharges at controlled voltage levels, typically around 7 kV. The electrode surfaces are polished to maintain consistent discharge characteristics and minimize unwanted noise in the recorded acoustic signals.

2.4.1.3 Acoustic Wave Generation and Propagation

Partial discharge events occurring within the void produce ultrasonic pressure waves that propagate through the oil medium. These waves travel outward from the discharge source and interact with the chamber walls before being detected by acoustic sensors. The characteristics of the emitted sound waves depend on factors such as discharge intensity, void size, and electrode configuration.

The oil-filled environment significantly enhances the propagation of ultrasonic waves, allowing high-frequency components to be captured with minimal signal distortion. This ensures that the recorded acoustic signals retain the essential features required for PD localization.

2.4.1.4 Ensuring Stability and Reproducibility

To maintain consistency across experiments, the APDS undergoes a validation process before data collection. This includes verifying the stability of the discharge source, calibrating the electrode spacing, and ensuring the dielectric properties of the transformer oil remain constant. The void geometry is inspected periodically to prevent variations that could affect acoustic signal characteristics.

The prepared APDS forms the core of the acoustic detection experiment, providing a reliable and reproducible source for studying PD behaviour in an oil-insulated system. The subsequent sections describe the experimental setup and sensor arrangements required for capturing and analysing the generated acoustic PD signals.

2.4.2 Partial Discharge Location Emulator (PDLE) for Acoustic Detection

The Partial Discharge Location Emulator (PDLE) for acoustic detection is specifically designed to simulate high-voltage environments and facilitate accurate localization of Partial Discharge (PD) events through acoustic wave propagation. Unlike the optical detection setup, the acoustic PDLE

incorporates an oil-filled tank [shown in Figure. 2.7], which serves as a controlled medium for ultrasonic wave transmission, ensuring consistent and repeatable experimental conditions.

Figure. 2.7. Actual photograph of PDLE.

2.4.2.1 Design and Structure

The PDLE for acoustic detection consists of a stainless-steel tank, approximately 40 cm in height and 32 cm in length and width, with a sealed acrylic window to allow optical inspection. The tank is filled with transformer oil, which provides a uniform acoustic medium and mimics real-world insulation conditions found in high-voltage transformers.
The top lid of the PDLE is designed to accommodate high-voltage (HV) electrode placement through a precision-sealed opening that prevents external contamination of the oil. The ground electrode is located at the base of the tank, ensuring a stable reference potential for PD generation.
The acoustic sensors are mounted on the inner walls of the tank, positioned to optimize wave capture and minimize reflections. The tank walls are acoustically treated to reduce unwanted reflections and ensure the captured signals originate primarily from the PD source rather than external noise or reverberations.

2.4.2.2 Simulated PD Source Placement

To standardize PD localization, a three-dimensional coordinate grid is defined within the PDLE. The Acoustic Partial Discharge Source (APDS) is positioned at predefined locations within this grid, ensuring consistency in data collection. The grid system provides multiple PD source positions,

allowing systematic analysis of PD localization across different spatial arrangements.

For single-source experiments, the APDS is placed at a central location within the tank, ensuring symmetrical wave propagation. For multiple-source experiments, additional APDS units are introduced at different grid positions, simulating complex PD interactions commonly observed in high-voltage equipment.

The Partial Discharge Location Emulator (PDLE box) (discussed in section) has been employed for the acoustic PD detection approach as shown in Figure. 2.7. The internal space of the box is divided uniformly with the use of a fictional grid to identify the 27 identical cubical places (numbered 1 through 27) inside the box, as illustrated in Figure. 2.8. Figure .2.6 illustrates the arrangement of electrodes. As seen in Figure. 2.8, the discharge source is maintained at 27 distinct cubical locations in a manufactured grid within the PDLE in order to accomplish the experimental results. The spots are numbered from 1 to 27.

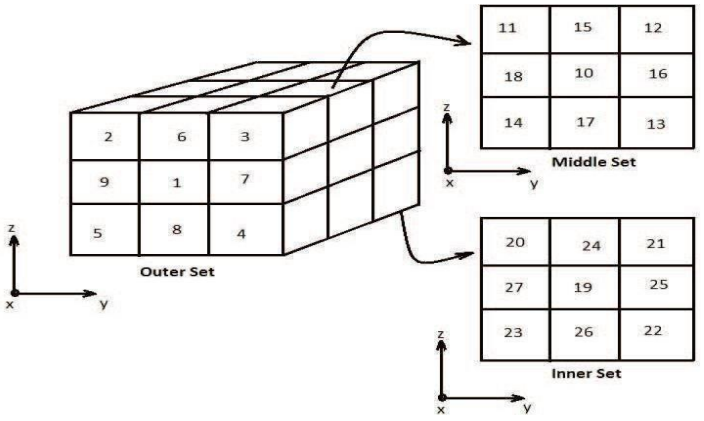

Figure. 2.8. a schematic of the fictitious cubical sections inside the PDLE

Table 2.2. Description of simulated PD events

Single location PD event	**Identifier**	**Multiple (two) location PD event**	**Identifier**
PD at cubical "1"	"SPDE1"	PD at cubical "1" and cubical "19"	"MPDE1"
…	…	…	…
PD at cubical "10"	"SPDE10"	PD at cubical "2" and cubical "22"	"MPDE8"
…	…	…	…
PD at cubical "27"	"SPDE27"	PD at cubical "27" and cubical "25"	"MPDE20"

In order to create PD sources at different positions inside the PDLE, it has been assumed that PDLE consists of 27 fictitious cubical sections. In Figure 2.8, a schematic of the fictitious cubical sections inside the PDLE has been presented. Hence, in this work 27 single location PD events have been simulated. For multiple PD sources, 2 electrode arrangements have been placed simultaneously in two different fictitious cubicles of PDLE. In this work 20 multiple location PD events have been simulated. The number of multiple location PD events is limited due to placement limitation and closeness of two electrode arrangements. A brief description of the simulated PD events has been given in Table.2.2.

2.4.2.3 Acoustic Wave Propagation in Oil Medium

The oil-filled environment of the PDLE ensures that ultrasonic waves generated by PD events propagate efficiently without significant attenuation. The low viscosity and high density of transformer oil enhance acoustic wave transmission, preserving high-frequency components essential for accurate PD localization.

Since acoustic waves travel at a relatively constant speed in transformer oil (~1400 m/s), the time-of-arrival method is used to determine the PD source location. The difference in arrival times of the acoustic signals at different sensors is analysed to reconstruct the exact discharge position.

2.4.2.4 Purpose and Functionality

The PDLE serves multiple critical functions in acoustic PD detection experiments. It provides a controlled and shielded environment, minimizing external acoustic noise that could interfere with PD signal detection. The oil-filled medium replicates practical high-voltage insulation conditions, allowing results to be extrapolated to real-world applications.

The standardized grid system ensures repeatability in experimental conditions, supporting the development of robust PD localization algorithms. The optimized sensor placement strategy improves detection accuracy, making the PDLE a vital component in acoustic PD research.
With its precisely controlled experimental setup, the PDLE for acoustic detection forms the foundation for reliable and reproducible PD studies. The next section will discuss the placement of the APDS within the PDLE to maintain optimal conditions for PD signal acquisition.

2.4.3 Placement of APDS within the PDLE

The placement of the Acoustic Partial Discharge Source (APDS) within the Partial Discharge Location Emulator (PDLE) is a crucial step in ensuring accurate simulation of Partial Discharge (PD) events and effective acoustic detection. Proper positioning of the APDS allows for consistent wave propagation, precise sensor data collection, and reliable PD localization.

2.4.3.1 Positioning Strategy

The APDS is submerged in transformer oil inside the PDLE to create a uniform acoustic propagation medium. The positioning of the APDS follows a three-dimensional coordinate grid system, ensuring controlled placement at predefined locations. The grid consists of multiple placement points, allowing systematic experimentation across different discharge locations.
For single-source experiments, the APDS is typically placed at the geometric centre of the PDLE, ensuring symmetrical wave propagation. In multi-source experiments, additional APDS units are positioned at separate predefined locations to simulate the interaction of multiple PD events. The placement is carefully adjusted to prevent overlapping acoustic waves that could lead to misinterpretation of signal data.

2.4.3.2 Electrode Placement and Alignment

The high-voltage (HV) electrode is inserted through a sealed opening in the PDLE lid and is precisely aligned with the APDS to ensure a stable and reproducible discharge. The ground electrode is positioned at the base of the tank, maintaining a consistent electrode gap required for controlled PD generation.
The alignment of the HV electrode with the void inside the APDS ensures that discharges occur in a predictable manner, producing consistent acoustic

signals. The electrode is secured using an adjustable mounting system, allowing fine-tuning of its position relative to the APDS.

2.4.3.3 Acoustic Wave Propagation Considerations

Since the speed of sound in transformer oil is approximately 1400 m/s, the placement of the APDS must consider wave reflection and attenuation. The distance from the tank walls and sensor locations is optimized to minimize unwanted reflections that could interfere with PD localization.
The APDS is placed at least 5 cm away from the nearest tank wall to reduce acoustic reflections. The positioning also ensures that direct waves reach the sensors before reflected waves, improving the accuracy of time-of-arrival calculations used in PD localization.

2.4.3.4 Multiple Source Configurations

For multi-source PD experiments, multiple APDS units are placed at distinct grid points within the PDLE. Additional HV electrodes are inserted through dedicated openings in the lid, allowing independent control of each discharge source. The minimum separation distance between sources is carefully maintained to prevent signal overlap and ensure clear identification of individual PD sources.

2.4.3.5 Validation of Placement

Before data acquisition begins, the placement of the APDS is validated through the following steps:

- Ensuring proper alignment of the HV and ground electrodes with the APDS void.
- Checking for air bubbles in the oil medium, which could distort acoustic wave propagation.
- Verifying that the discharge occurs consistently at the designated voltage threshold.

The precise placement of the APDS within the PDLE is fundamental to achieving accurate and repeatable acoustic PD detection. The next section will discuss the arrangement of acoustic sensors within the PDLE to capture the generated signals effectively.

2.4.3.6 Placement Strategy

The sensors are distributed across the five internal planes of the PDLE, avoiding symmetrical positioning to prevent ambiguity in PD source

Localization [shown in Figure. 2.9]. By utilizing an odd-plane sensor distribution, the risk of undetected or misinterpreted PD events due to equidistant reflections is minimized.
Sensors are positioned at the inner walls of the PDLE, with a typical configuration as follows:

- **S1** is placed on the front wall of the PDLE.
- **S2** is positioned on the back wall, directly opposite S1.
- **S3** is mounted on the left side wall.
- **S4** is mounted on the right side wall.
- **S5** is located at the bottom of the tank, aligned with the vertical axis.

Each sensor is secured using an oil-resistant coupling material, ensuring firm attachment to the PDLE structure while allowing efficient acoustic wave transmission.

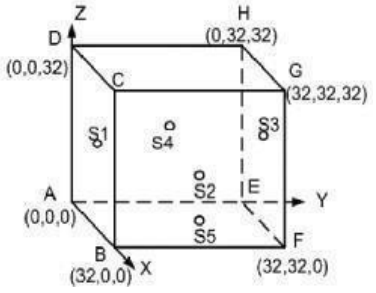

Figure. 2.9. Location and placement of acoustic sensors mounted on PDLE.

2.4.3.7 Acoustic Wave Propagation and Detection

Since acoustic waves travel at approximately 1400 m/s in transformer oil, the time difference of arrival (TDOA) method is used for PD localization. Sensors are placed at varying distances from the Acoustic Partial Discharge Source (APDS) to enable triangulation-based positioning.
Each sensor detects the PD-generated wave at a slightly different time, depending on its distance from the source. The difference in arrival times across sensors provides critical data for calculating the exact position of the PD event within the PDLE.
To minimize reflections from the tank walls, the sensors are mounted at least 5 cm away from any direct reflection surface. This reduces overlapping wavefronts and improves signal clarity.

2.4.3.8 Calibration and Sensitivity Adjustment

Before data acquisition, the sensors undergo calibration to ensure consistent sensitivity across all detection points. The calibration process includes:

- **Baseline noise measurement** to eliminate interference from background vibrations.
- **Gain normalization** to ensure all sensors operate at uniform sensitivity levels.
- **Frequency response adjustment** to focus on the ultrasonic spectrum relevant to PD emissions.

Each sensor is tested for **directional accuracy**, ensuring that detected signals correspond to actual PD events rather than external mechanical noise.

2.4.3.9 Purpose of the Odd-Plane Sensor Configuration

The use of an odd-numbered sensor distribution in the PDLE eliminates geometrical symmetry, preventing data gaps that could occur in equidistant sensor placements. This strategic placement enhances localization accuracy and ensures that even low-intensity PD events are reliably captured.

By optimizing sensor positions and utilizing advanced signal processing techniques, this arrangement provides a highly accurate acoustic PD detection system. The next section will discuss the experimental setup, integrating all components to conduct systematic PD detection trials.

2.4.4 Experimental Setup for Acoustic Detection

The experimental setup for acoustic detection of Partial Discharges (PD) integrates the Acoustic Partial Discharge Source (APDS), the Partial Discharge Location Emulator (PDLE), and acoustic sensors to create a controlled environment for studying PD-induced ultrasonic emissions [shown in Figure. 2.10]. This setup ensures reliable data acquisition and facilitates precise localization of PD events.

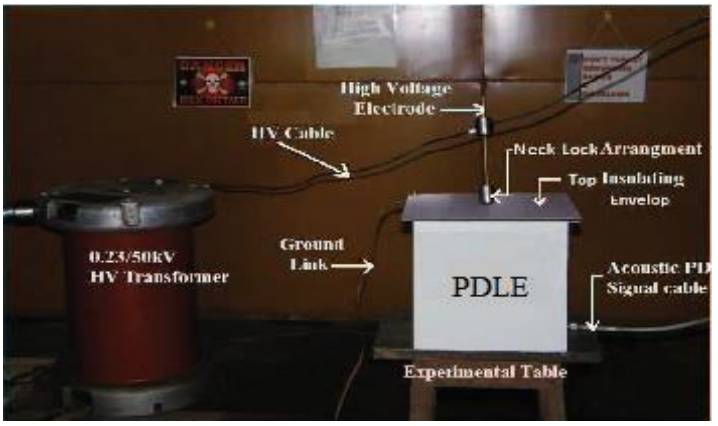

Figure. 2.10. Actual photograph of experimental setup of the acoustic partial discharge data acquisition in high voltage laboratory.

2.4.4.1 Key Components of the Setup

The Partial Discharge Location Emulator (PDLE) serves as the main enclosure for the experiment. It consists of a cylindrical stainless steel tank filled with transformer oil, which acts as the acoustic medium. The top lid contains precision-sealed perforations for inserting the high-voltage (HV) electrode, while the ground electrode is positioned at the base of the tank to establish a stable reference potential.

The Acoustic Partial Discharge Source (APDS) is an acrylic enclosure with a controlled void, submerged inside the PDLE to generate PD events. A high-voltage supply is applied across the electrodes to initiate discharge activity, producing ultrasonic waves that propagate through the oil.

The acoustic sensors are placed on five internal planes of the PDLE to capture pressure variations caused by PD-generated acoustic emissions. These sensors are equipped with preamplifiers and bandpass filters, ensuring high-fidelity signal detection within the 20 kHz – 500 kHz ultrasonic frequency range.

The high-voltage system includes a 0.23/50 kV, 10 kVA testing transformer, providing the required excitation voltage. A variable autotransformer regulates the input voltage, allowing controlled voltage ramping for PD initiation.

2.4.4.2 Assembly of the Setup

The experimental setup begins with positioning the APDS inside the PDLE at a predefined grid location. The HV electrode is inserted through a precision-sealed opening in the PDLE lid and carefully aligned with the APDS to ensure controlled discharge activity. The ground electrode is fixed at the bottom of the tank, maintaining a consistent electrical gap for PD initiation.
The high-voltage system is then connected, with the HV electrode linked to the secondary terminal of the testing transformer, while the primary terminal is grounded. This grounding configuration prevents voltage distortion and ensures a stable PD excitation voltage.
The acoustic sensors are mounted at the designated positions on the PDLE walls, with coupling materials ensuring optimal acoustic wave transmission. The sensor outputs are routed to a digitizer, which records the signals as time-domain waveforms for further analysis.

2.4.4.3 Experimental Procedure

The experiment starts with voltage application to the APDS. The voltage is increased gradually in steps of 1 kV until the PD inception voltage is reached, typically around 7 kV. To ensure continuous PD activity, a constant test voltage of 10 kV is applied during data acquisition.
Data recording involves capturing the ultrasonic signals emitted during PD events. The acoustic sensors detect the propagating pressure waves, converting them into electrical signals. These signals are digitized, normalized, and processed to extract key PD characteristics.
The experiment is conducted under two configurations:

- **Single-source PD experiments**, where one APDS is positioned inside the PDLE at a predefined grid location.
- **Multi-source PD experiments**, where multiple APDS units are activated simultaneously at different positions to analyse the interaction of multiple PD events.

2.4.4.4 Validation of Setup

Before data collection, the experimental setup undergoes a validation process to ensure reliable measurements. The HV system is tested for stable discharge operation, and the acoustic sensors are calibrated to maintain uniform sensitivity. The oil medium is inspected for air bubbles, as trapped air can distort acoustic wave propagation. The alignment of the APDS and

electrodes is verified to ensure that discharge activity occurs at the desired location.

2.4.4.5 Advantages of the Setup

The controlled environment of the oil-filled PDLE minimizes external acoustic noise, ensuring high signal fidelity. The odd-plane sensor arrangement enhances detection accuracy by eliminating symmetrical positioning errors. The high-frequency response of the sensors allows the detection of even low-intensity PD events, making the setup highly effective for real-world PD localization applications.

This experimental setup forms the foundation for acoustic PD detection and analysis. The next section will discuss the recorded acoustic PD data, presenting key findings and waveform characteristics obtained from the experiments.

2.4.5 Recorded Acoustic Partial Discharge Data

The recorded acoustic Partial Discharge (PD) data provides critical insights into the propagation characteristics of ultrasonic emissions generated during discharge events. By analysing these signals, the experimental setup enables precise localization of PD sources and the identification of unique acoustic patterns associated with different discharge scenarios.

2.4.5.1 Data Recording Methodology

Acoustic signals emitted during PD events are captured using wideband ultrasonic sensors placed at strategic locations inside the Partial Discharge Location Emulator (PDLE). These sensors convert the detected pressure waves into electrical signals, which are then amplified and digitized for further analysis. The data acquisition system records the signals in time-domain waveforms, preserving their amplitude, frequency, and phase characteristics.

To ensure data consistency, the recorded signals are normalized relative to the peak amplitude observed across all sensors. This normalization process eliminates variations due to sensor placement and ensures comparability across different experimental runs.

The data is collected under two configurations:

- **Single Location PD Events (SLPD)**, where a single Acoustic Partial Discharge Source (APDS) is placed at a predefined grid position.

- **Multiple Location PD Events (MLPD)**, where two or more APDS units are activated at different positions within the PDLE, simulating real-world multi-source discharge scenarios.

2.4.5.2 Key Observations

Analysis of the recorded acoustic PD data reveals distinct patterns that provide valuable insights into discharge behaviour.
For Single Location PD Events (SLPD), the intensity of recorded signals varies depending on the relative position of the APDS and the acoustic sensors. When the PD source is closer to a particular sensor, that sensor registers the highest signal intensity, with a gradual decrease in intensity at more distant sensors. This allows for accurate localization of the PD source using time-of-arrival (TOA) methods.
For Multiple Location PD Events (MLPD), overlapping acoustic wavefronts are observed, resulting in complex signal interactions. The recorded data shows distinct signal peaks corresponding to each source location, enabling differentiation between individual PD sources. By analysing arrival time differences at multiple sensors, precise localization of each discharge source is achieved.
The relationship between PD signals and the applied voltage waveform further confirms that most PD events occur near the zero-crossing points of the AC voltage cycle. This behaviour is consistent with discharge mechanisms in oil-insulated systems, where electric field fluctuations drive intermittent PD activity.
The effect of sensor positioning on signal characteristics is also evident in the recorded data. Sensors placed closer to the PD source detect sharper, higher-amplitude waveforms, while sensors located farther away record signals with increased attenuation and slight delays due to wave propagation effects.

2.4.5.3 Visualization and Data Interpretation

The recorded data is visualized through time-domain waveform plots, illustrating the amplitude variations of acoustic PD signals over time. These plots highlight key signal characteristics such as rise time, peak intensity, and decay profiles. The time-frequency representation of recorded acoustic PD data is shown in Figure. 2.11.
For SLPD, the waveforms exhibit a clear single-peak structure, where the peak amplitude correlates with the distance between the sensor and the PD source. For MLPD, multiple peaks are observed in the recorded signals, each corresponding to a distinct discharge source. The analysis of time delay between signal peaks allows precise triangulation of PD locations.

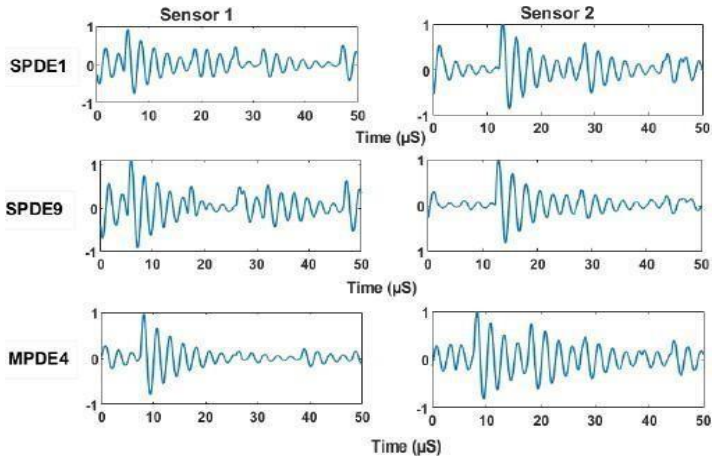

Figure. 2.11. The time frequency representation of Recorded Acoustic PD data of Sensor 1 and 2 for SPDE1, SPDE9 and MPDE4

2.4.5.4 Significance of Recorded Acoustic PD Data

The recorded acoustic PD data is instrumental in advancing PD detection and localization methodologies. The distinct signal patterns captured in SLPD and MLPD experiments provide a basis for the development of machine learning-based classification models for PD source identification.
Additionally, the dataset serves as a benchmark for validating acoustic PD detection frameworks, enabling improvements in sensor configurations and signal processing techniques. The insights gained from analysing recorded acoustic PD data contribute to early fault detection in high-voltage insulation systems, reducing the risk of catastrophic failures in power equipment.
The structured analysis of recorded acoustic PD data provides a comprehensive understanding of PD behaviour in oil-insulated systems. The next section will describe the database structure and organization of recorded acoustic PD data, ensuring systematic storage and retrieval for future studies.

2.4.6 Database Description for Acoustic PD Detection

The database for acoustic PD detection systematically stores and organizes the recorded ultrasonic signals, enabling further analysis, classification, and

validation of PD localization methods. The structured dataset serves as a benchmark for developing acoustic signal processing algorithms for PD detection in high-voltage systems.

2.4.6.1 Database Composition

The database consists of acoustic PD signals recorded from both Single Location PD Events (SLPD) and Multiple Location PD Events (MLPD). Each dataset includes time-domain waveforms captured from multiple sensors, allowing detailed analysis of PD source characteristics.

2.4.6.1.1 Single Location PD Events (SLPD)

For SLPD experiments, a single Acoustic Partial Discharge Source (APDS) is positioned at one of the predefined grid locations inside the Partial Discharge Location Emulator (PDLE). The ultrasonic signals generated by PD events are recorded across five acoustic sensors placed at strategic positions.
Each experiment consists of 40 recorded datasets per grid position, ensuring statistical reliability in signal analysis. The total number of datasets for SLPD is calculated as: 27 grid positions×40 datasets each=1080 datasets.

2.4.6.1.2 Multiple Location PD Events (MLPD)

For MLPD experiments, two or more APDS units are activated simultaneously at different positions within the PDLE. The objective is to simulate real-world scenarios where multiple PD sources coexist within a high-voltage system.
Acoustic signals from multiple PD sources are recorded across **five sensors**, capturing overlapping ultrasonic wavefronts. Each unique pair of PD locations generates **60 datasets**, leading to a total dataset count of:
20 unique pairs of grid positions×60 datasets each=1200 datasets.

2.4.6.2 Database Structure

The acoustic PD detection database is organized into two primary categories:

- **SLPD Data**: 1080 datasets from single-source experiments.
- **MLPD Data**: 1200 datasets from dual-source experiments.

Each dataset contains the following information:

- **Time-domain waveform recordings** from five ultrasonic sensors.
- **Grid position labels** indicating the precise location of the APDS.

- **Signal arrival time differences (Δt)** used for PD source localization.
- **Peak intensity values** to correlate signal strength with PD source proximity.
- **Normalized acoustic signal amplitudes** for comparative analysis.

2.4.6.3 Utility of the Database

The database provides a comprehensive resource for PD signal analysis, supporting various applications in high-voltage equipment monitoring. The recorded data enables:

- **Pattern Recognition**: Identification of characteristic acoustic PD signatures for different discharge types.
- **Localization Algorithm Development**: Implementation of time-of-arrival (TOA) and triangulation techniques for precise PD source detection.
- **Validation of Acoustic PD Detection Methods**: Benchmarking new detection techniques against a controlled dataset.

2.4.6.4 Examples of Data Patterns

Time-domain plots of recorded signals illustrate characteristic variations in acoustic PD signals.
For SLPD experiments, waveforms exhibit a single dominant peak, with amplitude variations corresponding to the distance between the sensor and the PD source. Sensors closer to the PD source capture high-amplitude signals, while those farther away record attenuated waveforms.
For MLPD experiments, waveforms contain multiple peaks, each corresponding to a distinct PD source. The arrival time difference between peaks provides crucial information for multi-source localization, allowing precise differentiation between simultaneous PD events.

2.4.6.5 Significance of the Database

The acoustic PD detection database serves as a reference dataset for developing and refining PD detection methodologies. By systematically cataloguing single-source and multi-source PD waveforms, the database ensures that experimental findings can be validated and reproduced in real-world applications.
The structured dataset contributes to advancements in machine learning-based PD classification, enabling automated detection of insulation faults in

high-voltage systems. Furthermore, the database provides insights into acoustic wave propagation in transformer oil, supporting the design of improved sensor configurations for industrial PD monitoring.
By compiling a large-scale dataset with precise localization information, the database plays a key role in enhancing the reliability and accuracy of acoustic PD detection techniques.

2.5 Optical Detection

Optical detection of Partial Discharges (PD) leverages light emissions from PD events, offering a non-intrusive and efficient way to monitor and localize discharges in high-voltage equipment. This section outlines the preparation, configuration, and setup for conducting experiments with the Optical Partial Discharge Source (OPDS), utilizing a custom-built Partial Discharge Location Emulator (PDLE).

The optical detection methodology employs specialized optical sensors to capture light signals emitted during PD events. These signals are analyzed to identify the type, location, and intensity of the discharges. The experimental framework is structured as follows:

Section 2.5.1 details the preparation of the Optical Partial Discharge Source (OPDS), including its design and fabrication to emulate realistic PD conditions.

Section 2.5.2 describes the electrode configuration and arrangement for generating partial discharges.

Section 2.5.3 introduces the Partial Discharge Location Emulator (PDLE), a controlled tank designed to simulate realistic high-voltage environments for PD localization experiments.

Section 2.5.4 explains the placement of the OPDS within the PDLE to achieve optimal experimental conditions.

Section 2.5.5 focuses on the arrangement of optical sensors inside the PDLE to maximize detection accuracy.

Section 2.5.6 provides a comprehensive overview of the experimental setup used for optical PD detection, including the integration of sensors and data acquisition systems.

Section 2.5.7 discusses the recorded optical PD data, illustrating the observed patterns and their correlation with PD events.

Section 2.5.8 elaborates on the database created from the recorded optical PD events for further analysis and development of detection frameworks.

By integrating advanced optical sensors and a structured experimental approach, this detection methodology provides a robust means for localizing PD events and understanding their characteristics in high-voltage systems.

2.5.1 Preparation of Optical Partial Discharge Source (OPDS) for Experiment

The Optical Partial Discharge Source (OPDS) is specifically designed to emulate real-world PD conditions and serve as a controlled source for experimental studies. This section outlines the process of creating and configuring the OPDS for use in optical PD detection experiments.

To position the PD source within the device at a designated location, the HV electrode is inserted through a perforation in the PDLE lid. Once the HV electrode reaches the desired vertical alignment, it is secured using a screw and collar mechanism. The earth electrode features a telescopic design and is linked to the PDLE body at ground potential. This setup is illustrated in Figure.2.12. For detecting multiple PD sources, two acrylic discs (PD sources) are placed concurrently at distinct positions within the PDLE.

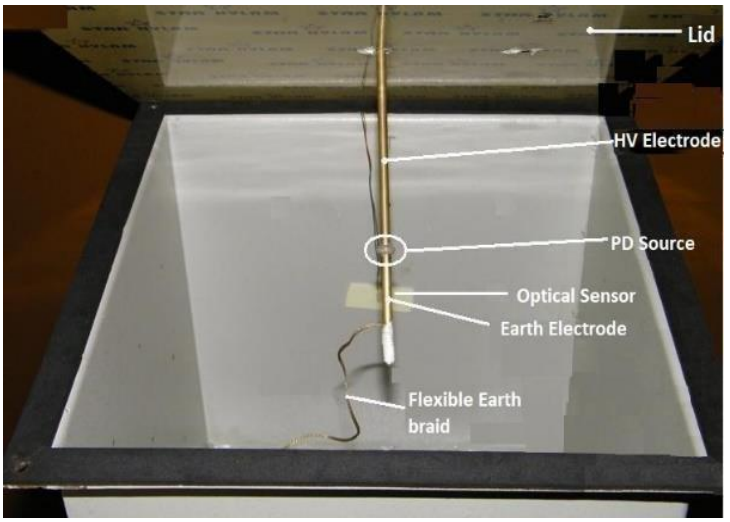

Figure. 2.12. Optical PD source placement inside the PDLE actual photograph.

2.5.1.1 Material Selection and Design

The OPDS is constructed using an acrylic disc as the insulating material, selected for its high optical transparency and ease of fabrication. Acrylic's optical properties enable the effective transmission of light signals generated during partial discharge events, making it ideal for the experiment. The OPDS is using an acrylic disc as the insulating material is represented in Figure. 2.13(a-b).

A deliberate void [illustrated in Figure. 2.13(a-b)] is introduced within the acrylic disc to mimic defects commonly found in high-voltage insulation systems. The void is precisely crafted with a diameter of 10 mm and a height of 3 mm, ensuring consistency and reproducibility in discharge generation.

2.5.1.2 Electrode Configuration

Two brass electrodes are used to sandwich the acrylic disc. One electrode is connected to a high-voltage (HV) source, while the other is grounded to simulate the electric field conditions found in actual high-voltage equipment. This setup ensures a high concentration of the electric field within the void, triggering partial discharges when voltage is applied.

2.5.1.3 Void Emulation

The artificially created void acts as a localized PD source, replicating internal discharges observed in high-voltage equipment. This design provides a controlled environment for studying PD behaviour and detecting light emissions using optical sensors.

Noteworthy is the deliberate creation of an artificial void within a transparent acrylic disc, aimed at inducing PD upon the application of electrical stress.

2.5.1.4 Precision Manufacturing

Acrylic discs are fabricated using laser cutting techniques to ensure dimensional accuracy and uniformity across all samples. This precision is critical for generating reliable and repeatable PD events, facilitating accurate sensor calibration and data acquisition.

2.5.1.5 Functionality

The OPDS is tailored to emit optical radiation across a wide spectrum, including ultraviolet (UV) and visible light. These emissions are captured and analyzed by optical sensors placed strategically within the experimental setup.

The prepared OPDS forms the core of the optical detection experiment, offering a reliable and reproducible source for studying partial discharges in controlled laboratory conditions.

2.5.2 Electrode Configuration and Arrangement for Optical Detection

The electrode configuration plays a critical role in generating consistent and measurable Partial Discharges (PD) within the Optical Partial Discharge Source (OPDS). This section outlines the design, placement, and setup of the electrodes for accurate PD emulation and subsequent optical detection.

2.5.2.1 Electrode Design and Material

The electrodes used in the experiment are made of brass, chosen for its excellent conductivity and durability. The design includes:

High-Voltage (HV) Electrode: Connected to the HV source to create the required electric field.

Ground Electrode: Maintained at earth potential to complete the electrical circuit.

The electrodes are precisely manufactured to ensure a uniform electric field distribution and minimize variability in PD behaviour.

2.5.2.2 Placement and Alignment

The acrylic disc containing the void is sandwiched between the HV and ground electrodes. The void is aligned such that the maximum electric field is concentrated within it, ensuring repeatable discharge initiation.

The HV electrode is inserted through a perforation in the Partial Discharge Location Emulator (PDLE) lid and secured at the desired vertical position using a locking mechanism [Figure .2.13(c)]. This design ensures stability and prevents misalignment during experiments. The ground electrode is fixed directly beneath the HV electrode, maintaining a consistent spacing across samples. The actual photograph of electrode placement inside PDLE is illustrated in Figure. 2.13(d).

2.5.2.3 Void-Induced PD Generation

The void within the acrylic disc acts as a defect site, where partial discharges occur due to localized electrical stress. When the applied voltage exceeds the PD inception voltage, discharges are triggered, emitting light signals captured by the optical sensors.

2.5.2.4 Electrode Dimensions

The dimensions of the electrodes are optimized to concentrate the electric field within the void. The effective area of contact ensures that the discharge behaviour is consistent across all experiments, facilitating reliable data collection.

2.5.2.5 Ensuring PD-Free Setup

Prior to experimentation, the electrode system and test equipment are inspected to ensure they are free from inherent PD activity. This step is crucial to avoid interference with the discharge signals from the OPDS.

This electrode configuration ensures the generation of stable and localized PD events, providing an ideal foundation for optical detection experiments.

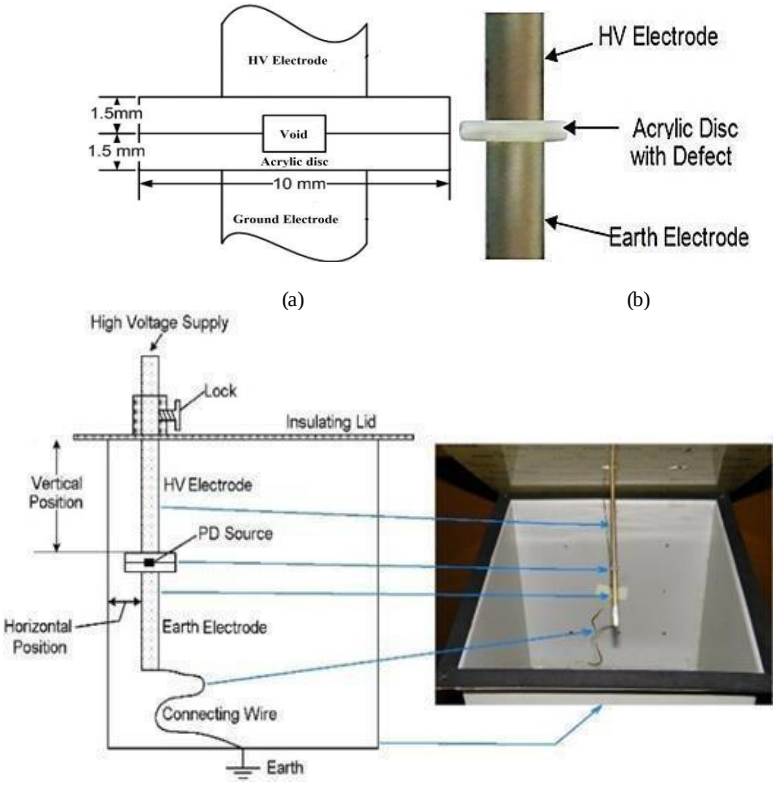

Figure. 2.13 (a) schematic of electrode arrangement with void and its dimension (b) Actual photograph of electrode arrangement (c) Schematic and (d) actual photograph of electrode placement inside PDLE.

2.5.3 Partial Discharge Location Emulator (PDLE) for Optical Detection

The Partial Discharge Location Emulator (PDLE) is a custom-designed experimental tank used to simulate high-voltage environments and accurately locate Partial Discharge (PD) sources. It provides a controlled and shielded environment for conducting optical PD detection experiments with minimal external interference.

Partial discharges from a localized source inside a cubical steel box with a side of 0.32 meters have been produced in the lab. The HV conductor is placed and held in place by an insulating substance on the box top. The Partial Discharge Location Emulator (PDLE) is the new name for this box. Additionally, the PDLE itself attenuates external loud signals or incoming electromagnetic waves. Multiple artificially created partial discharge sources have been developed within the PDLE. The same PDLE has also been applied to acoustic PD detection. To identify the optical signal produced by the PD source, optical sensors are mounted on the walls of the PDLE. The design and the real photo of the PDLE are displayed in Figure. 2.14(a) and 2.14(b) respectively. In order to emulate a PD source as well as to acquire a PD signature employing optical sensors, an experimental setup has been configured in the laboratory. For this purpose, a cubical steel box (each side of length 32cm) has been constructed. The box closely resembles the metallic enclosure of any HV equipment on a small scale. The box has been named as "Partial Discharge Location Emulator" or PDLE box. Schematic diagram of the PDLE box is shown in Figure .2.14(a). An actual photograph of the PDLE box has been shown in Figure .2.14(b). It should be mentioned here that the PDLE box yields an insulated top lid, which has been used to place and hold the high voltage (HV) conductor.

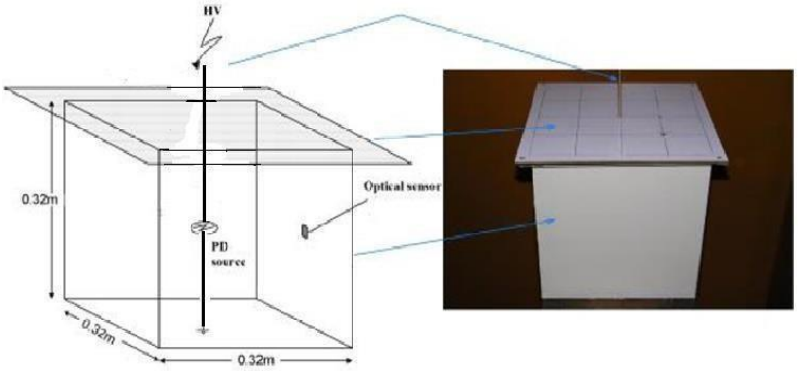

(a) (b)

Figure. 2.14. (a) Diagram of PDLE box with particular dimensions (b) Actual photographic view of PDLE box.

2.5.3.1 Design and Structure

The Partial Discharge Location Emulator (PDLE) is a cubical steel enclosure with each side measuring 32 cm. The tank closely resembles the metallic casing of high-voltage equipment, such as transformers, but on a smaller scale. Its compact size ensures that experiments can be conducted efficiently while retaining realistic conditions for PD source detection.

2.5.3.1.1 Key Structural Features

The PDLE incorporates several structural elements to optimize its performance in detecting and localizing Partial Discharge (PD) events. The outer layer consists of steel to minimize external electromagnetic interference (EMI), ensuring that only light signals emitted by the PD source are detected while external noise is reduced. The top lid of the PDLE is fabricated using an insulating material to allow the safe placement of the high-voltage (HV) electrode, providing electrical isolation. Pre-drilled holes in the top lid facilitate precise positioning of the HV electrode, enabling consistent placement of PD sources at various locations inside the tank.

2.5.3.1.2 Simulated PD Source Grid

An imaginary grid is defined inside the PDLE to standardize the placement of PD sources. The grid consists of 27 distinct positions labelled sequentially from 1 to 27. These positions are evenly distributed, maintaining an 8 cm clearance between each grid point and the tank walls. This structured layout ensures consistent experimental conditions and allows repeatable positioning of PD sources, facilitating detailed localization studies.

In this study conducted within the PDLE, 27 PD sources were strategically positioned across a hypothetical grid, marked as '•' in Figure. 2.15 and identified sequentially as 1 through 27. This grid is evenly distributed within the PDLE, maintaining an 8cm gap from all adjacent walls and between each experimental position. To simulate PD occurrences at various locations within the PDLE enclosure, a specific setup has been devised. This arrangement entails considering 27 distinct positions (indicated by '•' and labelled as '1a', '2a', '3a'... '9c' in Figure. 2.15) on an imaginary grid for placing the PD sources. It's worth noting that this imaginary grid is evenly distributed with an 8cm clearance from all surrounding walls and between experimental positions.

During experimentation, it was observed that gradually increasing the test voltage up to 7 kV resulted in discernible PD signals from the test sample. Variations in signal patterns were noticeable with the presence or absence of PD signal spikes above and below the 7 kV threshold. Consequently, the 7 kV threshold was determined as the PD inception voltage. To ensure the occurrence of partial discharges, experiments were conducted using a constant test voltage of 10 kV, which is slightly greater than the PD inception voltage. For data acquisition. For PD information capture, five optical sensors from Hamamatsu Photonics were installed at the center of the internal walls of the PDLE enclosure, excluding the top lid.

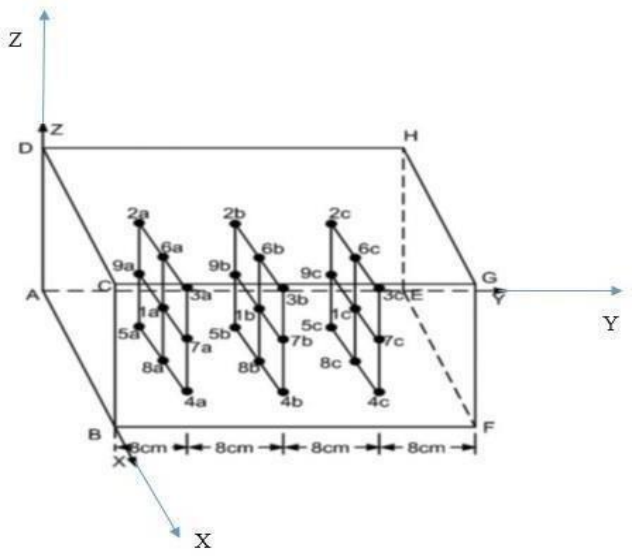

Figure. 2.15. The sources of discharge are placed at nodes 1 to 27 in Fictitious grid inside PDLE

When high voltage is applied to the HV electrode of Figure. 2.13(a), a partial discharge signal is generated due to a defect in the acrylic disc. The above- mentioned artificially created PD source has been placed at different locations inside the PDLE to record the PD data. To obtain data from multiple PD sources two such sources have been placed at two different locations within the PDLE.

2.5.3.1.3 Multi-Source Capability

The PDLE is designed to accommodate both single and multiple PD sources. Multiple acrylic discs with voids can be placed at different grid positions for experiments involving multiple PD sources. This configuration enables the generation of overlapping discharge patterns, effectively simulating complex real-world scenarios often encountered in high-voltage equipment.

2.5.3.1.4 Purpose and Functionality

The PDLE provides a realistic and controlled environment for studying PD emissions under conditions resembling those in actual high-voltage

equipment. It also acts as a framework for calibrating and testing the performance of optical sensors in detecting and localizing PD events. The structured grid, along with its double shielding and precise electrode placement features, ensures that the PDLE serves as a reliable and essential component for optical PD detection experiments.

2.5.4 Placement of OPDS within the PDLE

The placement of the Optical Partial Discharge Source (OPDS) within the Partial Discharge Location Emulator (PDLE) is a critical step in ensuring accurate simulation of Partial Discharge (PD) events and effective optical detection. This section details the procedure for positioning the OPDS to achieve optimal experimental results.

2.5.4.1 Procedure for Placement

The high-voltage (HV) electrode of the OPDS is inserted through a perforation in the insulated top lid of the PDLE. It is carefully lowered to the desired vertical position, aligning it with a predefined grid position inside the PDLE. A locking mechanism, such as a screw and collar system, is used to secure the HV electrode in place, ensuring stability during the experiment. The ground electrode is fixed directly beneath the HV electrode, maintaining a consistent gap dictated by the acrylic disc containing the void. This ground electrode is attached to the PDLE structure to establish a reliable electrical connection with the tank enclosure.

2.5.4.2 Grid Alignment

The OPDS is positioned at one of the 27 grid nodes defined within the PDLE. Each grid position is clearly marked to maintain consistency across experiments. For experiments involving multiple PD sources, multiple OPDS units can be placed simultaneously at distinct grid nodes. This configuration facilitates the study of interactions between PD sources and ensures that results reflect realistic conditions.

2.5.4.3 Ensuring Optimal Placement

To maximize the likelihood of partial discharge, the vertical alignment of the HV electrode is adjusted to concentrate the electric field within the void

of the acrylic disc. The acrylic disc is positioned such that its void lies precisely at the center of the electric field. This alignment is crucial for generating consistent PD events that are reproducible across experimental iterations.

2.5.4.4 Multiple Source Configurations

For experiments involving multiple PD sources, two or more OPDS units are positioned at separate grid nodes. Additional perforations in the PDLE lid are utilized to accommodate multiple HV electrodes. The distance between the sources is maintained to prevent electrical or optical interference, ensuring accurate detection of individual PD events and reducing the potential for overlapping signals.

2.5.4.5 Validation

Before starting the experiment, the placement of the OPDS is verified to ensure proper alignment with the grid and secure attachment of the electrodes. This verification process also includes confirming the absence of unintended discharge activity outside the void, which could affect the integrity of the results.

This carefully planned placement process ensures the reliability and repeatability of PD events, forming the foundation for robust optical detection experiments within the PDLE.

2.5.5 Optical Sensor Arrangement Inside the PDLE

The arrangement of optical sensors within the Partial Discharge Location Emulator (PDLE) is meticulously designed to avoid geometrical symmetry, ensuring comprehensive detection and localization of Partial Discharge (PD) events. By distributing sensors across an odd number of planes (5), potential blind spots caused by symmetry are eliminated, providing more reliable data acquisition.

2.5.5.1 Sensor Selection

The experiment utilizes Hamamatsu Photonics Model No. S7 184 sensors, which are chosen for their high sensitivity to optical emissions in the

UV spectrum (300–1000 nm), a range where PD events are known to radiate. These sensors are compact and robust, featuring an integrated amplifier and de-noising filter to simplify external circuitry requirements. With high signal amplification capabilities (up to 1300 times the photo current generated), these sensors provide precise and reliable detection.

The electrode system's configuration lacks universality, as its optimal radiation emission transpires within the UV spectrum, typically falling between 280 and 405 nm. PD emits radiation spanning from infrared to ultraviolet wavelengths. Hence, UV sensors featuring peak sensitivity within the 300 to 1000 nm range are integral to the present approach. For this study, sensors bearing the part number S7 184 from Hamamatsu Photonics are utilized; the data sheet contains information about these sensors' features. Hamamatsu Photonics is the manufacturer of this sensor. This sensor (Model No. S7 184) is made up of a signal processing circuit and a photo diode that can amp up to 1300 times the photo current it generates. Even with their limited active region, these photo ICs offer an output that is almost the same as that of photo diodes with an active area of 20 by 20 mm. Similar to a reverse biased photo diode, S7 184 can be utilized in the same manner and, for the most part, provide a load resistor attached to it with enough output voltage. Although this optical sensor is less expensive than comparable alternatives, it features an integrated amplifier and de-noising filter, which simplifies the external data acquisition circuitry. This sensor is utilized in this work because (i) its characteristics align with the optical Partial Discharge signal; (ii) it is reasonably priced; and (iii) it is incredibly compact.

2.5.5.2 Placement Strategy

Sensors are strategically distributed on the five internal planes of the PDLE to avoid symmetric positioning, ensuring no two sensors are located on geometrically equivalent planes. This odd-plane arrangement eliminates blind spots caused by symmetry and ensures effective detection of PD events, irrespective of their location within the tank.

Except for the upper lid, designated for housing the high voltage electrodes, the optical sensors are strategically located at the centres of each of the PDLE's five walls, simplifying their arrangement. The actual photograph and the location of the sensors are displayed in Figures. 2.16 (a) and 2.6 (b).

The PDLE's vertices are denoted by letters A through H, with their coordinates depicted in Figure. 2.16(a). Sensor1, labelled as S1, is positioned at the midpoint of the wall shared by the planes ABFE. Likewise, S2, S3, S4, and S5 are situated at the midpoints of the walls within the planes BCGF, CDHG, DAEH, and ADCB, correspondingly. The coordinates of these sensors are also provided in Figure. 2.16(a) to facilitate comprehension of their positions. It is clear from the data that odd numbers of sensors are required in order to prevent any planes of symmetry. The optimum outcome requires a minimum of 5 sensors, which are positioned at each of the box's 5 walls in order to identify the optical PD source. Some essential data from the PD source could be missed if fewer than five sensors are employed. Therefore, it might not be able to accurately identify the exact position of the PD. It makes sense that there isn't a universal plan for sensor placement in practical applications. An appropriate placement strategy for sensors must be chosen based on the application.

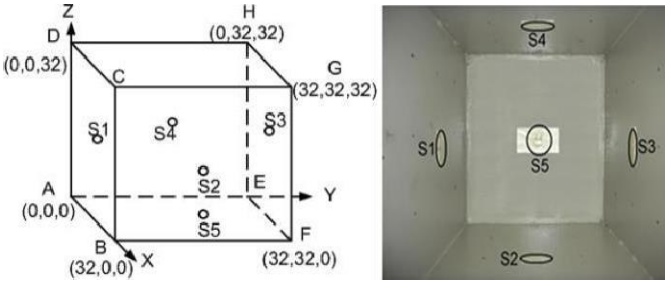

(a) ((b)

b

Figure. 2.16. (a) Schematic diagram of placement of sensors in PDLE Box, (b) Actual Photograph of the procured sensor for PD detection by optical method

The specific sensor positions are as follows:

S1 is located at the centre of the wall shared by vertices ABFE.

S2 is positioned at the centre of the wall shared by vertices BCGF.

S3 is placed at the centre of the wall shared by vertices CDHG.

S4 is situated at the centre of the wall shared by vertices DAEH.

S5 is mounted at the centre of the bottom wall, shared by all lower vertices.

These positions ensure that the sensors are evenly distributed, with no overlapping fields of view, allowing for accurate capture of emissions from any PD event within the PDLE.

2.5.5.3 Orientation and Calibration

The sensors are oriented perpendicular to the walls, facing the central volume of the PDLE to maximize their field of view. Calibration of the sensors is performed to ensure consistent sensitivity across all devices, compensating for minor variations in placement or environmental conditions.

2.5.5.4 Purpose of the Odd-Plane Configuration

The odd-plane configuration of sensors in the PDLE addresses several critical factors in experimental design. By avoiding geometrical symmetry, the risk of missed data is eliminated, especially when PD events occur at locations equidistant from symmetrically placed sensors. This deliberate asymmetry enhances detection accuracy, allowing even weak signals from distant or low-intensity PD events to be reliably captured.

Furthermore, the non-symmetric sensor distribution improves localization accuracy by generating unique signal patterns for different PD source positions. This configuration is also highly adaptable, accommodating varying grid layouts or multiple PD sources in experimental setups.

2.5.5.5 Real-World Implications

In practical applications, such as oil-filled transformers, this odd-plane sensor configuration ensures robust detection and localization of PD events. The methodology considers real-world installation constraints while maintaining reliable detection capabilities.

In real-world scenarios, like oil-filled transformers, where optical sensors could be strategically placed without any cost or technological restrictions, this methodology is acceptable for locating the PD source.

The odd-plane arrangement of sensors within the PDLE ensures consistent, reliable, and accurate data acquisition, forming a critical component of the optical detection methodology.

2.5.6 Experimental Setup for Optical Detection

The experimental setup for optical detection of Partial Discharges (PD) integrates the Optical Partial Discharge Source (OPDS), the Partial Discharge Location Emulator (PDLE), and optical sensors to create a controlled environment for studying PD phenomena. This section details the assembly and configuration of the components to ensure effective data acquisition and analysis.

The Figure. 2.17 displays schematic representation of the experimental setup for PD measurement by Optical method and the data acquisition system present in the high voltage laboratory at Jadavpur University, while Figure. 2.18 presents a photograph captured during the actual experiment.

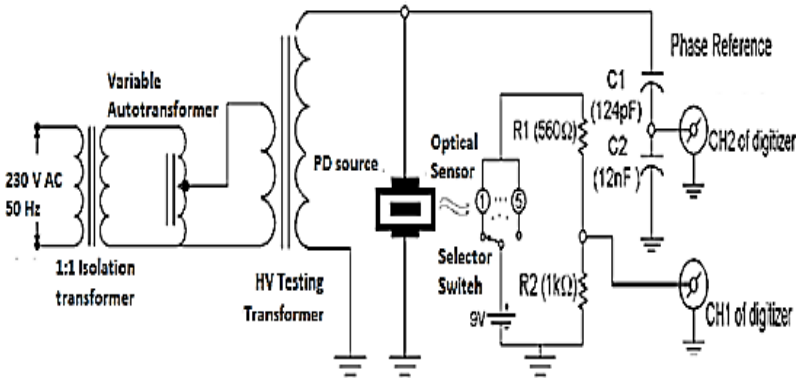

Figure. 2.17. Experimental set-up schematic diagram of optical PD measurement

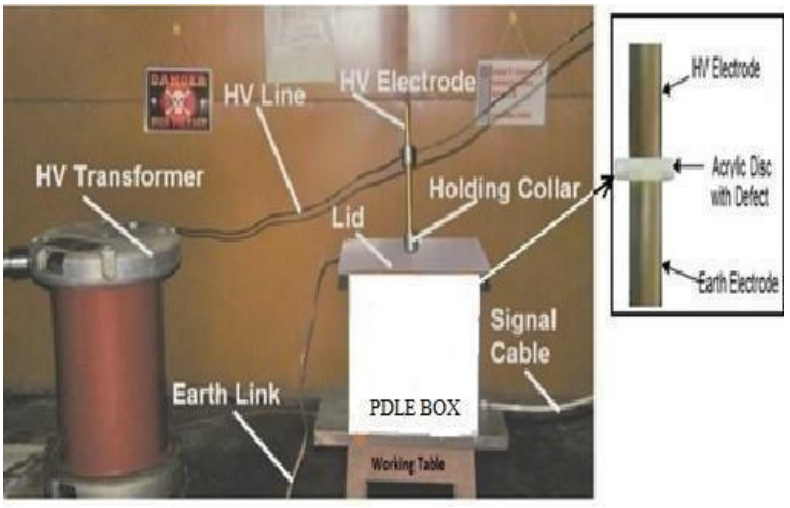

Figure. 2.18. Experimental Set-up actual photograph of optical PD data acquisition in high voltage laboratory at Jadavpur University

2.5.6.1 Key Components of the Setup

The experimental setup includes the following key components:

(a) The Partial Discharge Location Emulator (PDLE) is a cubical steel enclosure designed to simulate high-voltage environments. It features five internal sensor planes for placing optical sensors and perforations in the insulated top lid to position the high-voltage electrode of the OPDS accurately.

(b) The Optical Partial Discharge Source (OPDS) consists of an acrylic disc with a precisely crafted void to emulate real-world insulation defects. It is positioned within the PDLE at predefined grid points to maintain consistent experimental conditions.

(c) The optical detection relies on five Hamamatsu Photonics sensors (Model No. S7 184) mounted on the center of each internal wall of the PDLE, excluding the top lid. These sensors are oriented to face the center of the tank, ensuring maximum coverage.

(d) The high-voltage system includes a 0.23/50kV, 10kVA high-voltage testing transformer, which provides the required test voltage, and a variable autotransformer used to regulate the input voltage.

2.5.6.2 Assembly of the Setup

The experimental setup begins with positioning the OPDS. The high-voltage electrode is inserted through the insulated top lid of the PDLE and secured at the desired grid position. The ground electrode is fixed beneath the HV electrode to ensure proper alignment with the acrylic disc.

The high-voltage system is then connected. The HV electrode of the OPDS is attached to the secondary terminal of the testing transformer, while the primary of the transformer is grounded to allow third-harmonic current flow, preventing voltage distortion.

The optical sensors are mounted at the centers of the five PDLE walls, excluding the top lid. Calibration is performed to normalize sensitivity across all sensors, ensuring consistent and reliable data acquisition. The output signals from the sensors are routed to a digitizer, which records the light intensity signals as a function of time for further analysis.

2.5.6.3 Experimental Procedure

The experimental procedure begins with applying voltage. The voltage is gradually increased in steps of 1 kV until the PD inception voltage, approximately 7 kV, is reached. For data acquisition, a constant test voltage of 10 kV is applied, slightly above the inception voltage, to ensure continuous PD activity.

Data is recorded by optical sensors capturing light emissions from PD events. These signals are normalized and processed to identify patterns associated with the discharge. Experiments are conducted for both single and multiple PD source configurations, allowing an analysis of how source location affects sensor data.

Voltage was supplied to the HV electrode using a 0.23/50 kV, 10 kVA HV testing transformer to initiate PD discharge. In laboratory tests, distinct PD signals were observed upon gradually increasing the test voltage up to 7 kV, with noticeable differences in signal patterns above and below this threshold.

Hence, 7 kV was determined as the PD inception voltage. For data acquisition, a fixed test voltage of 10 kV, slightly higher than the inception voltage, was chosen to ensure partial discharge. Additionally, five optical sensors from Hamamatsu photonics were mounted at the center of the inside walls of the PDSE box (excluding the top lid) to capture PD information.

2.5.6.4 Validation of Setup

Before starting the experiment, the entire setup is inspected to ensure inherent PD-free operation, eliminating interference from undesired discharges. The stability and alignment of the OPDS and sensors are also verified to maintain repeatable and reliable measurements.

2.5.6.5 Advantages of the Setup

The controlled environment within the PDLE minimizes external interference, ensuring high accuracy. The odd-plane sensor arrangement avoids symmetry issues, significantly enhancing detection precision. The use of high-quality sensors enables reliable data collection, even for low-intensity PD events.

This experimental setup serves as the backbone of the optical PD detection methodology, providing the necessary framework for accurate localization and analysis of PD events under controlled conditions.

2.5.7 Recorded Optical Partial Discharge Data

The recorded optical data provides critical insights into the characteristics of Partial Discharge (PD) events, enabling accurate analysis and localization. This section presents the methodology for data recording and highlights the key observations obtained from the experiments.

In Figure. 2.19, the sensor data of partial discharge along with voltage waveform is shown. It is evident from Figure. 2.19 that most of the PD signals are concentrated near zero crossing of the voltage waveform which is reminiscent of the internal discharge. The Figure. 2.19 provided below is the time-magnitude plot of single location PD events.

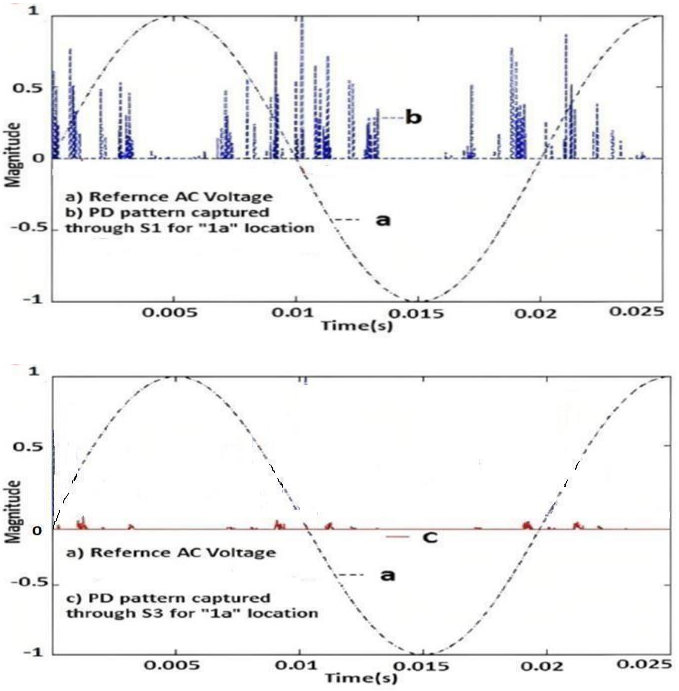

Figure. 2.19. Time domain plot of Sensor data with voltage waveform for single location PD events (a) Input supply signal, (b) and (c) are the response of Sensor 1 and Sensor 3 when PD occurs at location '1'.

Figure. 2.19 illustrates the acquired PD signal emanating from a solitary source positioned at 'SLPD1' and 'SLPD20', respectively. The Figure displays the recorded PD patterns attributed to sources at 'SLPD1' and 'SLPD20', denoted as 'MLPD20'. When considering individual PD instances situated at 'SLPD1' and 'SLPD20', they exhibit closer proximity to sensors 1 and 3, respectively. This sensor configuration remains applicable even in practical transformer scenarios. To mitigate handling challenges associated with oil-coated electrodes, an optically transparent material was adopted, yielding equivalent effects to oil.

In Figure. 2.20. a set of five datasets is acquired from the five sensors for a single PD source at a specific location (SLPD), with normalization conducted relative to the maximum value obtained among the five. Similarly, datasets

comprising five readings obtained in the case of multiple PD sources (MLPD) undergo normalization procedures.

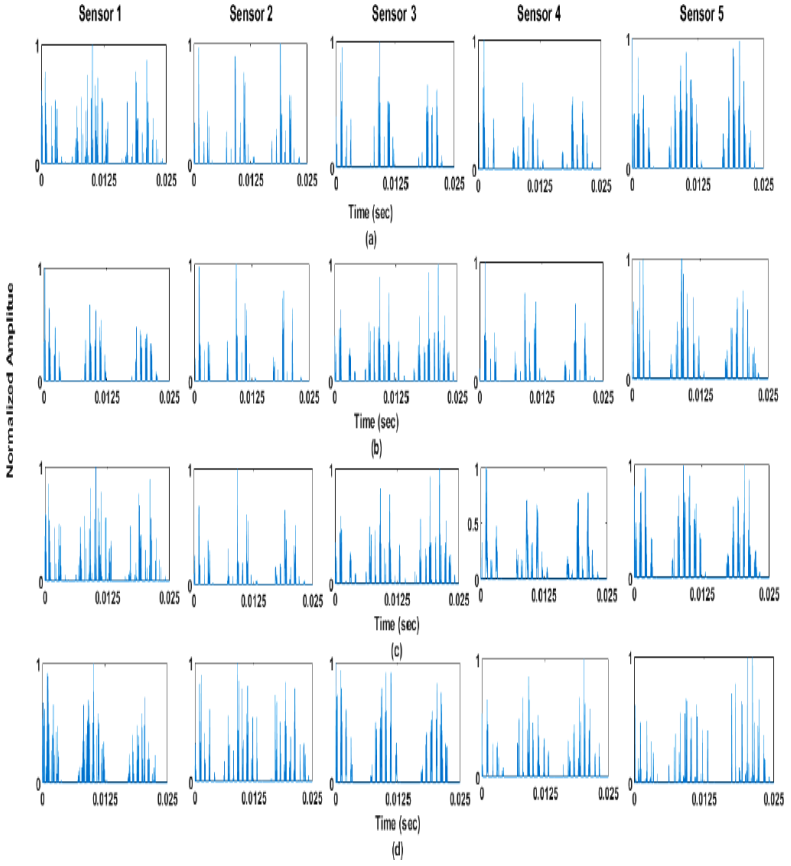

Figure. 2.20. Recorded PD patterns (normalized) for Recorded PD patterns (normalized) for (a) “SLPD1”, (b) “SLPD10” (c) “MLPD1” and (d) “MLPD8” events.

2.5.7.1 Data Recording Methodology

Signal Capture: Optical sensors mounted on the internal walls of the Partial Discharge Location Emulator (PDLE) detect light emissions from PD events. The light intensity signals are converted into electrical signals using built-in amplifiers in the sensors.

Data Digitization: The electrical signals are routed to a high-speed digitizer.

The digitizer records the signals as time-domain waveforms, preserving the temporal characteristics of PD events.

Normalization: To ensure uniformity in data representation, the recorded signals from all five sensors are normalized. Normalization is based on the maximum signal value detected among the five sensors during each PD event.

Single and Multiple PD Sources: For single PD source experiments, data is recorded for each predefined grid position in the PDLE. For multiple PD sources, data is captured with two sources simultaneously placed at different grid positions.

2.5.7.2 Key Observations

The analysis of recorded data reveals distinct patterns and characteristics that provide valuable insights into the behaviour and localization of Partial Discharge (PD) events. Key findings from the experiments are summarized in the following sections.

2.5.7.2.1 Single Location PD Events (SLPD)

For a single PD source, the intensity of recorded signals varies with the relative proximity of the source to each sensor. For instance, when the PD source is near Sensor S1, the signal captured by S1 exhibits the highest intensity compared to the others. This pattern is consistent across all grid positions, allowing for precise localization of the PD source.

2.5.7.2.2 Multiple Location PD Events (MLPD)

When two PD sources are placed simultaneously at distinct grid positions, overlapping light emissions are observed. The recorded data from multiple sensors shows distinctive patterns, enabling differentiation between the two sources and accurate localization.

2.5.7.2.3 Correlation with Voltage Waveform

Most PD signals are observed near the zero-crossing points of the applied voltage waveform, a characteristic indicative of internal discharges.

2.5.7.2.4 Effect of Grid Position

PD sources positioned closer to the PDLE walls produce stronger signals due to reduced light attenuation. Central positions exhibit relatively uniform signal distribution across sensors.

2.5.7.3 Visual Representation of Data

Time-domain plots of recorded signals are generated to visualize the captured PD patterns.

These plots reveal: Variations in signal intensity for single and multiple PD sources. Temporal characteristics of PD events, such as the duration and frequency of light emissions.

2.5.7.4 Applications of Recorded Data

Localization of PD Sources: The distinct signal patterns from different sensors facilitate accurate triangulation of PD locations.

Pattern Recognition: The recorded data serves as a foundation for developing algorithms to classify PD events based on their type and location.

Database Generation: The normalized and processed data is stored in a database, enabling further analysis and validation of detection frameworks.

The recorded optical PD data provides a comprehensive basis for understanding the behaviour of PD events and serves as a critical input for localization and detection methodologies.

2.5.8 Database Description for Optical PD Detection

The optical PD detection experiment generates a comprehensive database, serving as a foundation for analysing, classifying, and localizing Partial Discharge (PD) events. This section describes the database under structured subheadings for clarity which has been illustrated in Table 2.3.

Table 2.3. Description of created PD events

PD locations	Identifier	PD location	Identifier	PD locations	Identifier
“1a”	“SLPD1”	“8b”	“SLPD17”	“2a” & “3a”	“MLPD6”
“2a”	“SLPD2”	“9b”	“SLPD18”	“2a” & “4a”	“MLPD7”
“3a”	“SLPD3”	“1c”	“SLPD19”	“3a” & “5a”	“MLPD8”
“4a”	“SLPD4”	“2c”	“SLPD20”	“4a” & “5a”	“MLPD9”
“5a”	“SLPD5”	“3c”	“SLPD21”	“7a” & “9a”	“MLPD10”
“6a”	“SLPD6”	“4c”	“SLPD22”	“2b”& “3b”	“MLPD11”
“7a”	“SLPD7”	“5c”	“SLPD23”	“2b”& “4b”	“MLPD12”
“8a”	“SLPD8”	“6c”	“SLPD24”	“3b”& “5b”	“MLPD13”
“9a”	“SLPD9”	“7c”	“SLPD25”	“4b”& “5b”	“MLPD14”
“1b”	“SLPD10”	“8c”	“SLPD26”	“7b”& “9b”	“MLPD15”
“2b”	“SLPD11”	“9c”	“SLPD27”	“2c” &“3c”	“MLPD16”
“3b”	“SLPD12”	“1a” & 1c”	“MLPD1”	“2c” & “4c”	“MLPD17”
“4b”	“SLPD13”	“1a” & “2c”	“MLPD2”	“3c” & “5c”	“MLPD18”
“5b”	“SLPD14”	“1a” & “5c”	“MLPD3”	“4c” & “5c”	“MLPD19”
“6b”	“SLPD15”	“2a” & “1c”	“MLPD4”	“9c” & “7c”	“MLPD20”
“7b”	“SLPD16”	“7a” & “1c”	“MLPD5”	Total “20” MLPD events	
				Total “27” SLPD events	

In this work, two different types of PD event such as "single location partial discharge" (SLPD) event and "multiple location partial discharge" (MLPD) event have been emulated for this task. In the first (SLPD) event, one PD source has been placed in the fictious grid and discharge is made to occur. In this work, 27 different SLPD events were created where a PD source has been placed at each individual position in the fictious grid. Now, to create the MLPD event, two similar electrode arrangements have been simultaneously placed in any two different positions in the fictious grid through creating multiple holes at the top lid of the PDLE. In this work, 20 different combinations of MLPD events have been created. From Figure. 2.13(a) and Figure. 2.18, it is evident that the sample diameter is kept small in comparison to the distance between the two PD source locations. Therefore, the proposed sensor configuration can detect MLPD sources closer than 8 cm to each other with the same accuracy. In Table 2.3, a brief description of different created PD events has been presented. Now, for experimental investigation purposes, 40 datasets have been recorded for each SLPD event. Whereas, for each combination of MLPD events, a total of 60 datasets has been recorded. Hence, a database consisting of 2280 datasets {27 (number of SLPD events)
× (40 set) +20 (number of MLPD events) × (60 set)} have been prepared for this work. In Figure2.20 (a-d), time domain plots of PD signature (captured by all optical sensors) for "SLPD1", "SLPD10", "MLDP1" and "MPLD8" events have been shown respectively. From Figure2.20, it is clearly observed that the pattern of captured PD data changes with the type of PD event as well as with PD source location. Here, "SLPD1", "SLPD10" locations are considered, because "SLPD1 the location is nearest to the sensor S1 and location "SLPD10" is the midpoint of the grid. Therefore, it is possible to distinctly observe PD events of those two locations. Similarly, MLPD1 and MLPD8 are chosen in such a way that we clearly identify PD events those two locations. Hence, employing the acquired PD database, it is possible to detect not only the type of PD event but also to locate the PD sources through developing a suitable framework. In Figure. 2.19, the sensor data along with the voltage waveform is shown. It is evident from Figure. 2.19 that that most of the PD signals are concentrated near zero crossing of the voltage waveform which is reminiscent of the internal discharge.

2.5.8.1 Description of Classification Problems

In this study, one binary classification problem and two multiclass classification problems have been addressed. The brief description of the classification problems is presented in Table 2.4. The objective of the 1st classification problem is to classify single PD sources or multiple PD

sources. In this problem, the database has been segregated into 2 classes (SLPD and MLPD) according to the number of simultaneous PD events. The objective of the 2nd classification problem is classification of SLPD sources separately occurring at 27 locations. For the 3rd classification problem, the objective is to classify MLPD sources at 20 locations. Since, the PD originating from different locations will have different signatures (as captured by different sensors), hence using the proposed framework, classification of SLPD and MLPD events occurring at different locations is possible. Hence, for CP-II and CP-III problems, the database has been subdivided into 27 and 20 classes according to the position of PD sources for each event.

Table 2.4. Description of Classification Problems

Classification problem (CP)	Description	No of classes
CP1	Identification of the type of PD event	2
CP2	PD source location for SLPD event.	27
CP3	PD source location for MLPD event.	20

2.5.8.2 Database Composition

The database includes data recorded for both Single Location PD Events (SLPD) and Multiple Location PD Events (MLPD), ensuring broad coverage of experimental scenarios.

2.5.8.2.1 Single Location PD Events (SLPD)

In the case of SLPD experiments, a single Optical Partial Discharge Source (OPDS) is placed at one of the 27 grid positions inside the Partial Discharge Location Emulator (PDLE). Signals from all five optical sensors are recorded for each grid position. To ensure statistical reliability, 40 datasets are collected for each grid position. This results in a total of 1080 datasets for SLPD, calculated as 27 grid positions multiplied by 40 datasets per position.

2.5.8.2.2 Multiple Location PD Events (MLPD)

For MLPD experiments, two OPDS units are placed simultaneously at different grid positions to emulate multiple PD sources. Signals from all five optical sensors are recorded for each unique pair of grid positions. To ensure statistical reliability, 60 datasets are collected for each unique pair of

positions. This results in a total of 1200 datasets for MLPD, calculated as 20 unique pairs of grid positions multiplied by 60 datasets per pair.

2.5.8.3 Database Structure

The database is organized into two main categories: SLPD data and MLPD data. The SLPD data comprises 1080 datasets collected from single-source experiments, while the MLPD data includes 1200 datasets collected from dual-source experiments. Each dataset contains normalized light intensity values recorded from the five optical sensors, information identifying the PD source location(s) within the PDLE, and temporal alignment of the optical signals with the applied voltage waveform.

2.5.8.4 Utility of the Database

The database serves multiple purposes in advancing the study of PD detection. It facilitates pattern analysis by enabling the identification of distinct signal patterns corresponding to various PD event types and locations. Furthermore, the data supports the development of algorithms for accurately localizing PD sources within the PDLE. The database also acts as a benchmark for testing and validating optical detection techniques, ensuring the reliability of these methodologies.

2.5.8.5 Examples of Data Patterns

Time-domain plots of the recorded data reveal characteristic variations in signal intensity and distribution. For single-location PD events (SLPD), the recorded signals vary with the source's proximity to the sensors. For example, when the source is at grid position SLPD1, Sensor S1 captures the highest intensity signal, with decreasing intensity observed at sensors farther away. At central positions, such as SLPD10, the signal distribution is more uniform across sensors.

For multiple-location PD events (MLPD), overlapping signal patterns are recorded, with distinctive peaks corresponding to each source location. These patterns enable clear differentiation between the two sources and allow precise localization of each PD event.

2.5.8.6 Significance

The database provides a robust foundation for the development of scalable and precise optical PD detection techniques. By capturing diverse experimental scenarios, it ensures that these methodologies are applicable to real-world high-voltage equipment. The database supports detailed analysis, facilitates the development of localization frameworks, and enables reliable validation of detection methods.

2.6 Summary

This chapter presented the experimental setup and methodologies for detecting Partial Discharge (PD) events using electrical, optical and acoustic detection techniques. The chapter was structured to cover the preparation of PD sources, sensor arrangements, experimental configurations, and data acquisition methods, ensuring reliable and repeatable detection of PD activity in controlled laboratory conditions.

The Electrical or conventional detection (section 2.3) method pertains to PD testing while “offline”, which means the excitation voltage is provided via an external source. This set-up of electrical detection significantly helps to reduce external electromagnetic influences. It can provide accurate and reliable systems for PD measurements of HV equipment such as transformers, generators, switchgear and cable systems using applied voltage in laboratory or on-site testing environments. The electrical measurement of PD measures part of the current pulse that is initiated by the discharge mechanism. Different measured quantities are used in the industry. However, the apparent charge, in coulombs (C), is the most widely accepted unit. The measured values are usually in the ranges of picocoulombs (pC) or nanocoulombs (nC). The coupling capacitor is by far the most commonly used sensors. They usually consist of a high voltage capacitor that is connected in parallel to the test object. When a PD event occur, the energy stored in the coupling capacitor will supply part of the recharging current. The more energy that is stored in the capacitor, the higher the recharging current will be in case of a PD event. Therefore, a high capacitance value usually results in a higher sensitivity for PD measurement circuit using a coupling capacitor. When using a coupling capacitor, it is common to be able to also obtain the waveform of the supply voltage. This is needed for a phase synchronized PD measurement. It is also possible to connect the measuring impedance in series with the test object. When performing onsite measurement on HV apparatus, the size and cost of a coupling capacitor can become problematic. Therefore, they are some cases where it can be preferable to use alternative sensors.

The Acoustic Detection (Section 2.4) focused on capturing ultrasonic signals generated by PD discharges in an oil-insulated environment. The Acoustic Partial Discharge Source (APDS) was placed inside the PDLE, submerged in transformer oil to facilitate efficient acoustic wave propagation. A set of wideband ultrasonic sensors was arranged in a non-symmetrical configuration to ensure complete coverage of PD-generated signals. The experimental setup involved controlled voltage application, sensor calibration, and digitized data recording. The recorded acoustic PD data provided insights into signal arrival times, wave propagation characteristics, and the differentiation of single and multiple PD sources. A comprehensive database of acoustic PD data was developed, supporting advancements in PD detection and localization.

The Optical Detection (Section 2.5) focused on capturing light emissions generated by PD events. The Optical Partial Discharge Source (OPDS) was positioned within the Partial Discharge Location Emulator (PDLE), ensuring standardized placement across multiple experiments. A five-plane optical sensor arrangement was employed to eliminate symmetrical positioning errors, improving localization accuracy. The experimental setup integrated high-voltage excitation, sensor calibration, and data acquisition through a digitizer. The recorded optical PD data revealed characteristic light emission patterns, which were analyzed for intensity variations and correlation with applied voltage waveforms. A structured database of optical PD data was compiled, enabling future validation of detection frameworks and localization techniques.

The chapter also introduced systematic grid-based positioning for both optical and acoustic PD sources, ensuring repeatability in measurements. The collected datasets serve as benchmark references for developing advanced detection algorithms, including time-of-arrival (TOA) analysis, triangulation techniques, and machine learning-based PD classification models. The structured approach to PD detection in this chapter provides a foundation for improving real-world high-voltage insulation monitoring systems.

This summary concludes the experimental methodologies for PD detection presented in this chapter. The next chapter will focus on the analysis and interpretation of recorded PD signals, leveraging the compiled optical and acoustic datasets for detailed PD localization and pattern recognition.

This structured approach ensures reliable PD detection and supports the development of localization algorithms based on acoustic signal processing. The combination of electrical, acoustic and optical detection methodologies provides a comprehensive strategy for monitoring PD activity in high-voltage equipment.

Chapter 3

Identification and Classification of Partial Discharge Pulse Sequence based on Mathematical Morphology aided Bi-directional Long-Short Term Memory Network

3.1. Introduction

Partial discharge (PD) is a local and incomplete defect in some part of insulation due to electrical stress [7,9,10,12-19]. Types of PD defects in an insulation system can be classified as: 1) “internal discharge”; 2) “surface discharge”; and 3) “corona discharge.” Internal discharge mainly occurs in the presence of voids/cavities inside the insulation [7], [19]. On the other hand, surface discharge occurs on the external surface of insulation [7], [19]. Corona discharge is the partial breakdown of gaseous insulation that mainly occurs at the sharp edge of electrodes [7], [19]. It is to be noted that in the presence of PD defects, some portion of insulation failure happens.

However, the insulation can still endure electrical stress [7], [19], [9]. However, the presence of PD in an insulating material deteriorates the condition further and leads to complete failure of it [7], [19], [9]. Catastrophic breakdown of an insulating material can severely affect the reliability of an electrical system. Therefore, the accurate pattern recognition and classification of PD defects (sources) is necessary for the quality assessment of an insulation system. The existing literature reveals that phase resolved PD (PRPD) analysis is commonly used for representation of PD data. In PRPD analysis, the PD pulses are quantified with the help of occurrence of the phase angle (ϕ), magnitude of the charge (q), and the number of PD occurrences over predefined time duration (n). The corresponding PD data represented using PRPD patterns is commonly known as the ϕ–q–n plot [10]. The phase-resolved PD patterns are widely used in PD analysis purposes since the PD pulse characteristics can be represented more accurately using the PRPD patterns.

However, it has been reported in [19] that the local electric field intensity inside the defect determines the PD inception voltage and local field enhancement does not depend on the phase of the applied voltage [19]. Also, in the case of dc voltage, phase information is absent. Therefore, the PRPD pattern cannot provide a comprehensive representation of PD data. Considering the aforesaid limitation, a novel approach known as Pulse

Sequence Analysis (PSA)-based PD detection framework is presented in this chapter. According to the theory of PSA [11-16], the phase of the applied voltage upon which the discharges observed is not considered as a significant parameter. It is noteworthy to mention that the sequence of PD pulses has a great impact on PD defect identification. According to [19], the sequence of PD pulses is not treated as independent events. In fact, each subsequent PD pulse is strongly correlated with the previous ones. Thus, information regarding the phase is not required for PSA analysis, and hence, it can be used for PD measurement under dc voltage too. Considering the fact, in this work, PSA has been used to characterize the nature of PD defects. The advantage of PSA is that it can characterize different types of PD defect and can distinguish the discharges due to single or multiple discharge site [19]. For automated categorization of PD pulse sequences into PD defects, it is important to develop a robust pattern recognition framework. In [11], the application of convolutional neural network (CNN) on PD pulse sequence has been investigated to identify PD defect in a cable joint. However, the aforesaid paper did not focus on the classification of PD pulse sequence into "internal discharge," "surface discharge," and "corona discharge." In recent times [11,12,123,124], several machine learning and deep learning algorithms have been proposed to classify PD defects employing PRPD pattern and PD sensor data. Motivated by the aforesaid research works and considering the research gap, in this chapter, an attempt has been made to develop an automated framework which can classify PD pulse sequence into "internal discharge," "surface discharge," and "corona discharge." In the proposed framework, mathematical morphology (MM) has been used to extract local and meaningful information from PD pulse sequence data. Thereafter, a bidirectional long short-term memory (Bi-LSTM)-based deep neural network (DNN) has been configured to classify morphological features (extracted from PD pulse sequence). The Bi-LSTM-based deep network has been chosen in this work for the classification task due to the fact that it can learn the temporal properties of 1-D data in both forward and backward direction. In this work, the MM aided Bi-LSTM network is proposed to classify PD defects based on PSA. Besides, this chapter introduces several new composite MM operators to analyze PD pulse sequence.

3.2. Theory of Partial Discharge Pulse Sequence Analysis

In **Pulse Sequence Analysis (PSA)**, PD data are represented by computing the differences in the inception voltage across the void between consecutive

discharge pulses with the assumption that PD pulses at the time of discharge are highly correlated with each other [19]. In the other words, in PSA, the repetitive discharge pulses during the occurrence of PD are not treated as independent events; rather it assumes that every subsequent discharge pulse has some relation with the previous ones. Compared with phase resolved analysis, PSA provides better information regarding the PD processes occurring inside an insulation sample because the latter assumes that the localized electric field intensity at the site of the discharge is responsible for subsequent discharges [19]. Since the presence of localized space charge accompanied by electric field enhancement contributes to the discharge process, therefore, strong similarity between successive PD pulses must exist. Hence, in PSA analysis, instead of recording the phase angle of the applied voltage at which the PD occurs, more significance is given to the alteration in localized electric field intensity with time between successive discharges [19]. Now, the change in localized electric field occurs due to the alteration in supply voltage since the latter determines the residual charge, i.e. the localized electric field involved at the site of discharge, which triggers the initiation/ignition of the subsequent pulse. Thus, PSA is closely related to the actual physical discharge processes taking place within the insulation and appropriate parameters extracted from PSA can provide insight into the consecutive pulse correlation over the entire measuring duration [19]. The advantage of PSA is that information regarding the phase of the voltage signal is not required during PD measurements. Another advantage of PSA is that it can be applied for ac as well as dc PD measurement. The parameter details and PSA data acquisition method are described in the following section.

3.2.1. Limitations on Partial discharge phase resolved analysis

In conventional approach, PD data are usually represented as phase-resolved plots. In phase resolved plots, the acquired PD pulses are overlapped with the applied voltage which is sinusoidal in nature. Although the previously mentioned approach can provide insight into the type of PD occurring inside an insulating material, yet it has some limitations. Detailed investigations have revealed that although pulse heights can provide insight into the discharge severity, but the phase of the sinusoidal voltage at the PD inception is not a significant parameter to analyze PD data. The above declaration is true for solid or liquid insulation, where the PD inception voltage and not on the phase information of the applied voltage [19]. Also, it is well known that the information regarding the phase of the voltage signal is exceedingly significant in a PRPD.

The performance of PRPD-based PD recognition drastically reduces if the PD data lacks voltage reference [13]. Thus, it is apparent that a PRPD will malfunction if the voltage signal information is absent [13]. In addition, in the case of PD measurement under dc voltage, phase information is absent. Considering these aforesaid limitations of the conventional approach, PSA technique has been implemented in this work for better characterization and discrimination of PD pulses arising out of single as well as multiple defects present within the insulation.

3.2.2. Partial discharge pulse sequence analysis

(PRPS)Phase Resolved Pulse Sequence analysis (discussed in chapter 1, section 1.8.1.1) is a technique used in partial discharge (PD) measurement and analysis to extract valuable information about the characteristics of PD signals. It involves analysing the time-domain characteristics of the pulses emitted by partial discharge events. Here's an overview of pulse sequence analysis in PD. PD signals are captured using appropriate measurement techniques such as high-frequency current transformers (HFCT), ultrasonic sensors, or optical sensors. The PD signals are typically recorded as voltage or current waveforms. The recorded PD waveforms are pre-processed to remove noise and environmental issues that may affect the analysis. Filtering techniques, such as band pass or high-pass filters, can be applied to isolate the PD pulses from other interference. The PD pulses are detected and extracted from the pre-processed waveforms using various algorithms. Threshold-based methods, peak detection, or pattern recognition techniques may be used to identify individual pulses. Once the pulses are detected, they are segmented into individual events. This involves separating the pulses in time and amplitude, ensuring that each pulse is analyzed independently. Various time-domain and amplitude-related features are extracted from the segmented pulses. These features can include pulse duration, rise time, peak amplitude, pulse repetition rate, and pulse charge. These features provide insights into the characteristics of PD events. The extracted features are analyzed to identify patterns and correlations within the pulse sequence. Statistical analysis, clustering algorithms, or pattern recognition techniques can be used to identify specific patterns or classes of PD events. The analyzed pulse sequence data is interpreted to assess the severity, location, and type of partial discharge activity. Comparisons with established databases or expert knowledge can help in diagnosing the condition of the electrical insulation or identifying potential faults. By analyzing the pulse sequence data over time, trends and changes in

PD behaviour can be identified. Trend analysis can help in detecting early signs of insulation deterioration or the progression of faults. Pulse sequence analysis in PD provides valuable insights into the characteristics and behaviour of partial discharge events. It enables the identification of specific PD patterns, classification of PD types, and assessment of insulation condition. This analysis technique plays a crucial role in condition monitoring, maintenance decision-making, and ensuring the reliability and safety of electrical systems.

3.2.3. Pulse Sequence Analysis (PSA) Data Analysis

PD pulses are kept in phase-resolved pulse sequence (PRPS) format. The Δu features are important parameters to analyze the PSA for data acquisition. The recorded discharge signals which has been already illustrated in chapter 2, section 2.3.4.3 are analyzed in this section.

3.2.3.1. Methodology based on Mathematical Morphology Aided Bi-directional Long-Short Term Memory Network

3.2.3.1.1. Mathematical Morphology

MM proposed by Serra and Matheron is a popular mathematical tool widely used for pattern recognition [125], [126], [127], [128]. MM has been extensively used for analysis of image and time series data. In this study, MM has been used to analyse the PSA data to extract meaningful information for accurate identification of defects. In MM, the geometry of any pattern or data is manipulated by predefined element known as structure element (SE) to extract local and temporal characteristics [125]. The nature of SE in MM operation is completely empirical. In this task, 1-D flat SE {111} has been chosen to analyse PSA data, i.e., the n–Δu PD pattern. It should be mentioned here that the window length of SE has been taken "3" due to the fact that a large window will provide global information about the signal rather than local information. In MM, the basic MM operators are: 1) erosion; 2) dilation; 3) opening; and 4) closing.

The mathematical expression of erosion *E(i)* has been expressed as follows:

$$E(i) = (a \ominus s)(i) = \min\{a(i + j) - s(j)\} \quad (0 \le i \le I, 1 \le j \le M) \tag{3.1}$$

In this equation, "a" is the input n–1u pattern over a domain *A = (0, 1, ... , I − 1)*, whereas "s″ is SE over a domain *S = (0, 1, ... , M − 1), (M ≤ I).* Similarly, other basic MM operators, i.e., dilation *D(i)*, opening *O(i)*, and closing *C(i)* can be expresses as follows:

$$D(i) = (a \oplus s)(n) = \max\{a(i-j) + s(j)\} \quad (0 \le i \le N, 1 \le j \le M) \tag{3.2}$$

$$O(i) = (a \circ b)(i) = (a \Theta b \oplus b)(i) \tag{3.3}$$

$$C(i) = (a \bullet b)(i) = (a \oplus b \Theta b)(i) \tag{3.4}$$

It is noteworthy that erosion erodes the contour of the signal, whereas dilation expands any kind of sharp deviation in a signal [125], whereas *O(i)* smooth's the sharp edges of the contour and closing fills the narrow gaps present in the boundary [125]. Based on the basic MM operation some composite operators have been suggested in this chapter. The composite operators have been described through the following equations:

$$df_{de}(i) = D(i) - E(i) \tag{3.5}$$

$$df_{oc}(i) = O(i) - C(i) \tag{3.6}$$

$$avg_{de}(i) = \{D(i) + E(i)\}/2 \tag{3.7}$$

$$avg_{oc}(i) = \{O(i) + C(i)\}/2 \tag{3.8}$$

$$avg_3(i) = \{(avg_{de} \oplus s)(i) + (avg_{de} \Theta s)(i)\}/2 \tag{3.9}$$

$$avg_4(i) = \{(avg_{oc} \oplus s)(i) + (avg_{oc} \Theta s)(i)\}/2 \tag{3.10}$$

$$avg_5(i) = \{(avg_{de} \circ s)(i) + (avg_{de} \bullet s)(i)\}/2 \tag{3.11}$$

$$avg_6(i) = \{(avg_{oc} \circ s)(i) + (avg_{oc} \bullet s)(i)\}/2 \tag{3.12}$$

It is noteworthy that the composite MM operators proposed in this work can bring out inherent characteristics and sudden fluctuation in a PD pattern which aid in accurate feature extraction and subsequent defect classification.

3.2.3.1.2. Feature extraction

In this chapter, a 1-D $n - \Delta u$ PD patterns have been analysed through the aforesaid basic and composite MM operators to analyse the inherent

nonlinear characteristics of PD pattern. Based on the analysis, 36 MM features have been extracted. The description of extracted MM features has been given in Table.3.1.

Table3.1. Description of extracted MM features

Name	Features	Name	Features	Name	Features
F_1	variance of E(i)	F_13	variance of (i)	F_25	variance of (i)
F_2	skewness of E(i)	F_14	skewness of (i)	F_26	skewness of (i)
F_3	Kurtosis of E(i)	F_15	kurtosis of (i)	F_27	kurtosis of (i)
F_4	variance of D(i)	F_16	variance of (i)	F_28	variance of (i)
F_5	skewness of D(i)	F_17	skewness of (i)	F_29	skewness of (i)
F_6	kurtosis of D(i)	F_18	kurtosis of (i)	F_30	kurtosis of (i)
F_7	variance of O(i)	F_19	variance of (i)	F_31	variance of (i)
F_8	skewness of O(i)	F_20	skewness of (i)	F_32	skewness of (i)
F_9	kurtosis of O(i)	F_21	kurtosis of (i)	F_33	kurtosis of (i)
F_10	variance of C(i)	F_22	variance of (i)	F_34	variance of (i)
F_11	skewness of C(i)	F_23	skewness of (i)	F_35	skewness of (i)
F_12	kurtosis of C(i)	F_24	kurtosis of (i)	F_36	kurtosis of (i)

Thereafter, these 36 features have been given as input to the bidirectional LSTM classifier for automatic detection and classification PD source.

3.2.3.1.3. Bi-directional LSTM network

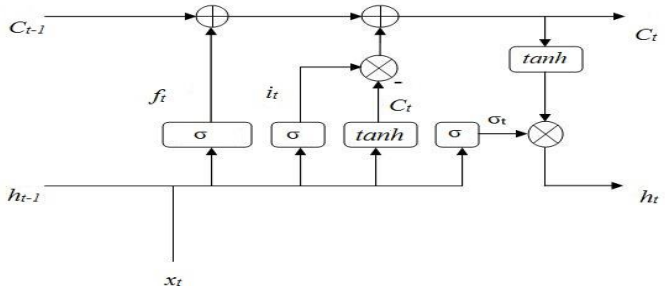

Figure. 3.1. Structure of a LSTM cell.

The long short-term memory network (LSTM) is a subset of the recurrent neural network (RNN) has been proven to be one off sequence classification tasks [129-134]. LSTM network, an efficient deep learning framework, can solve the problem related to vanishing gradient or exploding which is present in traditional RNN network through adding gate function in RNN dynamics [22]. The LSTM network consists of three gate functions, i.e., "input," "forget," and "output" (as shown in Figure. 3.1). The first one, i.e., "input" remember specific information, whereas "forget" has been used to drop information and "output" determines the input in the memory to become an output [130], [131]. Bidirectional LSTM or Bi-LSTM, which is an extension of traditional LSTM can increase performance related to sequence classification tasks. Bi-LSTM trains two independent LSTM networks instead of one LSTM network [132]. In the first network, input sequence has been fed in normal time order, whereas in the second network reverse copy of the input sequence has been fed. This allows the network to extract forward and backward data about input sequence at each time step, which can provide further context to the network and consequences in fuller learning on the problem. The detailed description about bi-LSTM has been discussed in these papers [130-134].

3.2.3.1.4. Bi- LSTM network configuration

For classification of $n-\Delta u$ PD patterns, a Deep Neural Network (DNN) based on Bi-LSTM has been configured. The configured DNN consists of two Bi-LSTM layers: one dropout layer and one softmax classification layer. The number of hidden units in the first and second Bi-LSTM layer of the proposed network is 100 and 50, respectively. In the softmax layer, the softmax activation function transforms the above-mentioned scores into a probabilistic value and estimates the class output. It is noteworthy to mention that a dropout layer has been used in this proposed network to counter overfitting issue. The dropout rate in the dropout layer has been taken as 0.5. A brief outline of the proposed DNN has been shown in Figure. 3.2. In Figure. 3.3, a brief representation of the proposed framework is shown.

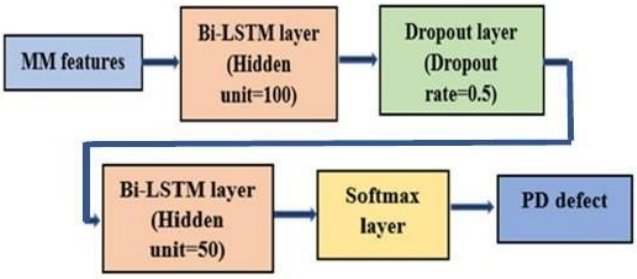

Figure. 3.2. Overview of proposed deep neural network based on bi-LSTM.

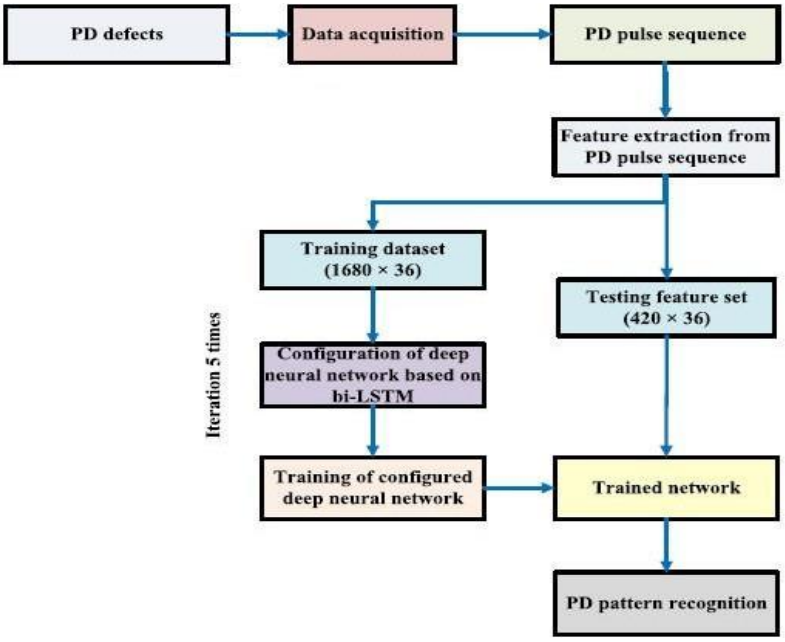

Figure. 3.3. Infographic of proposed methodology.

3.3. Results and Discussions

In this chapter, a total of 1500 PD data (500 for each class) has been acquired. From each $n-\Delta u$ PD pattern, a total of 36 MM features (as described in Table 3.2) have been extracted. Thereafter, these features have been subsequently fed to the configured Bi-LSTM network (described in Section IV) for the determination of classification. It should be stated here that the performance of the suggested framework has been attained after a fivefold cross validation (CV) strategy. In the fivefold CV strategy, 4/5th of the feature set (i.e., 1200 × 36) or 43200 features have been used to train the configured Bi-LSTM network, whereas the remaining 1/5th of the feature set (i.e., 300 × 36) or 10 800 features have been considered for testing purpose. It is pertinent that the learning rate of configured Bi-LSTM network is an important parameter. A high learning rate may cause DNN to learn rapidly. In such case, a loss of the DNN will be high, whereas low learning rate may lead to optimal learning of the network. Therefore, it is essential to find a suitable learning rate for the proposed DNN. In this work, learning rate has been adjusted using a random search optimization method.

It is essential to state that the minimum loss value of a configured DNN has been regarded as a cost function for the optimization technique here. The training for the proposed Bi-LSTM network has been done for 25 epochs. The mini batch size has been kept as 20, whereas the loss function used in the classification is “cross entropy.”

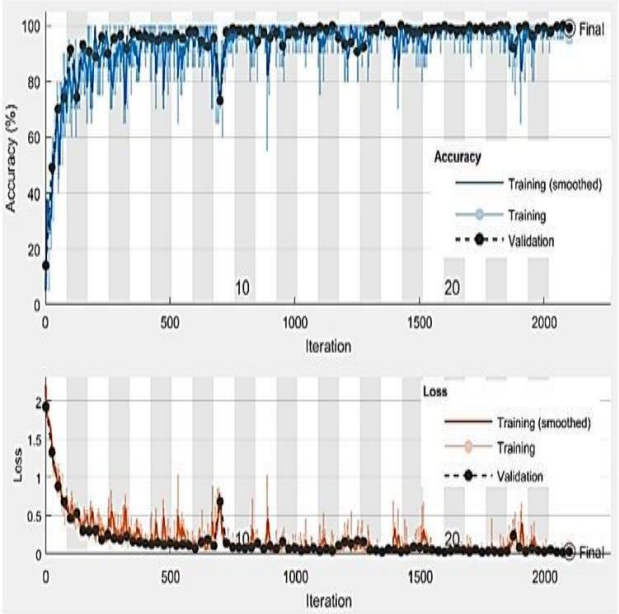

Figure. 3.4. Training performance of configured bi-LSTM network.

The training performance of the proposed DNN has been shown in Figure.3.4. In this Figure. 3.4, the top part shows the accuracy deviations against iteration number, whereas the bottom part indicates the cross-entropy loss of the proposed DNN with iteration number. The time required to train the network is around 4 min. It should be mentioned here that the training time has been computed on a system having an Intel1 Core2 2.5-GHz i5 processor with 8- GB RAM. Performance of the proposed framework is reported in Table. 3.2.

Table.3.2. Performance of proposed framework

Value	Accuracy (%)	Precision (%)	Specificity (%)	F1 score (%)
Minimum	98.333	98.348	99.722	98.339
Maximum	99.047	99.107	99.841	99.052
Mean	98.761	98.797	99.793	98.767
Standard deviation	0.312	0.328	0.051	0.3098

3.3.1. Classification result

In this chapter, the classification result of the suggested framework has been assessed by four metrics, that is the accuracy, precision or sensitivity, specificity, and F1 score. The mathematical expression of the parameters has been presented through the following equations:

$$Accuracy = \frac{TP + TN}{TP + FP + TN + FN} \tag{3.13}$$

$$Sensitivity = \frac{TP}{FP + TP} \tag{3.14}$$

$$Specificity = \frac{TN}{FP + TN} \tag{3.15}$$

$$F1score = \frac{TP}{TP + \frac{(FP + FN)}{2}} \tag{3.16}$$

In (3.13) – (3.16), true positive (TP) and true negative (TN) refers to the appropriately classified PD defects, whereas false negative (FN) and false positive (FP) refers to the incorrectly classified events. The maximum value, minimum value, mean value, and standard deviation of the aforesaid metrics have been summarized in Table.3.2. On the basis of Table.3.2, it can be said that the suggested framework has shown better performance. It is also noticed that the standard deviations of the classification metrics are very low, which indicates robustness of the proposed framework. In Table 3.3, the performance of the suggested feature-based deep learning framework has been compared with standalone deep learning framework. In the standalone deep learning framework, $n-\Delta u$ PD patterns are directly fed to a configured Bi-LSTM network for PD pattern recognition. According to Table.3.3, it can be noticed that the suggested feature-based Bi-LSTM framework has significantly better than the standalone deep learning framework.

Table.3.3. Comparative study with standalone deep learning framework

Method	Accuracy (%)	Precision (%)	Specificity (%)	F1 score (%)
Standalone bi-LSTM	95.63±0.85	95.61±0.86	99.41±0.10	94.34±0.84
Feature-based bi-LSTM	**98.76±0.31**	**98.79±0.33**	**99.79±0.05**	**98.77±0.31**

3.3.2. Comparative study of varying number of hidden units in Bi-LSTM layer

In the suggested DNN, it is important to discover the optimal number of hidden units in the Bi-LSTM layers. Therefore, a rigorous analysis has been performed to identify the optimal configuration. In this rigorous analysis, a number of hidden units in the first Bi-LSTM layer have been varied from 50 to 200 (in step of 50). In addition, the number of hidden units in the second Bi-LSTM layer has been varied from 30 to 60 (in step of 10). From the result presented in Table 3.4, the optimal number of hidden units in the first Bi-LSTM layer is 100, whereas the optimal number of hidden units in the second Bi-LSTM layer is 50.

Table.3.4. Performance analysis varying the number of hidden units

Hidden unit in the 1st layer	**Hidden unit in the 2nd layer**	**Accuracy (%)**
50	30	97.89
	40	97.99
	50	98.11
	60	98.35
100	30	98.43
	40	98.63
	50	**98.76**
	60	98.71
150	30	98.43
	40	98.56
	50	98.51
	60	98.45
200	30	98.33
	40	98.54
	50	98.42
	60	98.32

3.3.3. Analysis with different number of folds

The performance of the suggested framework has also been analysed for different number of fold value. In Figure. 3.5, the performance of the recommended framework has been presented for fold value 2–6. Based on Figure. 3.5, the performance has been increased with fold value and after fivefold, the performance is almost the same. Considering this fact, a fivefold CV procedure has been implemented.

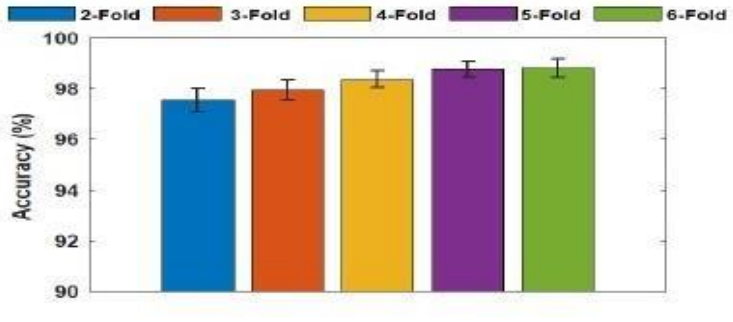

Figure 3.5. Mean recognition performance varying no. of folds.

3.3.4. Comparative study with other deep learning-based approaches

In comparative study, the efficacy of a configured Bi-LSTM network has been compared with other Deep Neural Network (DNN) models like classical LSTM and One-Dimensional (1-D) Convolutional Neural Network (CNN). For this purpose, 1-D CNN and LSTM networks have been configured. For LSTM network, the Bi-LSTM layers in the suggested network (as shown in Figure3.3) have been replaced with LSTM layers (keeping the number of hidden units the same). In contrary, configured 1-D CNN network consists of two convolution layers, two max pooling layers, one dense layer, and a softmax layer. In Table.3.6, PD pattern recognition performance of configured DNNs is presented. It should be mentioned that extracted MM features (as described in Section 3.2.3, Table 3.1) have been used as input to the aforementioned configured DNNs. According to Table.3.5, it can be noticed that the Bi-LSTM-based deep network has outperformed the other deep learning frameworks.

Table.3.5. Comparative study with other deep learning aided approach

Deep learning Method	Accuracy (%)	Precision (%)	Specificity (%)	F1 score (%)
Classical LSTM	98.29±0.46	97.69±0.48	99.61±0.06	97.70±0.44
1-D CNN	98.09±0.61	98.09±0.61	99.67±0.08	98.10±0.60
Proposed Bi-LSTM	**98.76±0.31**	**98.79±0.33**	**99.79±0.05**	**98.77±0.30**

Among other deep learning frameworks, classical LSTM yields better performance followed by 1-D CNN. In order to understand the significant differences among three classifiers (CNN, LSTM, and proposed Bi-LSTM) in terms of classification performances, Tukey–Kramer post-hoc analysis test was performed, which revealed that there are no significant differences between three classifiers indicating that the robust performance of the proposed model.

3.3.5. Comparative study with machine learning based approach

In this section, the proposed framework based on the Bi-LSTM network has been compared with standard machine learning based approaches. In machine learning-based approach, MM features extracted from $n-\Delta u$ PD patterns are subsequently fed to four standard machine learning classifiers, i.e., Gaussian Naive Bayes (GNB), k-nearest neighbourhood (KNN), support vector machine (SVM), and random forest (RF). Here, also fivefold CV technique has been implemented to evaluate the classification performance. Detailed description about the classifiers may be found in [16], [26], [27], and [28]. Based on the results presented in Figure. 3.6, it may be observed that the mean recognition performance of RF is better, while the performance of GNB is inferior. Tukey–Kramer post-hoc analysis was also performed which indicated significant differences in performance with probability ($p < 0.01$) between GNB and RF classifiers. For the rest of the classifiers, no significant variation is observed. However, based on analysis, it has also been observed that the suggested feature-based deep learning framework has significantly outperformed machine learning-based approaches, which signifies robustness of the proposed deep learning framework.

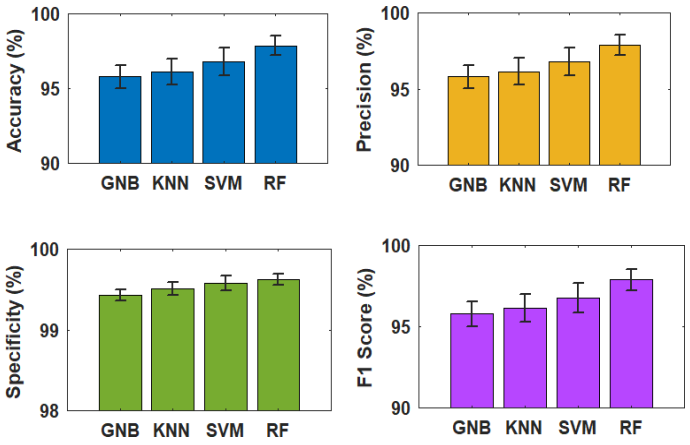

Figure. 3.6. Recognition performance with different machine learning based approach.

3.4. Conclusions

In this chapter, a novel method for automated identification of defects in an insulation system is proposed based on the PD measurement. For this purpose, a sequence of PD pulses has been recorded from three common artificial faults and was consequently, kept in PRPS format. Thereafter, the pattern of PD pulse sequence patterns has been analysed using Mathematical Morphology (MM), and some novel morphological features have been proposed in this work for recognition of PD defects. The features were fed to a deep learning-based proposed Bi-LSTM network for automatic classification and identification. From the result, it can be said that the suggested framework can detect different types of PD defects accurately. Besides the suggested technique yielded better results compared with the other deep learning frameworks. Thereafter, it can be inferred that suggested feature-based Bi-LSTM network can be employed for real-time identification of different types of PD defects in an insulation system.

Chapter 4

Identification and Locating Single and Multiple Partial Discharge Events by Time-frequency Representation aided Deep Transfer Learning Approach

4.1. Introduction

PD measurement through electrical methods is a well-established technique. However, it is difficult to measure PD location through electrical methods. Therefore, researchers have applied "acoustic sensors" [21-23], "optical sensors" [138], "ultrahigh frequency (UHF) sensors" [139], "radio frequency (RF) antennas" [140] for identification and location of PD events. Each technique has its own merits and demerits. It should be mentioned here that sensor-based PD detection techniques have some advantages such as using these sensors PD event can be accurately located without the need for measurements at the place of its occurrence. When PD occurs inside a high voltage equipment, PD sources produce sound waves, which propagate through the insulation. These waves can be detected by the application of acoustic sensors [21,23]. Compared to other techniques, acoustic sensor-based techniques have some advantages, like acoustic sensors are cost-effective, acoustic sensors are immune to external electrical and electromagnetic interference. However, acoustic sensor measurements can be affected by external mechanical noise [20]. Acoustic sensor-based PD source identification and location has been reported in existing literature [20,21,23,138]. In [21], an application of wavelet kernel convolutional neural network (WK-CNN) has been reported to locate PD within a power apparatus. Although the aforesaid method returned promising results in PD detection, it requires high computational cost to train the model. Also, the performance of the aforesaid method under noisy background has not been presented. Considering the shortcomings, this chapter presents a framework to locate PD source within HV equipment employing acoustic sensors. In this work, an experimental setup has been configured where artificial PD events have been emulated inside the Partial Discharge Location Emulator (PDLE) already discussed in chapter 2, which resembles an HV equipment under test. Several acoustic sensors have been placed outside of walls to capture sound waves emitted by the PD sources inside the equipment.

4.2. Analysis of acoustic Partial Discharge

In this section, PD of acrylic disc was measured by acoustic sensor method as discussed in Chapter 2, Section 2.4. The captured PD signatures corresponding to each acoustic sensor are then analysed in a joint time-frequency frame, and the time-frequency representation (TFR) images have been fed to a pre-trained VGGNet16 for automated feature extraction. The application of the pre-trained VGGNet16 allows automated feature extraction from TFR images while eliminating the high computation cost associated with training deep architectures. Finally, the deep features are fed to classifiers for identifying the PD source location. According to the results, this method has shown satisfactory performance in both noise-free and strongly noisy environments.

4.2.1. Time-frequency representation of PD acoustic signals

In Figure2.11 (in Chapter 2), PD acoustic signals (recorded through sensors S1 and S2) correspond to PD events “SPDE1”, “SPDE9”, and “MPDE4” are depicted respectively. Based on the visual inspection of the recorded acoustic signal, it can be said that the characteristics of the acoustic signal change with the PD event location as well as the number of PD sources. Therefore, the PD acoustic signals have been analysed in joint time-frequency space in order to extract some meaningful information through which PD source location can be predicted.

Various methods exist for analysing the time-frequency characteristics of non-stationary signals, as discussed in the literature. One notably popular technique is the Smoothed Pseudo Wigner Ville distribution (SPWVD). This method is particularly relevant in analysing the time-frequency aspects of PD (partial discharge) acoustic signals, which are represented as complex 2-D matrices. These matrices are visualized as time-frequency representation (TFR) plots, offering valuable insights into the location of PD sources. The SPWVD technique introduces cross-term reducing windows simultaneously

in both the time and frequency domains. The mathematical expression of "Smoothed Pseudo Wigner Ville distribution" of PD acoustic signal a(t) can be represented as [20]

$$SPWVD(t, f) = \int_{-\infty}^{\infty} x(\frac{\tau}{2}) x^*(-\frac{\tau}{2}) \int_{-\infty}^{\infty} y(t-t').....$$
$$.....a(t'+\frac{\tau}{2}) a^*(t'-\frac{\tau}{2}) dt' e^{-j2\pi ft} d\tau \quad (4.1)$$

In equation (4.1), *x(t)* signifies a cross-term reducing window in the time domain whereas *y(t*) signifies the window which reduces cross-terms in frequency domain. It is noteworthy to mention here that the length and type of the cross-term reducing windows can be selected independently. These windows, represented by *x(t)* and *y(t)* in equation (4.1), independently allow for the selection of their length and type. Compared to traditional methods like short-time Fourier transform (STFT), continuous wavelet transform (CWT), and Wigner Ville distribution (WVD), SPWVD offers superior time-frequency resolution in TFR image plots due to its unique approach. The resulting TFR image plots after applying SPWVD to PD signals are termed SPWVD images. Figure. 4.1 presents SPWVD images of PD acoustic signals captured from different sensors for various PD events, illustrating the changing characteristics of TFR plots with respect to PD events. To enhance PD location prediction within power apparatus, this chapter proposes a technique based on transfer learning, utilizing TFR image plots as input data.

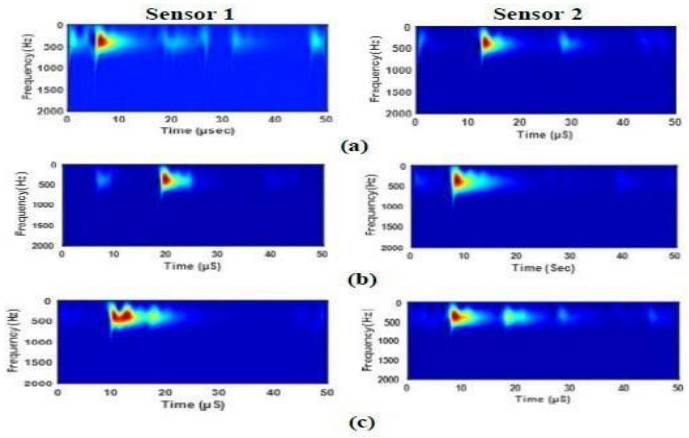

Figure. 4.1. Time-frequency SPWVD images for PD event (a) "SPDE1", (b) "SPDE9" and (c) "MPDE4" respectively.

4.2.2. Automated Deep Feature Extraction using Transfer Learning

In traditional machine learning-based approach, feature extraction from time-frequency representation of PD signal requires manual intervention. This is an unsophisticated process and requires qualitative and quantitative analysis for decision-making [141,142]. In this regard, deep learning has gained popularity. Among the deep learning algorithms, convolutional neural network (CNN) is a popular technique that can learn spatial features in an image adaptively and automatically. Detailed information about CNN can be found out in [9-10]. Although CNN is very efficient in image analysis related tasks, training of CNN from scratch requires massive computational time. Therefore, transfer learning (TL) has been introduced for automated feature extraction from the input TFR image plot of a PD signal. In TL, knowledge learnt previously from a pretrained CNN model can be applied for a new work. The advantage of the TL aided approach is that it can significantly reduce computational time of the model, which is not required to be trained from scratch. In this work, VGGNet16 has been implemented for automated feature extraction. VGGNet16 is a series network comprising 13 convolutional layers, 5 pooling layers and 3 fully connected layers respectively [143].

In the next section, a brief overview of the proposed model has been presented.

4.2.3. Proposed Model

The application of wavelet kernel convolutional neural network (WK-CNN) has been reported for PD location within a power apparatus [21]. Although this method has shown promising results in PD location, it requires high computational cost to train the model. Additionally, the performance of this method under noisy conditions has not been presented. An overview of the proposed framework for PD location within a power apparatus has been depicted in Figure. 4.2. As shown in Figure. 4.2, the proposed framework uses 5 acoustic sensors data (installed at 5 different walls of the PDLE box) for PD localization. In this proposed framework, PD signal acquired from the respective sensor has been converted into an SPWVD image. Thereafter, the SPWVD image corresponding to each sensor has been resized to 227×227×3 dimensions and individually fed to VGGNet16 for automated feature extraction. It should be mentioned here that during feature extraction, the last fully connected layer of VGGNet16 has been removed and feature has been extracted from the fully connected layer "fc6". It is pertinent to mention here that 4096 deep features have been extracted from each SPWVD image correspond to 5 acoustic sensors. The extracted deep feature vectors correspond to 5 sensors have been fused together through average feature fusion. It is pertinent to note here that using the average fusion strategy, the multi-sensor PD data can be effectively synthesized for final classification. Finally, the fused feature vector has been an input to a bidirectional long short memory (Bi-LSTM) network to predict the location of PD sources during single and multiple PD events. It is pertinent to mention here that in a Bi-LSTM network, sequential correlation in a feature vector is analysed in both directions forward (past to future) or backwards (future to past) at each time step [144]. The proposed Bi-LSTM network in the work consists of a sequential "input layer", followed by a "Bi-LSTM layer", "dropout layer", and a "classification layer" with "softmax activation" at the end [145,146]. As the dimension of the fused feature 4096×1, the neuron value of sequential input layer of the Bi-LSTM network is 4096. It should be further noted that the number of hidden units in the Bi-LSTM layer has been taken as 200 whereas the dropout rate in the dropout layer has been kept as 50%. Finally, based on the probabilistic scores obtained in the classification layer, the output class has been predicted.

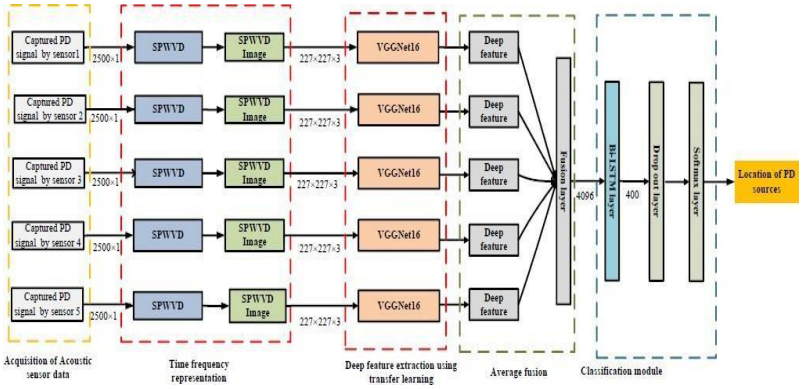

Figure. 4.2. Overview of proposed framework

4.2.4. Training Implementation

In the classification module training, the following training hyper-parameters were set an initial learning rate of 0.001, 60 epochs, a minimum batch size of 40, and utilized the "cross entropy" loss function. Additionally, the Adam optimizer was employed to adjust the learning rate after each iteration. Notably, the training for the classification module was executed on a system configured with an NVidia GTX 1650 GPU and 8 GB of RAM.

4.3. Results and Discussions

4.3.1. Classification Performance Analysis

In this work, a total of 20 set of data have been acquired for each PD event. Additionally, to augment the database and investigate the performance under noisy environment, white Gaussian noise of 20dB, 25dB, 30dB, 35dB, and 40dB signal to noise ratio (SNR) values have been added to each data systematically. Hence, the database consists of 47(no. of PD event)} × 20 (no. of set) × 6 (1 raw data + 5 additive noise levels) =5,640 number of datasets. In order to assess classification performance of the work, it utilized a 5-fold cross-validation technique and classification performance was evaluated using three statistical parameters: accuracy, sensitivity, and specificity. In Table.4.1, classification performance of the proposed approach has been presented.

Table.4.1. Classification performance

Accuracy (%)	Sensitivity (%)	Specificity (%)
98.27±0.65	98.47±0.56	98.13±0.79

4.3.2. Performance analysis under noisy environment

In real life there is a possibility that acoustic sensor data gets contaminated with background noise. Hence, the performance of the proposed approach has been checked under different noise contamination levels. Based on the results given in Table.4.2, it may be noticed that classification performance of the proposed framework has dipped with the noise contamination severity. However, the performance of the proposed framework under the noise background is within the acceptable range. Hence, it may be inferred that the proposed approach can deliver reliable performance in PD source localization within a power apparatus if the recorded acoustic sensor data is contaminated with background noise.

Table.4.2. Performance analysis at different noise level

Noise level(dB)	Accuracy (%)	Sensitivity (%)	Specificity (%)
RAW data	98.84±0.87	99.03±0.75	98.72±0.91
40	98.72±0.72	98.91±0.61	98.58±0.79
35	98.62±0.63	98.83±0.54	98.49±0.71
30	98.29±0.73	98.47±0.67	98.15±0.82
25	97.85±0.54	98.02±0.42	97.67±0.64
20	97.31±0.64	97.54±0.53	97.19±0.75

4.3.3. Performance comparison with other time-frequency representation

In order to obtain better insight about the efficacy of the proposed framework, the performance of the proposed transfer learning approach involving other time-frequency imaging techniques is also being investigated. For this purpose, the TFR images of recorded acoustic PD signals have been obtained through other time-frequency methods such as “Short Time Fourier Transform” (STFT), “Continuous wavelet transform” (CWT) and “Wigner Ville distribution” (WVD), respectively. Thereafter, the TFR plots correspond to five acoustic sensors that are separately fed to VGGNet16 for automated feature extraction. After that, the extracted deep feature vectors

correspond to 5 acoustic sensors and are fused together and fed to the Bi-LSTM network for classification purposes. Based on the result presented in Table.4.3, it can be observed that the proposed SPWVD TFR image aided framework has returned 0.66%, 0.54% and 0.37% better mean accuracy compared to "STFT", "CWT" and "WVD" TFR image aided framework respectively.

Table.4.3. Performance analysis with other time-frequency imaging technique

Time-frequency method	Accuracy (%)
STFT	97.61±0.92
CWT	97.73±0.98
WVD	97.90±0.87
SPWVD	98.27±0.65

4.3.4. Comparison with existing work

In order to establish superiority, the performance of the proposed framework has been compared with existing methods available in the literature where acoustics sensors were employed for locating PD. From the results given in Table.4.4, it can be inferred that the proposed framework gives superior result (in terms of accuracy) compared to existing methods.

Table.4.4. Performance comparison with existing work

Literature	Accuracy (%)
[23]	92.80
[21]	97.64
This chapter	98.27

4.4. Conclusions

This chapter presents an innovative framework to distinguish partial discharge source location within a power equipment. This framework requires acoustic sensors, which can be installed on the outside wall of a power equipment without any constraints. It has been noticed that data acquired by acoustic sensors contains information about the location of PD sources and number of PD sources within power equipment. Hence, the

acoustic PD data has been analysed in time-frequency space and the time-frequency representation has been fed to a transfer learning aided framework to extract relevant information about PD source location. Finally, the extracted features corresponding to each acoustic sensor have been fused together and fed to a train classification module for PD localization. The advantages of the proposed framework are mentioned below,

(a) The proposed framework employs deep transfer learning, which eliminates the requirement of manual feature extraction from time-frequency representation.
(b) As deep transfer learning has been used in this chapter, the problem of high computation time during training of a deep network can be effectively countered.
(c) The proposed framework is very effective under a noisy background. Hence, it is very suitable for real life application.

Therefore, it can be inferred that the proposed framework is very suitable for real life PD localization within power equipment.

Chapter 5

Detection and Locating Single and Multiple Partial Discharge using Novel Deep Learning Framework

5.1. Introduction

PD can occur at both single as well as multiple locations within a HV equipment [21-24]. Considering the advantages as stated earlier, this chapter investigates the feasibility of using optical sensors to locate PD events. The optical PD measurement relies upon detection of the light energy emitted due to various excitation and ionization processes taking place during the occurrence of PD activities [22-24, 148]. Since the emitted light radiations vary with the location of PD sources, hence optical PD measurement can provide key information regarding the location of PD events within the HV equipment. Apart from that, optical PD measurement techniques are also advantageous because of their ability to withstand high temperatures, resistance to chemical corrosion, safety from electric spark, larger bandwidth etc. [22-24, 148]. Moreover, optical PD measurement is immune to noise and electromagnetic interferences (EMI) thereby making it suitable for field measurements [22-24]. Keeping in mind the above advantages, the application of optical sensors for locating PD events has been reported in existing literature [22-24]. However, a major limitation of the aforesaid works is that they rely on manual feature extraction from the signature of optical sensors for locating PD events. Extraction of manual features requires expertise in signal processing and it may generate redundant features, which are very much unsophisticated [143]. Moreover, inability to extract relevant features may lead to poor information about the location of PD events. As a consequence, the reported accuracy of the existing methods is poor. Considering the limitations of the existing methods, a novel deep learning framework is proposed in this chapter for detection and locating the PD sources employing optical sensors. In this present work, an experimental set up has been designed to generate single as well as multiple PD events at different locations within an air insulated steel tank or box known as Partial Discharge Location Emulator (PDLE) mentioned in chapter 2, section 2.5.3. The PD events have been captured using five optical sensors placed on the wall of the tank or box. The captured PD signatures were

initially analysed through a 1-D local binary pattern (1-D LBP) to capture the local information. Therefore, a multi-channel fusion hybrid deep network (MCFCNN-BiLSTM) has been configured for classification of LBP transformed PD signatures. Using this proposed network, Local Binary Pattern (LBP) transformed PD signatures correspond to each optical sensor that have been processed simultaneously and separately through a multi-channel convolutional module. It is important to mention here that each channel of the multi-channel convolutional module can automatically extract meaningful features from the LBP transformed PD signature corresponding to each optical sensor, which can eliminate the problems associated with manual feature extraction. A weighted feature fusion strategy has been introduced in this network to combine the deep features learnt from each single channel. Prior to classification (using softmax activation function), the fused deep features were sequentially passed though the bi-directional long short-term memory (BiLSTM) to boost the recognition performance. It has been observed that a proposed network can accurately detect PD occurring at one location or multiple locations with very high accuracy.

5.2. Optical Partial Discharge Analysis

The Optical Partial Discharge signals are captured by optical sensors are reported in chapter 2, section 2.5.7. The methodology of The Optical Partial Discharge data analysis is illustrated in this section in step by step format.

5.2.1. 1-D Local Binary Pattern

The concept of the 1-D local binary pattern (1-D LBP) used in this work, is derived from the concept of 2-D local binary pattern which is widely used in computer vision for recognition of image textures [149,150]. The fundamental operation of 1-D LBP is similar to the image texture operator, where instead of pixels, data points in a time series are analyzed sequentially. The computation of the 1-D LBP requires selection of a window of particular length (P+1), where P is an even number. For all the data points, lying within the window, a center data point is selected such that it has P/2 data points in its neighbourhood. Now, a binary code of the center data is generated by comparing (thresholding) it with the neighbourhood data points lying within the window [150-152]. The binary code is then converted to a decimal value and the 1-D LBP code of the center element is obtained. The process iteratively traverses along the entire signal in a sequential manner and thus 1-

D LBP code of the entire signal is obtained [150-152]. A mathematical expression to generate the 1-D LBP code of the center element is given by:

$$1DLBP = \sum_{i=1}^{p+1} G(x_i - x_c)2^{i-1} \tag{5.1}$$

where, $G(x_i - x_c) > 1$, if $x_i > x_c$ else, $G(x_i - x_c) = 0$, if $x_i < x_c$.

It is imperative from the above equation that the 1-D LBP code of a time series varies from 0-2*P*. Thus, by using equation (5.1), any time series data can be converted to an LBP domain. Figure. 5.1 shows the computation steps of the1-D LBP code of an exemplary time series with P=8. It should be mentioned here that selection of optimal window length is very important during 1-D LBP operation of a signal. If window length is kept small, then local fluctuations present in a signal can't be captured properly. If a large window size is chosen, then it will provide information about global variation present in a signal rather than the local fluctuations. Considering the fact, in this work window length during the 1-D LBP operation of PD signature has been kept as "9" i.e., P value has been kept as 8. It has been observed that with the P value equal to 8, the local fluctuations present in a PD signature can be captured effectively. In Figure. 5.2, 1-D LBP transformed PD signature (captured from sensor 1) for "SLPD1", "SLPD10", "MLDP1" and "MPLD8" events have been shown respectively. From Figure. 5.2, it is evident that LBP transformed PD signatures are different with respect to type of PD occurrence and PD location. The LBP transformed PD signatures (captured by all sensors) are thereafter fed to a multi-channel fusion hybrid deep network for automated identification and locating of PD events.

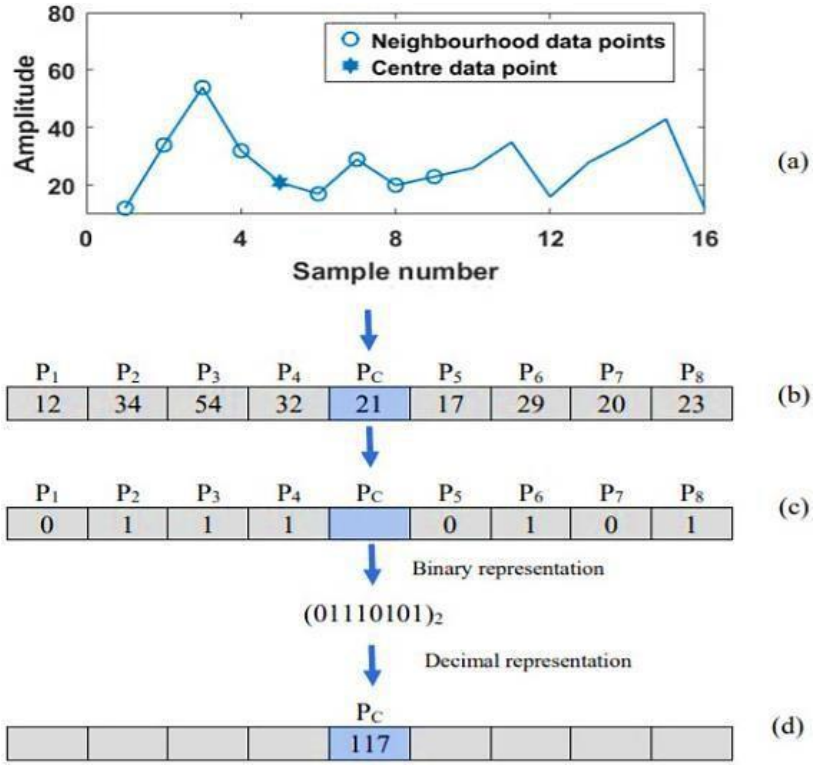

Figure. 5.1. Computation steps of 1-D LBP code (a) an exemplary time series, (b) value of datapoints within the window length, (c) binary code generated by thresholding it with the neighbourhood data points and (d) decimal representation

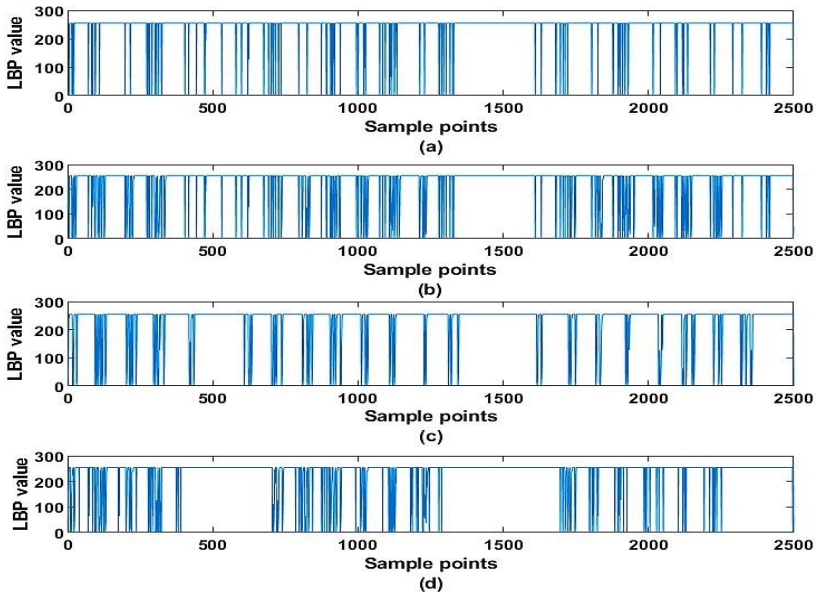

Figure. 5.2. LBP transformed PD signature (captured by sensor 1) for (a) "SLPD1", (b) "SLPD10" (c) "MLPD1"and (d) "MLPD8" event

5.5.2. Convolutional Neural Network (CNN)

Convolutional neural network (CNN) is a popular deep learning algorithm. It has been widely applied in image pattern recognition and signal pattern recognition related problems due to its excellent automated feature learning capability [21, 147, 143]. In CNN, input data (1-D/2-D) can be processed to a new feature representation field through convolutional and pooling operation. In a convolutional layer, 1-D or 2-D data is mapped onto a high dimensional feature map through a series of filter known as "kernel filter" [143, 147,152]. It should be mentioned here that the convolutional layer is very effective for ~~to~~ bringing out inherent information of input data. Following the convolutional layer, the pooling layer reduces the dimension of the convolved feature map and sets up a feature map with a high degree of uniform and spatial structure. Fully connected layer in a CNN has been used as a classifier, which makes the decision based on the feature learned by the convolution/pooling operation. Detailed description of CNN has been avoided in this paper as the concept of CNN is well known. However, more details about CNN have been given in [147].

5.5.3. Bidirectional Long Short Memory (Bi-LSTM)

While CNNs excel at extracting rich information from input data, they lack the ability to analyze the sequential nature of the data. To address this limitation, a hybrid deep network has been developed by integrating CNNs with Bidirectional Long Short-Term Memory (BiLSTM) networks. BiLSTM, an extension of the traditional LSTM architecture, enhances the capability of capturing sequential patterns by incorporating two LSTM cells operating in opposite directions [153-155]. Unlike traditional LSTMs, which only capture sequential characteristics in one direction, BiLSTM can analyze input sequences both forwards and backwards at each time step. In this hybrid framework, BiLSTM is utilized to analyze the sequential features of CNN-extracted deep features in both directions.

5.5.4. Proposed Network Configuration

In this chapter, an end-to-end multi-channel fusion hybrid deep network (MCFCNN-BiLSTM) has been proposed for accurate identification and finding the location of PD events employing PD signature captured by an optical sensor. A schematic diagram of the proposed "MCFCNN-BiLSTM" network has been given in Figure. 5.3. From Figure. 5.3, it can be noticed that the proposed network consists of five-channel convolution modules. It is worth mentioning here that the LBP transformed PD signature (obtained after 1-D LBP operation of captured PD signature) corresponds to each sensor has been given as input to the respective channel of the multi-channel convolution module. The idea behind this multi-channel convolution module is that through each channel, LBP transformed PD signature corresponding to the respective sensor can be processed independently and simultaneously for automated feature learning. In this multi-channel convolution module, the convolutional structure of each channel has been kept identical i.e., each channel utilizes four 1-D convolutional layers and two 1-D maxpooling layers. An overview of the convolutional structure has been depicted in Figure. 5.4 in this chapter. It should be mentioned here that in the 1-D convolutional layers, the kernel filter size has been kept as "1×4" whereas the number of kernel filters has been kept as "32", "32", "64" and "64" respectively.The pooling window size (PS) of the 1-D maxpooling layer has been kept as "2". It should be mentioned here that in max pooling, the feature with maximum value within a pooling window has been selected. After the convolutional and pooling operation, the pooling output has been expanded into 1-D feature vector by the flatten layer.

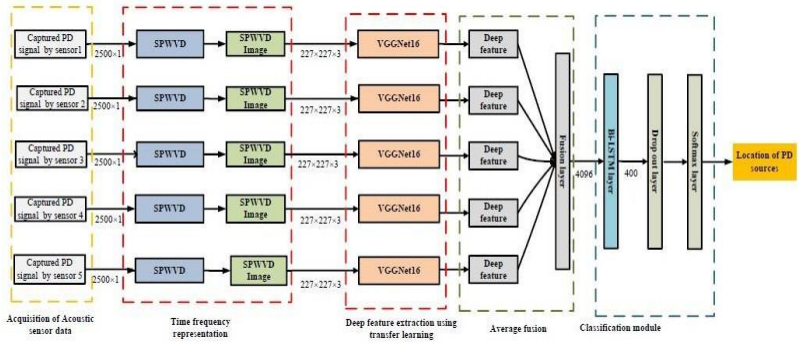

Figure. 5.3. Architecture of proposed "MCFCNN-BiLSTM" network

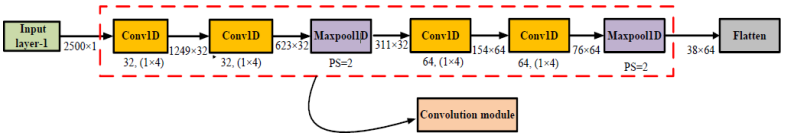

Figure. 5.4. Overview of a convolution module

Thereafter, flattened output corresponds to each channel has been fused together through a fusion layer. The fused output "v" can be mathematically expressed as:

$$v = \sum_{i=1}^{5} w_i . u_i \tag{5.2}$$

In equation (5.2), "u_i" is the flattened output corresponding to i^{th} channel whereas "w_i" indicates the fusion weight of the flattened output "u_i". It is worth mentioning here that the fusion weight of channel has been learned during the training process. It should be mentioned here that through the weighted fusion strategy, the multi-sensor PD data can be effectively synthesized for final classification. After this fusion, the fused output is fed to a BiLSTM layer where sequential correlation of the fused output has been learned. Here, it's important to highlight the configuration of the BiLSTM

layer. The State activation function is set to "tanh" while the Gate activation Function is set to "sigmoid". Additionally, the BiLSTM layer is configured with 200 hidden units. Subsequently, the output of the BiLSTM layer is passed to two consecutive fully connected layers. The first fully connected layer consists of 100 hidden units, while the number of hidden units in the last fully connected layer matches the number of classes in the classification problem. Finally, the softmax layer utilizes the probabilistic scores from the last fully connected layer to predict the output classes.

5.5.5. Training Implementation

The "MCFCNN-BiLSTM" architecture was developed within the PyTorch v1.7.1 framework. Training took place on a system equipped with an Intel(R) Core(TM) i7-2.2 GHz processor, 8 GB RAM, and a 4 GB NVIDIA GTX graphics card. Hyperparameters such as the learning rate (1e-3), minibatch size (60), and loss function (cross entropy) were set prior to training. The Adam optimizer was utilized for optimization, with the loss function updated after each iteration. To prevent overfitting, an early stopping technique was applied, wherein training ceased if there was no significant reduction in validation loss (≥0.002) over 10 consecutive epochs. This technique effectively mitigated overfitting concerns. Additionally, a 5-fold cross-validation approach was employed to assess the network's validation performance. This involved partitioning the database into 5 subsets, with 4 used for training and 1 for validation in each fold. The evaluation was based on the weights obtained from the epoch with the lowest validation loss. The training duration for the "CP1," "CP2," and "CP3" classification problems was approximately 15 minutes and 37 seconds, 14 minutes and 51 seconds, and 15 minutes and 14 seconds, respectively.

5.5.6. Performance Metric

In order to evaluate performance of each classification problem, three metrics namely, accuracy (Acc), Precision (Pre), and specificity (Spe) have been applied. Mathematical formulae of the aforesaid metrics have been described using (5.3) - (5.5) as:

$$(Acc)(\%) = \frac{TN + TP}{TN + TP + FP + FN} \times 100 \tag{5.3}$$

$$(spe)(\%) = \frac{TN}{FP + TN} \times 100 \tag{5.4}$$

$$(Sen)(\%) = \frac{TP}{TP + FN} \times 100 \tag{5.5}$$

Here, "*TN*" and "*TP*" indicate the "Truly-Negative or falsely-classified" and "Truly-Positive or correctly-classified cases, respectively. Similarly, "*FN*" and "*FP*" represent the corresponding false-negative and false-positive conditions, respectively. Hence, the metrics can be computed from the confusion matrices obtained for the respective classification problems.

5.6. Results and Discussions

5.6.1. Classification Result

This section reports the results and statistical analysis of the proposed framework for each classification problem (reported in Table.5.1). A 5-fold classification strategy has been adopted in this study, performance metrics have been reported (in Table.5.1) in terms of their mean and standard deviation values. Based on the results presented in Table.5.1, it can be said that the proposed framework can accurately identify whether the PD is occurring at one location or multiple locations within an insulated system. It has been also observed that the accuracy of correctly identifying the location of PD sources for both SLPD and MLPD events is also very high. Compared to MLPD, the accuracy of PD location classification is marginally better for SLPD events. This may be explained by the fact that the presence of two PD sources in a close vicinity resulted in some misclassifications in location classification for MLPD events, which is absent in the case of SLPD events. However, as far as accuracy and other metrics are concerned, the overall performance of the proposed framework is very much acceptable. Additionally, it has been observed that the standard deviation values of the performance metrics are very small, which suggests that the proposed framework is very robust. Hence proposed framework can be implemented in real-time to identify and localize the single and multiple PD sources within an air-insulated system like HV switchgears, bus bar panels, cable termination boxes etc.

Table 5.1. Performance of proposed "MCFCNN-bilstm" network

CP	Acc (%)	Spe (%)	Sen (%)
CP1	99.17 ± 0.27	99.00 ± 0.59	99.35 ± 0.53
CP2	98.61 ± 0.49	98.54 ± 0.68	98.83 ± 0.57
CP3	97.58 ± 0.65	97.35 ± 0.86	97.82 ± 0.79

5.6.2. Comparative analysis of varying the Kernel Filter Size

The size of a kernel filter can affect the feature learning capability of model [147]. If the size of the kernel filter is small, it can cause information loss. Whereas large kernel filter can cause redundant computation and increases the computational complexity of a model [147]. Hence, the performance of the proposed network (for each classification problem) has been investigated varying the kernel filter size from "1×1" to "1×6". It may be observed from Figure. 5.5, that accuracy of the proposed network increases at first and then becomes steady. This observation is true for all classification problems. However, the training time of a proposed network increases with the increment of kernel filter size. Considering this issue, the kernel filter size in the proposed "MCFCNN-BiLSTM" network has been considered as "1×4".

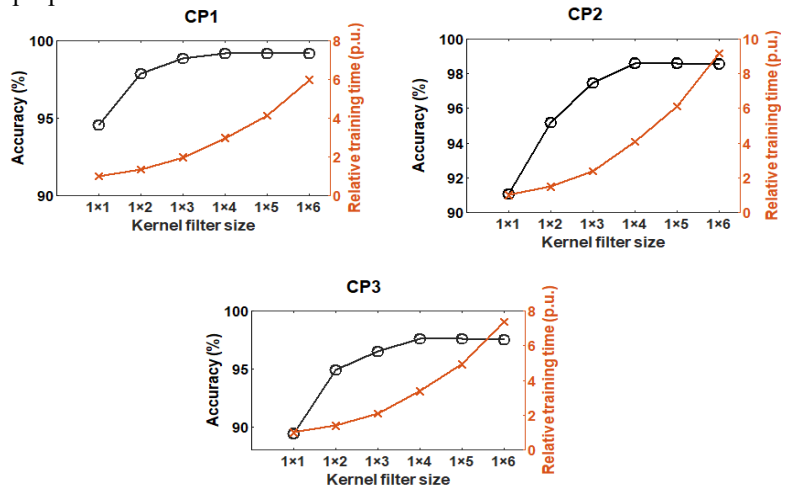

Figure. 5.5. Performance analysis varying kernel size for the proposed "MCFCNN-BiLSTM" network

5.6.3. Impact of Local Binary Transformation

In this section, the effectiveness of the 1-D LBP transformation has been investigated for each classification task. For this purpose, the performance of the proposed "MCCNN-BiLSTM" network has been investigated with raw PD signatures obtained from each PD sensor as input. According to the result presented in Table.5.2, it can be inferred that the proposed "MCFCNN-BiLSTM" network yields better classification accuracy (for all classification problems) with LBP transformed PD signature as input. This is because in LBP transformed PD signature, local fluctuations present in a PD signature can be captured effectively which aided in improved recognition performance. Therefore, it can be said that the1-D LBP transformation strategy adopted in this work is effective and impactful.

Table.5.2: Comparison with "Raw data" as input to proposed network

Input applied to proposed network	Mean Accuracy (%)		
	CP1	CP2	CP3
Raw PD signature	90.38	89.77	88.83
LBP transformed PD signature	99.17	98.61	97.58

5.6.4. Comparison with existing methods

The performance of the proposed framework is compared with some existing methods where optical sensors have been employed for PD detection. It is evident from Table 5.3, that the proposed framework is better than all existing methods in terms of PD detection accuracy. This is because, unlike the existing methods, the proposed framework utilizes a multi-channel convolution module for automated feature extraction. This has resulted in rich and relevant feature extraction from each sensor data compared to the existing methods where mere handcrafted feature extraction method has been employed. So, the proposed method is superior compared to the existing methods which is evident from the results given in Table.5.3.

Table.5.3: Comparative analysis with existing methods

Reference	Feature extraction mode	Accuracy (%)
[22]	Manual	87.3
[23]	Manual	92
[24]	Manual	95.6
This work	Automated	99.17

5.7. Conclusions

In the present work, an automated framework using muti-channel fusion hybrid MFCNN-BiLSTM deep network is proposed for identification and finding the location of PD events employing the signatures obtained from five wall mounted optical sensors. It has been observed that PD signatures obtained from optical sensors contain significant information which can be used to detect the type as well as the location of PD events. It has been also revealed that 1-D LBP is capable of capturing meaningful information from PD signatures on a local scale which aid in better classification accuracy. Using the proposed method, accuracy of 99.17% is obtained for classification of SLPD and MLPD events. Considering the PD localization problem, an accuracy of 98.61% and 97.58% has been obtained for location classification of SLPD and MLPD events, respectively. In comparison with different variants of multi-channel fusion deep network, the performance of the proposed "MCFCNN-BiLSTM" network has been found to be superior. Thus, the proposed framework can be implemented to develop an automated system for identification of the type of PD event as well as localization of the PD events. The advantage of the proposed method is that it can be mounted on the wall of HV equipment without any significant alteration of the normal operation. However, one limitation of the proposed PD detection framework is that it is applicable for PD detection inside an air insulated HV equipment only and cannot be used for PD detection inside an opaque medium. Moreover, in this study, only void discharge was chosen as an emulated PD source, other common PD sources like corona and surface discharge is not considered in this work. In the future, the proposed method will be validated on other PD sources to determine the efficacy of the proposed method. Also, the trained hybrid deep learning model will be implemented in hardware using either a microcontroller or FPGA based low-cost embedded system for automated detection of type and location of PD events inside any HV equipment at site.

Chapter. 6

Conclusions and Future Scope of work

6.1. Conclusions

This thesis has investigated various techniques for the detection and measurement of partial discharges (PD) in electrical systems. The research aimed to contribute to the enhancement of PD diagnostics, which are critical for ensuring the reliability and safety of high voltage equipment. The analysis of electrical measurement techniques revealed the effectiveness of traditional PD detection methods such as electrical impedance measurement and apparent charge measurement. However, challenges such as interference from background noise and sensitivity to system parameters necessitate the development of advanced signal processing algorithms to improve detection accuracy and reliability. Through a comprehensive literature review and experimental studies, a range of PD detection methods, including electrical, optical, and acoustic techniques have been explored. The findings suggest that each method possesses unique advantages and limitations, and the selection of the most suitable technique depends on factors such as application requirements, system configuration, and environmental conditions.

In this study, pulse sequence analysis, optical, and acoustic sensor-based methods for partial discharge (PD) detection in high voltage systems have been explored. The research aimed to advance PD detection techniques, which are crucial for ensuring the reliability and safety of electrical infrastructure. Through extensive literature review and experimental investigations, these have demonstrated the efficacy of pulse sequence analysis techniques in detecting and characterizing PD events. Advanced signal processing algorithms are employed to extract valuable information from the recorded signals, enabling accurate identification and localization of PD sources.

Furthermore, this study investigated the potential of optical and acoustic sensors as alternative means for PD detection. It is found that these sensors offer distinct advantages, such as non-intrusiveness and high sensitivity, making them promising methods for future PD monitoring systems. The integration of multiple sensing modalities, such as combining electrical measurements with optical or acoustic sensors, holds great potential for enhancing the accuracy and reliability of PD detection systems. By

comparing the objectives, applications, accuracy, analysis and advantages of different techniques of PD detection, it can achieve a more comprehensive understanding of PD phenomena and improve the effectiveness of condition monitoring strategies.

6.2. Future scope of work

Overall, the findings presented in this thesis underscore the importance of continued research and development in the field of PD detection. By advancing our understanding of PD phenomena and exploring innovative sensing technologies, it can enhance the reliability and efficiency of high voltage systems, ultimately contributing to the sustainable operation of modern electrical grids. Future research directions may include further optimization of signal processing algorithms, validation of sensor performance in real-world conditions, and integration of multiple sensing modalities for comprehensive PD monitoring solutions. Additionally, our investigation into optical and acoustic PD detection methods demonstrated their potential for non-intrusive and remote monitoring of PD activity. These methods offer advantages such as high sensitivity, spatial resolution, and the ability to operate in harsh environments, making them promising methods for future PD diagnostics applications.

Finally, this thesis has provided valuable insights into PD detection and measurement techniques, highlighting the importance of continued research and development. By advancing our understanding of PD phenomena and exploring innovative sensing technologies, it can minimize the risks associated with insulation degradation, minimize downtime, and enhance the reliability of electrical systems. Future research directions may include further optimization of sensor performance, validation of techniques in real-world operating conditions, and the development of advanced data analysis methodologies for predictive maintenance applications.

References

[1] O. Kessler, "The importance of partial discharge testing: PD testing has proven to be a very reliable method for detecting defects in the insulation system of electrical equipment and for assessing the risk of failure," IEEE Power Energy Mag., vol. 18, no. 2, pp. 62–65, 2020.

[2] High-voltage test techniques – Partial discharge measurements, IEC 60270:2000, 2000.

[3] W. J. K. Raymond *et al,* "Partial discharge classifications: review of recent progress," Measurement, vol. 68, pp. 164–181, 2015.

[4] M. G. Danikas, N. Gao, and M. Aro, "Partial discharge recognition using neural networks: A review,"Electr. Eng., vol. 85, no. 2, pp. 87–93, 2003.

[5] A. Mas'ud *et al,* "Artificial Neural Network Application for Partial Discharge Recognition: Survey and Future Directions," Energies, vol. 9, no. 8, p. 574, Jul. 2016.

[6] Barrios *et al,* "Partial discharge classification using deep learning methods—survey of recent progress," Energies, vol. 12, no. 13, p. 2485, Jun. 2019.

[7] B. Chatterjee, "Studies on some novel aspects of measurement and data acquisition techniques in HV systems," Ph.D. dissertation, Jadavpur Univ., Kolkata, India, 2009.

[8] Suganya Govindarajan, Adolfo Morales, Jorge Alfredo Ardila-Rey, Narasimman Purushothaman,"A review on partial discharge diagnosis in cables: Theory, techniques, and trends, Measurement", Elsevier, Volume 216,2023.

[9] C. Pan, J. Tang, and K. Wu, "The effect of PD process on the accumulation of surface charges," IEEE Trans. Plasma Sci., vol. 44, no. 11, pp. 2545–2552, Nov. 2016.

[10]A. Mas'ud, J. Ardila-Rey, R. Albarracin, and F. Muhammad-Sukki,"An ensemble-boosting algorithm for classifying partial discharge defects in electrical assets," Machines, vol. 5, no. 3, p. 18, Aug. 2017.

[11]H. R. Mirzaei, A. Akbari, and M. Allahbakhshi, "Partial discharge identification using pulse sequence analysis and neural network," in Proc. 16th Int. Symp. High Voltage Eng., Johannesburg, South Africa, 2009, pp. 1–4.

[12]J. Jiang, B. Zhang, Z. Li, P. Ranjan, J. Chen, and C. Zhang, "Partial discharge features for power electronic transformers under high-frequency pulse voltage," IEEE Trans. Plasma Sci., vol. 49, no. 2, pp. 845–853, Feb. 2021.

[13]C.-K. Chang, H.-H. Chang, and B. K. Boyanapalli, “Application of pulse sequence partial discharge based convolutional neural network in pattern recognition for underground cable joints,” IEEE Trans. Dielectr. Electr. Insul., vol. 29, no. 3, pp. 1070–1078, Jun. 2022.

[14]A. A. Mas’ud, B. G. Stewart, S. G. McMeekin, and A. Nesbitt, “Partial discharge pattern classification for an oil-pressboard interface,” in Proc. IEEE Int. Symp. Electr. Insul., San Juan, PR, USA, Jun. 2012, pp. 122–126.

[15]D.-H. Oh, H.-S. Kim, and B.-W. Lee, “Novel diagnostic method of DC void discharge in high temperature superconducting cable based on pulse sequence analysis,” IEEE Trans. Appl. Supercond., vol. 30, no. 4, pp. 1–5, Jun. 2020.

[16]X. Zhang et al., “Review on detection and analysis of partial discharge along power cables,” Energies, vol. 14, no. 22, p. 7692, Nov. 2021.

[17]V. Basharan, W. I. Maria Siluvairaj, and M. Ramasamy Velayutham,“Recognition of multiple partial discharge patterns by multi-class support vector machine using fractal image processing technique,” IET Sci., Meas. Technol., vol. 12, no. 8, pp. 1031–1038, Nov. 2018.

[18]S. Lu, H. Chai, A. Sahoo, and B. T. Phung, “Condition monitoring based on partial discharge diagnostics using machine learning methods: A comprehensive state-of-the-art review,” IEEE Trans. Dielectr. Electr. Insul., vol. 27, no. 6, pp. 1861–1888, Dec. 2020.

[19]S. Chakravorti, D. Dey and B. Chatterjee, “Recent Trends in the Condition Monitoring of Transformers Power Systems,” London: Springer, 2013.

[20]S. S. Roy and S. Chatterjee, "Partial Discharge Detection Framework Employing Spectral Analysis of Horizontal Visibility Graph," IEEE Sensors J., vol. 21, no. 4, pp. 4819-4826, 2021.

[21]B. Ganguly et al., "Wavelet Kernel-Based Convolutional Neural Network for Localization of Partial Discharge Sources Within a Power Apparatus," IEEE Trans. Ind. Informat., vol. 17, no. 3, pp. 1831-1841, 2021.

[22]S. Biswas, C. Koley, B. Chatterjee and S. Chakravorti, "A methodology for identification and localization of partial discharge sources using optical sensors," IEEE Trans. Dielect. Elect. Insul., vol. 19, no. 1, pp. 18-28, 2012.

[23]S. Biswas, D. Dey, B. Chatterjee and S. Chakravorti, "An approach based on rough set theory for identification of single and multiple partial discharge source," International Journal of Electrical Power & Energy Systems, vol. 46, pp. 163-174, 2013.

[24]S. Bag, A. K. Pradhan, S. Das, S. Dalai and B. Chatterjee, "S-Transform Aided Random Forest Based PD Location Detection Employing Signature of Optical Sensor," IEEE Trans. Power Del., vol. 34, no. 4, pp. 1261-1268, 2019.

[25]M. R. Hussain, S. S. Refaat and H. Abu-Rub, "Overview and Partial Discharge Analysis of Power Transformers: A Literature Review," in *IEEE Access*, vol. 9, pp. 64587-64605, 2021.

[26]G. A. Hussain, W. Hassan, F. Mahmood, M. Shafiq, H. Rehman and J. A. Kay, "Review on Partial Discharge Diagnostic Techniques for High Voltage Equipment in Power Systems," in *IEEE Access*, vol. 11, pp. 51382-51394, 2023.

[27]J. M. Rodríguez-Serna, R. Albarracín-Sánchez, F. Garnacho, F. Álvarez and J. Ortego, "Partial Discharges Measurements for Condition Monitoring and Diagnosis of Power Transformers: A Review," *2019 6th International Advanced Research Workshop on Transformers (ARWtr)*, Cordoba, Spain, 2019, pp. 83-88

[28]N. Rosle, N. A. Muhamad, M. N. K. H. Rohani and M. K. M. Jamil, "Partial Discharges Classification Methods in XLPE Cable: A Review," in *IEEE Access*, vol. 9, pp. 133258-133273, 2021.

[29]R. Schwarz and M. Muhr, “Experience with optical partial discharge detection,” Mater. Sci.-Poland, vol. 27, no. 4/2, pp. 1140–1146, 2009.

[30]S. Govindarajan *et al*., "Development of Hankel Singular-Hypergraph Feature Extraction Technique for Acoustic Partial Discharge Pattern Classification", Energies, vol. 14, no. 6, 2021.

[31]S. Biswas, D. Dey, B. Chatterjee, and S. Chakravorti, “Cross-spectrum analysis based methodology for discrimination and localization of partial discharge sources using acoustic sensors,” IEEE Trans. Dielect. Elect. Insul., vol. 23, no. 6, pp. 3556–3565, 2016.

[32]R. Ghosh, B. Chatterjee and S. Dalai, "A method for the localization of partial discharge sources using partial discharge pulse information from acoustic emissions," in *IEEE Transactions on Dielectrics and Electrical Insulation*, vol. 24, no. 1, pp. 237-245, Feb. 2017.

[33]S. Polisetty, A. El-Hag, and S. Jayram, “Classification of common discharges in outdoor insulation using acoustic signals and artificial neural network,” High Volt., vol. 4, no. 4, pp. 333–338, Dec. 2019.

[34]M. Kunicki and D. Wotzka, “A Classification Method for Select Defects in Power Transformers Based on the Acoustic Signals,” Sensors, vol. 19, no. 23, p. 5212, Nov. 2019.

[35]M. Harbaji, K. Shaban, and A. El-Hag, “Classification of common partial discharge types in oil-paper insulation system using acoustic signals,” IEEE Trans. Dielectr. Electr. Insul., vol. 22, no. 3, pp. 1674–1683, Jun. 2015.

[36]C. Boya, M. Ruiz-Llata, J. Posada, and J. A. Garcia-Souto,“Identification of multiple partial discharge sources using acoustic emission technique and blind source separation,” IEEE Trans. Dielectr. Electr. Insul., vol. 22, no. 3, pp. 1663–1673, Jun. 2015.

[37]Xing, C.; Zang, Q.; He, R.; Zhao, J.; Wang, L.; Dai, L.; Shi, R.; Wang, S.; Ma, G. Phase Stability Control of Optical Fiber Partial Discharge Ultrasonic Sensing System. *Sensors* **2022**, *22*, 8495.

[38]Y. Wang *et al*, “Multi-scale analysis and pattern recognition of ultrasonic signals of PD in a liquid/solid composite of an oil-filled terminal,” Energies, vol. 13, no. 2, p. 366, Jan. 2020.

[39]E. T. Iorkyase, C. Tachtatzis, I. A. Glover, and R. C. Atkinson, “RF based location of partial discharge sources using received signal features,” High Volt., vol. 4, no. 1, pp. 28–32, Mar. 2019.

[40]E. T. Iorkyase *et al*, “Improving RF-based partial discharge localization via machine learning ensemble method,” IEEE Trans. Power Deliv., vol. 34, no. 4, pp. 1478–1489, Aug. 2019.

[41]S. Anjum, S. Jayaram, A. El-Hag, and A. N. Jahromi, “Detection and classification of defects in ceramic insulators using RF antenna,” IEEE Trans. Dielectr. Electr. Insul., vol. 24, no. 1, pp. 183–190, Feb. 2017.

[42]Z. Li *et al*, "UHF partial discharge localization algorithm based on compressed sensing," IEEE Trans. Dielectr. Electr. Insul., vol. 25, no. 1, pp. 21–29, Feb. 2018.

[43]C. Boya, G. Robles, E. Parrado-Hernández, and M. Ruiz-Llata, "Detection of partial discharge sources using UHF sensors and blind signal separation," Sensors, vol. 17, no. 11, p. 2625, Nov. 2017.

[44]H. Hou, G. Sheng, S. Li, and X. Jiang, "A novel algorithm for separating multiple PD sources in a substation based on spectrum reconstruction of UHF signals," IEEE Trans. Power Deliv., vol. 30, no. 2, pp. 809–817, Apr. 2015.

[45]Álvarez, F.; Garnacho, F.; Ortego, J.; Sánchez-Urán, M.Á. Application of HFCT and UHF Sensors in On-Line Partial Discharge Measurements for Insulation Diagnosis of High Voltage Equipment. *Sensors* **2015**, *15*, 7360-7387.

[46]C. Boya, G. Robles, E. Parrado-Hernández, and M. Ruiz-Llata, "Detection of partial discharge sources using UHF sensors and blind signal separation," Sensors, vol. 17, no. 11, p. 2625, Nov. 2017.

[47]X. Zhou *et al,* "Research on transformer partial discharge UHF pattern recognition based on CNN-lSTM," Energies, vol. 13, no. 61, pp. 1–13, Dec. 2019.

[48]Uwiringiyimana, Jean Pierre & Khayam, Umar & Harjo, Suwarno & Montanari, Gian. (2022). Comparative Analysis of Partial Discharge Detection Features Using a UHF Antenna and Conventional HFCT Sensor. IEEE Access. PP. 1-1. 10.1109/ACCESS.2022.3212746.

[49]A. Pfeffer, S. Coenen, S. Tenbohlen, Sacha. M. Markalous, T. Strehl: "Onsite experiences with multi-terminal IEC PD measurements and UHF PD measurements", Proceedings 17th ISH, Cape Town, South Africa, 2009.

[50]A. Pfeffer, S. Tenbohlen, and S. Kornhuber, ''Pulse-sequence analysis of partial discharges in power transformers,'' in Proc. 17th Int. Symp. High Voltage Eng., Dec. 2011, pp. 1–5.

[51]Hoof, Martin and Rainer Patsch. “Analyzing partial discharge pulse sequences-a new approach to investigate degradation phenomena.” *Proceedings of 1994 IEEE International Symposium on Electrical Insulation* (1994): 327-331.

[52]M.Hoof, R. Patsch Pulse-sequence analysis: a new method for investigating the physics of PD-induced ageing. IEE Proceedings - Science, Measurement and Technology, Volume 142, Issue 1, 1995 , p. 95 – 101

[53]Patsch, Rainer and F. Berton. “Pulse Sequence Analysis - a diagnostic tool based on the physics behind partial discharges.” *Journal of Physics D* 35 (2002): 25-32.

[54]C. -K. Chang, H. -H. Chang and B. K. Boyanapalli, "Application of Pulse Sequence Partial Discharge Based Convolutional Neural Network in Pattern Recognition for Underground Cable Joints," in *IEEE Transactions on Dielectrics and Electrical Insulation*, vol. 29, no. 3, pp. 1070-1078, June 2022

[55]Lee, G.-Y.; Kim, N.-H.; Kim, D.-E.; Kil, G.-S.; Kim, S.-W. The Design, Fabrication, and Evaluation of a Phase-Resolved Partial Discharge Sensor Embedded in a MV-Class Bushing. *Sensors* **2023**, *23*, 9844.

[56]R. Yao *et al*, “A New Discharge Pattern for the Characterization and Identification of Insulation Defects in GIS,” Energies, vol. 11, no. 4, p. 971, Apr. 2018.

[57]Patsch, Rainer & Berton, Farhad. (2001). Pulse Sequence Analysis - a diagnostic tool based on the physics behind partial discharges. Journal of Physics D: Applied Physics. 35. 25. 10.1088/0022-3727/35/1/306.

[58]R. Patsch. “Pulse sequence analysis - what does it tell us about multiple discharge sites?” Seventh International Conference on Dielectric Materials, Measurements and Applications, 1996, p. 133 – 136.

[59] Iwata, Shinya and Ryota Kitani. “Phase-resolved partial discharge analysis of different types of electrode systems using machine learning classification.” *Electrical Engineering* 103 (2021): 3189 - 3199.

[60] Altenburger, R & Heitz, Christoph & Timmer, Jens. (2002). Analysis of phase-resolved partial discharge patterns of voids based on a stochastic process approach. Journal of Physics D: Applied Physics. 35. 1149. 10.1088/0022-3727/35/11/309.

[61] Kasinathan, Elanseralathan and Amit Mahajan. “Phase Resolved PD Patterns In Electric Treeing.” (2020).

[62] Suwarno, "Phase resolved measurement and simulation of partial discharges in solid and liquid insulating materials," *Proceedings of 2014 International Symposium on Electrical Insulating Materials*, Niigata, Japan, 2014

[63]T. Shahsavarian *et al*., "A Review of Knowledge-Based Defect Identification via PRPD Patterns in High Voltage Apparatus," in *IEEE Access*, vol. 9, pp. 77705-77728, 2021.

[64]M. Karimi, M. Majidi, H. MirSaeedi, M. M. Arefi and M. Oskuoee, "A Novel Application of Deep Belief Networks in Learning Partial Discharge Patterns for Classifying Corona, Surface, and Internal Discharges," in *IEEE Transactions on Industrial Electronics*, vol. 67, no. 4, pp. 3277-3287, April 2020.

[65] Strachan, Scott & Rudd, S. & McArthur, Stephen & Judd, Martin & Meijer, S. & Gulski, E.. (2008). Knowledge-based diagnosis of partial discharges in power transformers. Dielectrics and Electrical Insulation, IEEE Transactions on. 15. 259 - 268.

[66] Thayoob, Yasmin Hanum Md et al. “Characterization of Phase Resolved Partial Discharge waveforms from instrument transformer using statistical signal processing technique.” *2015 IEEE International Conference on Signal and Image Processing Applications (ICSIPA)* (2015): 355-360.

[67] Okamoto, Tatsuki and Masafumi Yashima. “Partial discharge characteristics on applied sine wave voltage frequency with IEC(b) electrode system.” *2017 3rd International Conference on Condition Assessment Techniques in Electrical Systems (CATCON)* (2017): 355-360.

[68]S. Misak *et al*, "A novel approach of partial discharges detection in a real environment," *Int. Conf. Environ. Electr. Eng. (EEEIC),* 2016.

[69]P. Xie, "Analysis of fault of insulation aging of oiled paper of a largescale power transformer and the prediction of its service life," IEEJ Trans. Electr. Electron. Eng., vol. 14, no. 8, pp. 1139–1144, Aug. 2019.

[70]Y. Jia and Y. Zhu, "Partial discharge pattern recognition using variable predictive model-based class discrimination with kernel partial least squares regression," IET Sci. Meas. Technol., vol. 12, no. 3, pp. 360–367, May 2018.

[71]L. S. Lumba, U. Khayam, and R. Maulana, "Design of pattern recognition application of partial discharge signals using artificial neural networks," *Int.Conf. Electr. Eng. Informatics (ICEEI),* 2019, pp. 239–243.

[72]T. R. Sukma *et al,* "Classification of partial discharge sources using waveform parameters and phase-resolved partial discharge pattern as input for the artificial neural network," *Int. Conf. Cond. Monit. Diagnosis (CMD),* 2018.

[73]A. A. Soltani and A. El-Hag, "Denoising of radio frequency partial discharge signals using artificial neural network," Energies, vol. 12, no.18, p. 3485, Sep. 2019.

[74]S. Kainaga, A. Pirker, and U. Schichler, "Identification of partial discharges at DC voltage using machine learning methods," *Int. Symp. High Volt. Eng. (ISH),* 2017.

[75]G. Luo, D. Zhang, K. J. Tseng, and J. He, "Impulsive noise reduction for transient earth voltage-based partial discharge using wavelet-entropy," IET Sci. Meas. Technol., vol. 10, no. 1, pp. 69–76, Jan. 2016.

[76]S. Polisetty, A. El-Hag, and S. Jayram, "Classification of common discharges in outdoor insulation using acoustic signals and artificial neural network," High Volt., vol. 4, no. 4, pp. 333–338, Dec. 2019.

[77]A. Dobrzycki, S. Mikulski, and W. Opydo, “Using ANN and SVM for the detection of acoustic emission signals accompanying epoxy resin electrical treeing,” Appl. Sci., vol. 9, no. 8, p. 1523, Apr. 2019.

[78]J. He *et al*, “Partial discharge pattern recognition algorithm based on sparse self - coding and extreme learning machine,” *IEEE Conf. Energy Internet Energy Syst. Integr. (EI2)*, 2018.

[79]Q. Q. Zhang, H. Song, and G. H. Sheng, “Online sequential extreme learning machine for partial discharge pattern recognition of transformer,” *IEEE Power Eng. Soc. Transm. Distrib. Conf. (T&D)*,2018.

[80]A. A. Mas’ud, B. G. Stewart, and S. G. McMeekin, “An investigative study into the sensitivity of different partial discharge φ-q-n pattern resolution sizes on statistical neural network pattern classification” Measurement, vol. 92, pp. 497–507, Oct. 2016.

[81]Mas’ud, A.A.; Ardila-Rey, J.A.; Albarracín, R.; Muhammad-Sukki, F.; Bani, N.A. Comparison of the Performance of Artificial Neural Networks and Fuzzy Logic for Recognizing Different Partial Discharge Sources. *Energies* **2017**, *10*, 1060.

[82]M. Majidi, M. S. Fadali, M. Etezadi-Amoli, and M. Oskuoee, “Partial discharge pattern recognition via sparse representation and ANN,” IEEE Trans. Dielectr. Electr. Insul., vol. 22, no. 2, pp. 1061–1070, Apr. 2015.

[83]J. He *et al*, “Partial discharge pattern recognition algorithm based on sparse self - coding and extreme learning machine,” *IEEE Conf. Energy Internet Energy Syst. Integr. (EI2)*, 2018.

[84]Q. Q. Zhang, H. Song, and G. H. Sheng, “Online sequential extreme learning machine for partial discharge pattern recognition of transformer,” *IEEE Power Eng. Soc. Transm. Distrib. Conf. (T&D)*,2018.

[85]J. Jineeth, R. Mallepally, and T. K. Sindhu, "Classification of Partial Discharge Sources in XLPE Cables by Artificial Neural Networks and Support Vector Machine," *IEEE Electr. Insul. Conf. (EIC)*, 2018, pp. 407–411.

[86]H. M. M. G. T. Herath *et al*, "Comparison of supervised machine learning techniques for PD classification in generator insulation," *IEEE Int. Conf. Ind. Inf. Syst. (ICIIS)*, 2017, pp. 1–6.

[87]S. Wang, Y. Xia, C. Ping, and G. Xue, "Study on SF6 gas on-line monitoring method based on machine learning," *IEEE Inf. Technol. Mechatronics Eng. Conf. (ITOEC)*, 2018, pp. 240–244.

[88]V. Kecman, *Support Vector Machines: Theory and Applications*. Springer Science & Business Media,2005.

[89]J. Gao, Y. Zhu, and Y. Jia, "Pattern recognition of unknown partial discharge based on improved SVDD," IET Sci. Meas. Technol., vol. 12, no. 7, pp. 907–916, Oct. 2018.

[90]T. Le, D. Tran, W. Ma, and D. Sharma, "A unified model for support vector machine and support vector data description," *Int. Jt. Conf. Neural Networks (IJCNN)*, 2012.

[91]G. Robles, E. Parrado-Hernández, J. Ardila-Rey, and J. M. Martínez-Tarifa, "Multiple partial discharge source discrimination with multiclass support vector machines," Expert Syst. Appl., vol. 55, pp. 417–428, Aug. 2016.

[92]I. Mitiche *et al*, "Classification of EMI discharge sources using time–frequency features and multi-class support vector machine," Electr. Power Syst. Res., vol. 163, pp. 261–269, Oct. 2018.

[93]S. Wang, C. Ping, and G. Xue, "Transformer partial discharge pattern recognition based on random forest," J. Phys. Conf. Ser., vol. 1176, no. 6, p. 062025, Mar. 2019.

[94]I. H. Kartojo, Y. B. Wang, G. J. Zhang, and Suwarno, "Partial discharge defect recognition in power transformer using random forest," *IEEE Int. Conf. Dielectr. Liq. (ICDL)*, 2019.

[95]X. Peng *et al*, "Random forest based optimal feature selection for partial discharge pattern recognition in HV cables," IEEE Trans. Power Deliv., vol. 34, no. 4, pp. 1715–1724, Aug. 2019.

[96]M. X. Zhu *et al*, "Localization of multiple partial discharge sources in air-insulated substation using probability-based algorithm," IEEE Trans. Dielectr. Electr. Insul., vol. 24, no. 1, pp. 157–166, Feb. 2017.

[97]X. Peng *et al*, "Rough set theory applied to pattern recognition of partial discharge in noise affected cable data," IEEE Trans. Dielectr. Electr. Insul., vol. 24, no. 1, pp. 147–156, Feb. 2017.

[98]M. X. Zhu *et al*, "Localization of multiple partial discharge sources in air-insulated substation using probability-based algorithm," IEEE Trans. Dielectr. Electr. Insul., vol. 24, no. 1, pp. 157–166, Feb. 2017.

[99]H. Janani and B. Kordi, "Towards automated statistical partial discharge source classification using pattern recognition techniques," High Volt., vol. 3, no. 3, pp. 162–169, Sep. 2018.

[100]W. L. Woon, A. El-Hag, and M. Harbaji, "Machine learning techniques for robust classification of partial discharges in oil-paper insulation systems," IET Sci. Meas. Technol., vol. 10, no. 3, pp. 221–227, May 2016.

[101]I. Goodfellow, B. Yoshua, and C. Aaron, *Deep Learning*, MIT Press, 2016.

[102]Y. Lecun, Y. Bengio, and G. Hinton, "Deep learning," Nature, vol. 521, no. 7553, pp. 436–444, May 2015.

[103]V. M. Catterson and B. Sheng, "Deep neural networks for understanding and diagnosing partial discharge data," *IEEE Electr. Insul. Conf. (EIC)*, 2015, pp. 218–221.

[104]L. Duan *et al*, "Identification of partial discharge defects based on deep learning method," IEEE Trans. Power Del., vol. 34, no. 4, pp. 1557–1568, Aug. 2019.

[105]Y. Wang *et al*, "Partial discharge pattern recognition of gas-insulated switchgear via a light-scale convolutional neural network," Energies, vol. 12, no. 24, p. 4674, Dec. 2019.

[106]X. Wan *et al*, "Pattern recognition of partial discharge image based on one-dimensional convolutional neural network," *Int. Conf. Cond. Monit. Diagnosis (CMD)*, 2018.

[107]N. Puspitasari *et al*, "Partial discharge waveform identification using image with convolutional neural network," *Int. Univ. Power Eng. Conf. (UPEC)*, 2019, pp. 1–4.

[108]Y. Yang *et al*, "Research on partial discharge diagnosis based on data augmentation and convolutional neural," IOP Conf. Ser. Mater. Sci. Eng., vol. 677, no. 5, p. 052101, Dec. 2019.

[109]H. Song, J. Dai, G. Sheng, and X. Jiang, "GIS partial discharge pattern recognition via deep convolutional neural network under complex data source," IEEE Trans. Dielectr. Electr. Insul., vol. 25, no. 2, pp. 678–685, Apr. 2018.

[110]Y. Wang *et al*, "A MobileNets convolutional neural network for GIS partial discharge pattern recognition in the ubiquitous power internet of things context: optimization, comparison, and application," IEEE Access, vol. 7, pp. 150226–150236, Oct. 2019.

[111]Q. Che *et al*, "Partial discharge recognition based on optical fiber distributed acoustic sensing and a convolutional neural network," IEEE Access, vol. 7, pp. 101758–101764, Jul. 2019.

[112]G. Li *et al*, "Partial discharge patterns recognition with deep Convolutional Neural Networks," *Int. Conf. Cond. Monit. Diagnosis (CMD)*, 2016, pp. 324–327.

[113]K. Banno, Y. Nakamura, Y. Fujii, and T. Takano, "Partial discharge source classification for switchgears with transient earth voltage sensor using convolutional neural network," *Int. Conf. Cond. Monit. Diagnosis (CMD)*, 2018.

[114]M. A. Khan, J. Choo, and Y. H. Kim, "End-to-end partial discharge detection in power cables via time-domain convolutional neural networks," J. Electr. Eng. Technol., vol. 14, no. 3, pp. 1299–1309, May 2019.

[115]W. L. Woon, Z. Aung, and A. El-Hag, "Intelligent monitoring of transformer insulation using convolutional neural networks," *Int. Work. Data Anal. Renew. Energy Integr. (DARE)*, 2018, pp. 127–136.

[116]Q. Zhang, J. Lin, H. Song, and G. Sheng, "Fault identification based on PD ultrasonic signal using RNN, DNN and CNN," *Int. Conf. Cond. Monit. Diagnosis (CMD)*, 2018.

[117]X. Peng *et al*, "A Convolutional neural network-based deep learning methodology for recognition of partial discharge patterns from highvoltage cables," IEEE Trans. Power Del., vol. 34, no. 4, pp. 1460–1469, Aug. 2019.

[118]K. Firuzi, M. Vakilian, B. T. Phung, and T. R. Blackburn, "Partial Discharges Pattern Recognition of Transformer Defect Model by LBP & HOG Features," IEEE Trans. Power Deliv., vol. 34, no. 2, pp. 542–550, Apr. 2019.

[119]B. Adam and S. Tenbohlen, "Classification of multiple PD sources by signal features and LSTM networks," *IEEE Int. Conf. High Volt. Eng. Appl. (ICHVE)*, 2019.

[120]M. T. Nguyen, V. H. Nguyen, S. J. Yun, and Y. H. Kim, "Recurrent neural network for partial discharge diagnosis in gas-insulated switchgear," Energies, vol. 11, no. 5, p. 1202, May 2018.

[121]G. Li *et al*, "Partial discharge recognition with a multi-resolution convolutional neural network," Sensors, vol. 18, no. 10, Oct. 2018.

[122]X. Zhou *et al*, "Research on transformer partial discharge UHF pattern recognition based on CNN-LSTM," Energies, vol. 13, no. 61, pp. 1–13, Dec. 2019.

[123]K. Sun, R. Li, L. Zhao, and Z. Li, "Feature extraction based on time series topological analysis for the partial discharge pattern recognition of high-voltage power cables," Measurement, vol. 217, Aug. 2023, Art. no. 113009.

[124]M. Hoof, B. Freisleben, and R. Patsch, "PD source identification with novel discharge parameters using counter propagation neural networks," IEEE Trans. Dielectr. Electr. Insul., vol. 4, no. 1, pp. 17–32, Feb. 1997.

[125]A. K. Das, B. Ghosh, S. Dalai, and B. Chatterjee, "Sensing surface contamination of metal oxide surge arrester through resistive leakage current signal analysis by mathematical morphology," IEEE Sensors J., vol. 20, no. 16, pp. 9460–9468, Aug. 2020.

[126]G. Matheron, Random Sets and Integral Geometry. New York, NY, USA:Wiley, 1975.

[127]S. Gautam and S. M. Brahma, "Overview of mathematical morphology in power systems—A tutorial approach," in Proc. IEEE Power Energy Soc. Gen. Meeting, Calgary, AB, Canada, Jul. 2009, pp. 1–7.

[128]M. Stasolla and X. Neyt, "Combining wavelets and mathematical morphology to detect changes in time series," in Proc. Prog. Electromagn. Res. Symp. Fall (PIERS FALL), Singapore, 2017, pp. 1015–1020.

[129]A. K. Das, S. Dalai, and B. Chatterjee, "Deep learning–based surface contamination severity prediction of metal oxide surge arrester in power system," IET Sci., Meas. Technol., vol. 15, no. 4, pp. 376–384, Jun. 2021.

[130]B. Ganguly, A. Ghosal, A. Das, D. Das, D. Chatterjee, and D. Rakshit, "Automated detection and classification of arrhythmia from ECG signals using

feature-induced long short-term memory network," IEEE Sensors Lett., vol. 4, no. 8, pp. 1–4, Aug. 2020.

[131]M. Geng, W. Zhou, G. Liu, C. Li, and Y. Zhang, "Epileptic seizure detection based on stockwell transform and bidirectional long short term memory," IEEE Trans. Neural Syst. Rehabil. Eng., vol. 28, no. 3, pp. 573–580, Mar. 2020.

[132]S. Xiang, Y. Qin, C. Zhu, Y. Wang, and H. Chen, "Long short-term memory neural network with weight amplification and its application into gear remaining useful life prediction," Eng. Appl. Artif. Intell., vol. 91, May 2020, Art. no. 103587.

[133]A. Shrestha, H. Li, J. L. Kernec, and F. Fioranelli, "Continuous human activity classification from FMCW radar with bi-LSTM networks," IEEE Sensors J., vol. 20, no. 22, pp. 13607–13619, Nov. 2020.

[134]H. Li, A. Shrestha, H. Heidari, J. Le Kernec, and F. Fioranelli, "Bi-LSTM network for multimodal continuous human activity recognition and fall detection," IEEE Sensors J., vol. 20, no. 3, pp. 1191–1201, Feb. 2020.

[135]F. F. Chamasemani and Y. P. Singh, "Multi-class support vector machine (SVM) classifiers—An application in hypothyroid detection and classification," in Proc. 6th Int. Conf. Bio-Inspired Computing: Theories Appl., Penang, Malaysia, Sep. 2011, pp. 351–356.

[136]I. Banerjee, S. S. Mullick, and S. Das, "On convergence of the class membership estimator in fuzzy k-nearest neighbor classifier," IEEE Trans. Fuzzy Syst., vol. 27, no. 6, pp. 1226–1236, Jun. 2019.

[137]A. K. Das, S. Dalai, and B. Chatterjee, "Cross stockwell transform aided random forest based surface condition identification of metal oxide surge arrester employning leakage current signal," in Proc. IEEE Region 10 Symp. (TENSYMP), Dhaka, Bangladesh, Jun. 2020,

[138]S. Bag *et al*., "S-Transform Aided Random Forest Based PD Location Detection Employing Signature of Optical Sensor," IEEE Trans. Power Del., vol. 34, no. 4, pp. 1261-1268, 2019.

[139]S. Zheng *et al*., "Location of PDs inside transformer windings using UHF Methods," IEEE Trans. Dielectrics Elect.Insul., vol. 21, no. 1, pp. 386–393, 2014.
[140]M. K. Chen *et al*., "RF detection of partial discharge in current transformer," 2007 International Power Engineering Conference (IPEC 2007), 2007, pp. 193-196.
[141]S. Govindarajan *et al*., "Development of Hankel Singular-Hypergraph Feature Extraction Technique for Acoustic Partial Discharge Pattern Classification", Energies, vol. 14, no. 6, 2021.
[142]S. K. Khare, V. Bajaj and U. R. Acharya, "SPWVD-CNN for Automated Detection of Schizophrenia Patients Using EEG Signals," IEEE Transactions on Instrumentation and Measurement, vol. 70, pp. 1-9, 2021, Art no. 2507409, doi: 10.1109/TIM.2021.3070608.
[143]A. K. Das, S. Chatterjee, B. Chatterjee and S. Dalai, "Cross Spectrum Aided Surface Condition Assessment of Metal Oxide Surge Arrester Employing Convolutional Neural Network," IEEE Trans. Dielectrics Elect.Insul., vol. 28, no. 6, pp. 2134-2143, 2021.
[144]S. Shao, S. McAleer, R. Yan and P. Baldi, "Highly Accurate Machine Fault Diagnosis Using Deep Transfer Learning," IEEE Trans. Ind. Informat., vol. 15, no. 4, pp. 2446-2455, 2019.
[145]K. Simonyan and A. Zisserman, "Very deep convolutional networks for large-scale image recognition," 2014, art xiv: 1409.1556.
[146]M. Geng, W. Zhou, G. Liu, C. Li, and Y. Zhang, "Epileptic seizure detection based on stockwell transform and bidirectional long short-term memory," IEEE Tra pp. 1775–1778.

[147]X. Peng et al., "A Convolutional Neural Network-Based Deep Learning Methodology for Recognition of Partial Discharge Patterns from High-Voltage Cables," IEEE Trans. Power Del., vol. 34, no. 4, pp. 1460-1469, 2019.
[148]R. Schwarz and M. Muhr, "Experience with optical partial discharge detection," Mater. Sci.-Poland, vol. 27, no. 4/2, pp. 1140–1146, 2009.
[149]P. Prasad Chandra, S. Singha Roy and S. Chatterjee, "Neuromuscular Disease Detection Employing 1D-Local Binary Pattern of Electromyography Signals,"

2020 IEEE Applied Signal Processing Conference (ASPCON), pp. 272-276, Kolkata, 2020

[150]A. K. Jaiswal and H. Banka, "Local pattern transformation-based feature extraction techniques for classification of epileptic EEG signals," Biomedical Signal Processing and Control, vol. 34, pp. 81-92, 2017.

[151]Y. Kaya, M. Uyar, R. Tekin and S. Yıldırım, "1D-local binary pattern-based feature extraction for classification of epileptic EEG signals," Applied Mathematics and Computation, vol. 243, pp. 209-219, 2014.

[152]Y. Liu, X. Yan, C. Zhang and W. Liu, "An Ensemble Convolutional Neural Networks for Bearing Fault Diagnosis Using Multi-Sensor Data," Sensors, vol. 19, no. 23, 2019.

[153]M. Geng, W. Zhou, G. Liu, C. Li and Y. Zhang, "Epileptic seizure detection based on stockwell transform and bidirectional long short-term memory," IEEE Trans. Neural Syst. Rehabil. Eng., vol. 28, no. 3, pp. 573-580, 2020.

[154]A. Shrestha, H. Li, J. Le Kernec and F. Fioranelli, "Continuous human activity classification from FMCW radar with Bi-LSTM networks," IEEE Sensors J., vol. 20, no. 22, pp. 13607-13619, 2020.

[155]M. F, Aslan, M. F. Unlersen, K. Sabanci and A. Durdu, "CNN-based transfer learning–BiLSTM network: A novel approach for COVID-19 infection detection", Applied Soft Computing, vol. 98, Article no. 10691, 2021.

Rakesh Das
23.05.2025